

STUDY OF SCOUR AROUND PERMEABLE SPURS

A THESIS

*Submitted in fulfilment of the
requirements for the award of the degree*

of

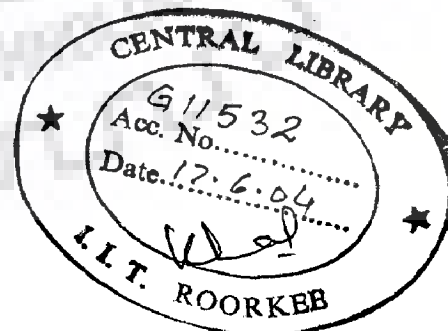
DOCTOR OF PHILOSOPHY

in

WATER RESOURCES DEVELOPMENT

By

SHAGOOFTA RASOOL SHAH



**WATER RESOURCES DEVELOPMENT TRAINING CENTRE
INDIAN INSTITUTE OF TECHNOLOGY ROORKEE
ROORKEE-247 667 (INDIA)**

OCTOBER, 2001

CANDIDATE'S DECLARATION


I hereby certify that the work which is being presented in this thesis entitled "**STUDY OF SCOUR AROUND PERMEABLE SPURS**" in fulfillment of the requirement for the award of the **Degree of Doctor of Philosophy** and submitted in Water Resources Development Training Centre, of the Indian Institute of Technology Roorkee is an authentic record of my own work carried out during the period from January 1999 to October 2001 under the supervision of **Dr. Nayan Sharma** and **Dr. C.S.P. Ojha**.

The matter presented in this thesis has not been submitted by me for the award of any other degree in this or any other university.

October 2001


(SHAGOOFTA RASOOL SHAH)

This is to certify that the above statement made by the candidate is true to the best of our knowledge.


23.10.2001

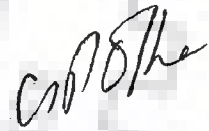
Dr. Nayan Sharma

Professor

Dept. of WRDTC

IIT, Roorkee

Roorkee, INDIA



Dr. C.S.P. Ojha

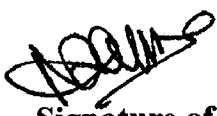
Associate Prof.

Dept. of Civil Engg.

IIT, Roorkee

Roorkee, INDIA

The Ph.D. Viva-Voca examination of Shagoofta Rasool Shah, Research Scholar has been held on 6th April, 2002

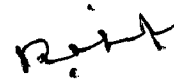


Signature of Supervisor (s)



Devadutta Das

Signature of H.O.D.



Signature of External Examiner

ABSTRACT

Increasing economic costs of river protection works in India have led to the adoption of permeable spurs in practice. However, research on different types of permeable spurs is not developed to the same extent as that on solid spurs, bridge piers and abutments. Different types of permeable spurs have come into existence. However, permeable pile spurs are being favoured in north and north-eastern region of India. To use these pile spurs in field, one needs to know the development of scour as well as equilibrium scour. The present study basically fills this gap. It examines various types of permeable spurs to assess the merits associated with the pile permeable spur. It is observed that these spurs experience minimum scour. Based on the study of bed condition in certain experiments, the variables influencing scour have been identified and used to model the equilibrium scour depth in case of pile permeable spurs. Use of different scaling parameters is also examined in the model development. Based on lab experiments, a model is calibrated for scour depth estimation. Subsequently, the use of the model is tested against field data. The predictions are satisfactory in certain cases only and are found dependant on the type of calibrated model. An approach for the estimation of scour in transient condition is suggested and an insight into the future work is also provided.

ACKNOWLEDGEMENT

I take this opportunity to record my sincere gratitude and indebtedness to Dr. Nayan Sharma, Professor, Water Resources Development Training Centre I.I.T Roorkee and Dr. C.S.P. Ojha, Associate Professor, Department of Civil Engineering I.I.T Roorkee, for their expert guidance, constant encouragement, constructive criticism and very fruitful discussions at various stages of the research work presented in this thesis.

I am extremely thankful to Prof. Devadutta Das, Head of Water Resources Development Training Centre I.I.T Roorkee, for providing funding and all technical assistance and Prof. Gopal Chauhan, Chairman APC, WRDTC I.I.T Roorkee, for his continuous moral encouragement during this research work.

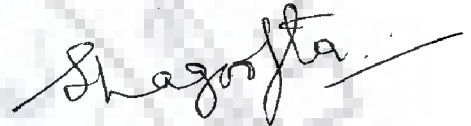
My infinite thanks are due to Dr. Farooq Abdullah, Honorable Chief Minister, Jammu and Kashmir for removing all hurdles in order to enable me to carry out this research work.

I express my sincere thanks to Dr. S.C Handa, Professor and Co-ordinator, Quality Improvement Program I.I.T Roorkee and his staff for all their support and to my sponsors those are All India Council for Technical Education and Regional Engineering College Hazratbal, Jammu and Kashmir for their financial support to undertake this Doctoral study.

I am also grateful to all the lab staff of WRDTC for their co-operation during the experimental phase. Thanks are also due to all my friends who assisted me in one way or the other at times.

On top of every thing I acknowledge the discipline my parents, Mr. Gulam Rasool Shah and Mrs. Gulam Fatima Qurashi imbided in me and the immense love, encouragement and sacrifice given by my husband Dr. Mohd. Naim Manhas and absolute help of Almighty God what proved to be my sole power to go ahead at all the stages.

But in my whole effort the angelic soul who suffered the most at my hands is my darling of all, elder son Adnan Naim who could not get enough love and care from my side which was due to him at his age and a little brunt was beared by my younger son Numair Naim too.



Shagoofta

(Mrs. SHAGOOFTA RASOOL SHAH)

CONTENTS

DESCRIPTION	Page No.
CANDIDATE'S DECLARATION	i
ABSTRACT	ii
ACKNOWLEDGEMENT	iii
CONTENTS	v
LIST OF TABLES	viii
LIST OF FIGURES	xi
LIST OF PLATES	xvi
NOTATIONS	xviii
CHAPTER 1 : INTRODUCTION	1
1.1 General	1
1.2 Objectives of the Study	3
1.3 Organisation of Thesis	4
CHAPTER 2 : REVIEW OF LITERATURE	6
2.1 General	6
2.2 Certain Scour Depth Models on Solid Spurs	7
2.3 Permeable Groynes	17
2.3.1 Slotted spur	18
2.3.2 Advantages and disadvantages of permeable groynes	19
2.4 Studies on Permeable Spurs	20
2.5 Certain Observations from Field	25
2.6 Concluding Remarks	25

CHAPTER 3 : EXPERIMENTAL PROGRAMME	27
3.1	Introduction 27
3.2	Laboratory Flumes and other Accessories 28
3.2.1	Flume used in first phase 28
3.2.2	Flume used in second phase 31
3.2.3	Materials used 33
3.3	Experimental Procedure 34
3.4	Phase One Model Experiments 39
3.5	Phase Two Pile Spur Experiments 64
3.6	Phase Three Field Experiments 65
3.6.1	Field experimental procedure 67
3.7	Summary 68
CHAPTER 4 : PRELIMINARY ASSESSMENT OF SCOUR AROUND DIFFERENT PERMEABLE SPURS	72
4.1	Introduction 72
4.2	Assessment of Melville's Approach 73
4.3	Data Analysis 76
4.4	Results and Discussion 79
4.5	Testing of Melville's Approach Using Permeable Spur Experiments 86
4.6	Bed Profiles in Case of Permeable Spurs 86
4.7	Summary 89
CHAPTER 5 : STEADY STATE MODELLING OF SCOUR	92
5.1	Introduction 92
5.2	Functional Relationships for Scour 92
5.3	Calibration of the Scour Relationship 94
5.4	Calibration of Dimensionless Relationships 97
5.5	Validation of Calibrated Relationships 102
5.6	Summary 104

CHAPTER 6 : MODELLING OF TRANSIENT SCOUR		
	VARIATION	108
6.1	Introduction	108
6.2	Analysis of Lab. Experiments For Transient Scour	108
6.3	Temporal Variation During an Unsteady State Flow	125
6.4	Application to Field Data	127
6.5	Significance of Temporal Scour Study	132
CHAPTER 7 : GENERAL DISCUSSION		134
CHAPTER 8 : CONCLUSIONS AND SCOPE FOR FUTURE WORK		
	FUTURE WORK	146
8.1	Conclusions	146
8.2	Scope for Future Work	148
REFERENCES		149
APPENDIX		154

LIST OF TABLES

Table No.	Description	Page No.
Table 3.1	The sieve analysis of the sediment material of $d_{50} = 0.424$ mm	34
Table 3.2	Sieve analysis of the sediment material of $d_{50} = 2.8$ mm	34
Table 3.3 a	Pertinent data related to experiment on solid spur (fig. 3.8a)	48
Table 3.3 b	Pertinent data related to experiment on spur model with round holes of 6 mm dia. (fig. 3.8 b)	48
Table 3.3 c	Pertinent data related to experiment on spur model with alternate rows of round holes of dia. 1 cm and 4mm (fig. 3.8 c)	48
Table 3.3 d	Pertinent data related to experiment on spur model with two rectangular holes in each row. Two rows in 8cm depth & three rows in 10 cm depth (Fig. 3.8 d)	48
Table 3.3 e	Pertinent data related to experiment on spur model with three rectangular holes in each row. The holes in the mid stream are open in mid stream side. Two rows in 8cm depth & three rows in 10 cm depth (fig. 3.8 e - 3.8 f)	49
Table 3.3 f	Pertinent data related to experiment on spur model with two vertical slots. Slots start from the test bed surface and are open on top (fig. 3.8 g)	49
Table 3.3 g	Pertinent data related to experiments on spur model with three vertical slots. Slots start from the test bed surface	

	and are open on top (Fig. 3.8 h)	50
Table 3.3 h	Pertinent data related to experiments on spur model with horizontal slots. Three rectangular, horizontally placed slots in 10 cm depth & two slots in 8cm depth. Slots are closed on mid stream side. 1 st slot starts from bed level (Fig. 3.8i)	50
Table 3.3 i	Pertinent data related to experiments on spur model with horizontal slots open on mid stream side. Three rectangular, horizontally placed slots in 10 cm depth & two slots in 8cm depth. 1 st slot starts from bed level (Fig. 3.8 j)	51
Table 3.3 j	Pertinent data related to experiments on pile spur model in form of pencils dia 0.85 cm each (Fig. 3.8 k to 3.8 l)	51
Table 3.3 k	Pertinent data related to experiments on two parallel rows of pile spur model in form of plate and pencils dia 0.85 cm each (fig. 3.8m to 3.8.n)	51
Table 3.4	The sieve analysis of the bed material of river Solani at the spur construction spots	68
Table 4.1	K_{θ} versus θ after Richardson et al. (1993)	75
Table 4.2	K_s for abutments after Melville (1997)	76
Table 4. 3	Range of parameters used by different investigators and the observed (d_{s0}) and calculated (d_{scm}) scour depths	77
Table 4. 4	Range of dimensionless parameters taken by different Investigators	78
Table 4. 5	Performance evaluation of Melville (1997) relationship	85

Table 5.1	Data related to different permeable pile spurs (Placed in Solani river) for steady state analysis (Width of pile spur = 6 cm, and width of Solani river as 30.0 m)	103
Table 5.2	Performance evaluation of different dimensionless scour Relationships	103
Table 6.1	Calibrated model parameters	124



LIST OF FIGURES

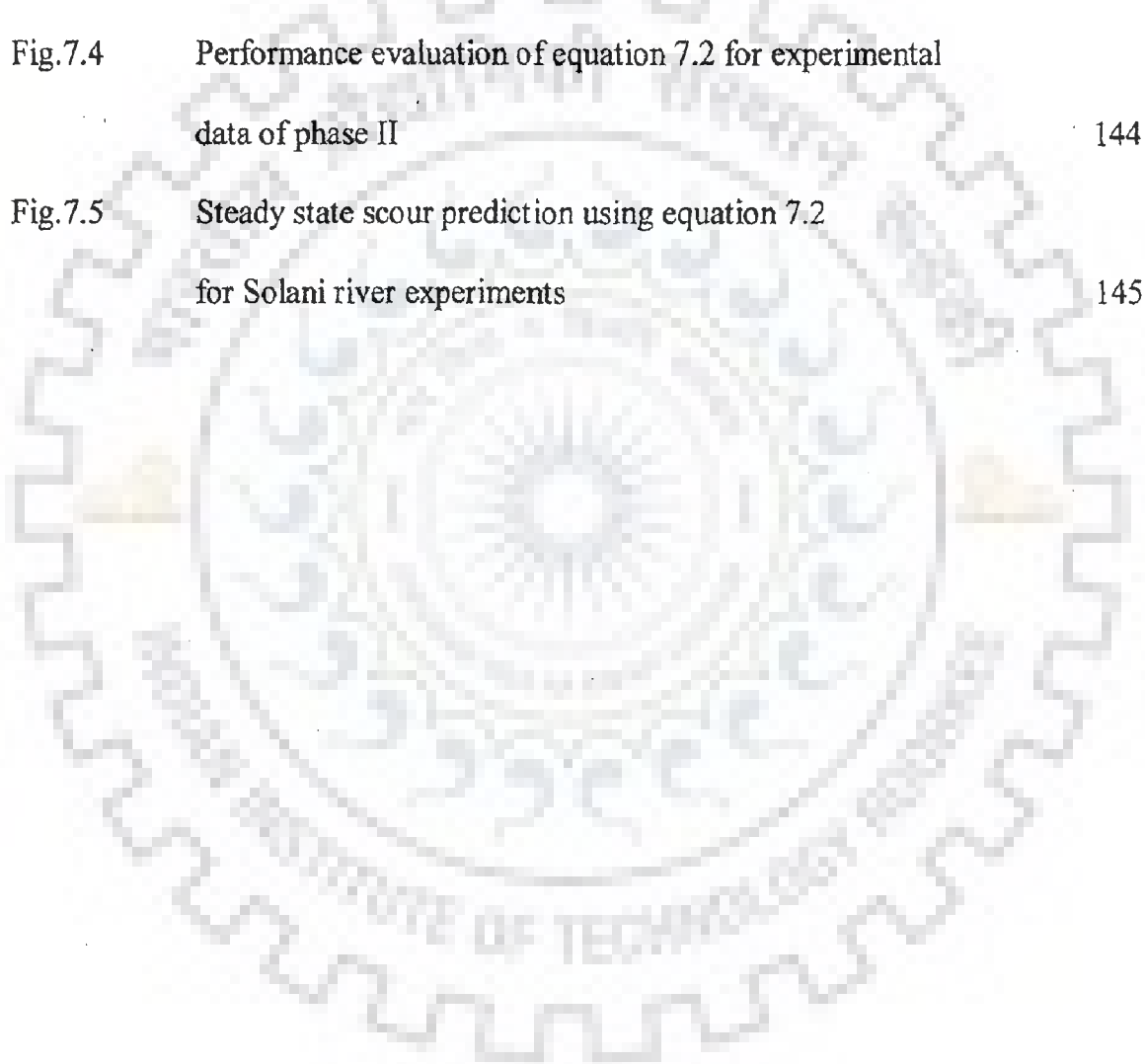
Figure No.	Description	Page No.
Fig. 2.1	Descriptive sketch of scour at permeable (pile) groyne	22
Fig. 3.1	Plan of first flume and its components used in phase -1 experiments	30
Fig. 3.2	Plan of second tilting flume and its components used in phase -2 experiments	32
Fig. 3.3	Cummulative frequency curve for coarse sand of $d_{50}=0.4\text{mm}$, ranging from 0.3mm to 0.6mm	35
Fig. 3.4	Cummulative frequency curve for fine gravel $d_{50}=2.8\text{ mm}$, ranging from 2 mm to 4 mm	35
Fig. 3.5	Calibration of V-notch	37
Fig. 3.6	Calibration chart for pitot tube	37
Fig. 3.7	Grid points in cross-section locations across the flume, for measurements of velocities	38
Fig. 3.8a	Model of zero permeability	40
Fig. 3.8b	Model with only one dimensional holes	40
Fig. 3.8c	Model with round holes of two different diameters	41
Fig. 3.8d	Model with two square/rectangular slits in each row	41
Fig. 3.8e	Model with three slits in each row slits opposite to spur-side-wall are open	42
Fig. 3.8f	Model with three rectangular slits in mid stream are	

	open on extreme edge	42
Fig. 3.8g	Model with 2 vertical slots through out the depth of flow	43
Fig. 3.8h	Model with 3 vertical slots through out the depth of flow	43
Fig. 3.8i	Model with only one rectangular slot in each row through out its length (The slits are closed on top, bottom, left and right)	44
Fig. 3.8j	Model with only one horizontal rectangular slot in each row which are open in mid stream side	45
Fig. 3.8k	Single row pile spur model made with two wooden pencils	45
Fig. 3.8l	Single row pile spur model made with four wooden pencils	46
Fig. 3.8m	Two parallel rows pile spur model made with eight wooden pencils	46
Fig. 3.8n	Two parallel plates with 3 vertical slots model	47
Fig. 4.1	Agreement between computed (Melville's approach 1999) and observed scour depths (Garde & Subramanya 1961)	80
Fig. 4.2	Agreement between computed (Melville's approach 1999) and observed scour depths (Nambudripad 1961)	81
Fig. 4.3	Agreement between computed (Melville's approach 1999) And observed scour depths (Ramu (a) (b) 1964)	82
Fig. 4.4	Agreement between computed (Melville's approach 1999) and observed scour depths (Tyagi 1973)	83
Fig. 4.5	Agreement between computed (Melville's approach 1999) and observed scour depths (Singh, 1993)	84
Fig. 4.6a	Variation of d_{50} / d_{scm} with permeability in $d_{50} = 0.424\text{mm}$ grain size and $b = 5\text{cm}$.	87
Fig. 4.6b	Variation of d_{50} / d_{scm} with permeability in	

	$d_{50} = 0.424\text{mm}$ grain size and $b = 10\text{cm}$.	87
Fig. 4.6c	Variation of d_{s0} / d_{scm} with permeability in $d_{50} = 2.8\text{mm}$ grain size and $b = 5\text{cm}$.	88
Fig. 4.6d	Variation of d_{s0} / d_{scm} with permeability in $d_{50} = 2.8\text{mm}$ grain size and $b = 10\text{cm}$.	88
Fig. 4.7	Interpolated bed profiles for experiment no. P1E5	90
Fig. 4.8	Interpolated bed profiles for experiment no. P1A5	91
Fig. 5.1	Scour depth in relation to F_r ($p = 15\%$, $b = 5\text{ cm}$, $d = 2.8\text{ mm}$)	96
Fig. 5.2	Scour depth in relation to beta ($F_r = 0.12$, $b = 5\text{ cm}$, $d = 2.8\text{ mm}$)	96
Fig. 5.3a	Agreement between computed and observed scour depth for pile spurs ($d = 2.8\text{ mm}$, $b = 50\text{ mm}$)	98
Fig. 5.3b	Agreement between computed and observed scour depth for pile spurs ($d = 2.8\text{ mm}$, $b = 100\text{ mm}$)	98
Fig. 5.3c	Agreement between computed and observed scour depth for pile spurs ($d = 0.424\text{ mm}$, $b = 50\text{ mm}$)	99
Fig. 5.3d	Agreement between computed and observed scour depth for pile spurs ($d = 0.424\text{ mm}$, $b = 100\text{ mm}$)	99
Fig. 5.4a	Performance evaluation of various equations to judge the Suitable scaling parameters (Spur type RA)	105
Fig. 5.4b	Performance evaluation of various equations to judge the Suitable scaling parameters (Spur type RB)	105
Fig. 5.4c	Performance evaluation of various equations to judge the Suitable scaling parameters (Spur type RC)	106
Fig. 5.4d	Performance evaluation of various equations to judge the Suitable scaling parameters (Spur type RD)	106

Fig. 6.1(a)to(n)	Temporal variation of scour depth under steady flow (lab.data)	110- 123
Fig. 6.2	Quasi steady state discretisation of a hypothetical discharge	126
Fig. 6.3	Variation of discharge in Solani river during field experiments	126
Fig. 6.4 a	Variation of scour in Solani river for experiment nos. RA-1 to RA-4 with pile spur of porosity 20%	128
Fig. 6.4b	Variation of scour in Solani river for experiment nos. RB-1to RB-4 with pile spur of porosity 40%	128
Fig. 6.4c	Variation of scour in Solani river for experiment nos. RC-1 TO RC-4 with pile spur of porosity 60%	129
Fig. 6.4d	Variation of scour in Solani river for experiment nos. RD-1 TO RD-4 with pile spur of porosity 80%	129
Fig. 6.5a	Agreement between observed and computed scour for RA type permeable spurs	131
Fig. 6.5b	Agreement between observed and computed scour for RB type permeable spurs	131
Fig. 6.5c	Agreement between observed and computed scour for RC type permeable spurs	133
Fig. 6.5d	Agreement between observed and computed scour for RD type permeable spurs	133
Fig. 7.1	Agreement between computed and observed scour/width of pile spur ($d=0.424$ mm, $b=50$ mm)	139
Fig. 7.2a	Agreement between observed and computed scour for RA type permeable spurs	140
Fig. 7.2b	Agreement between observed and computed scour	

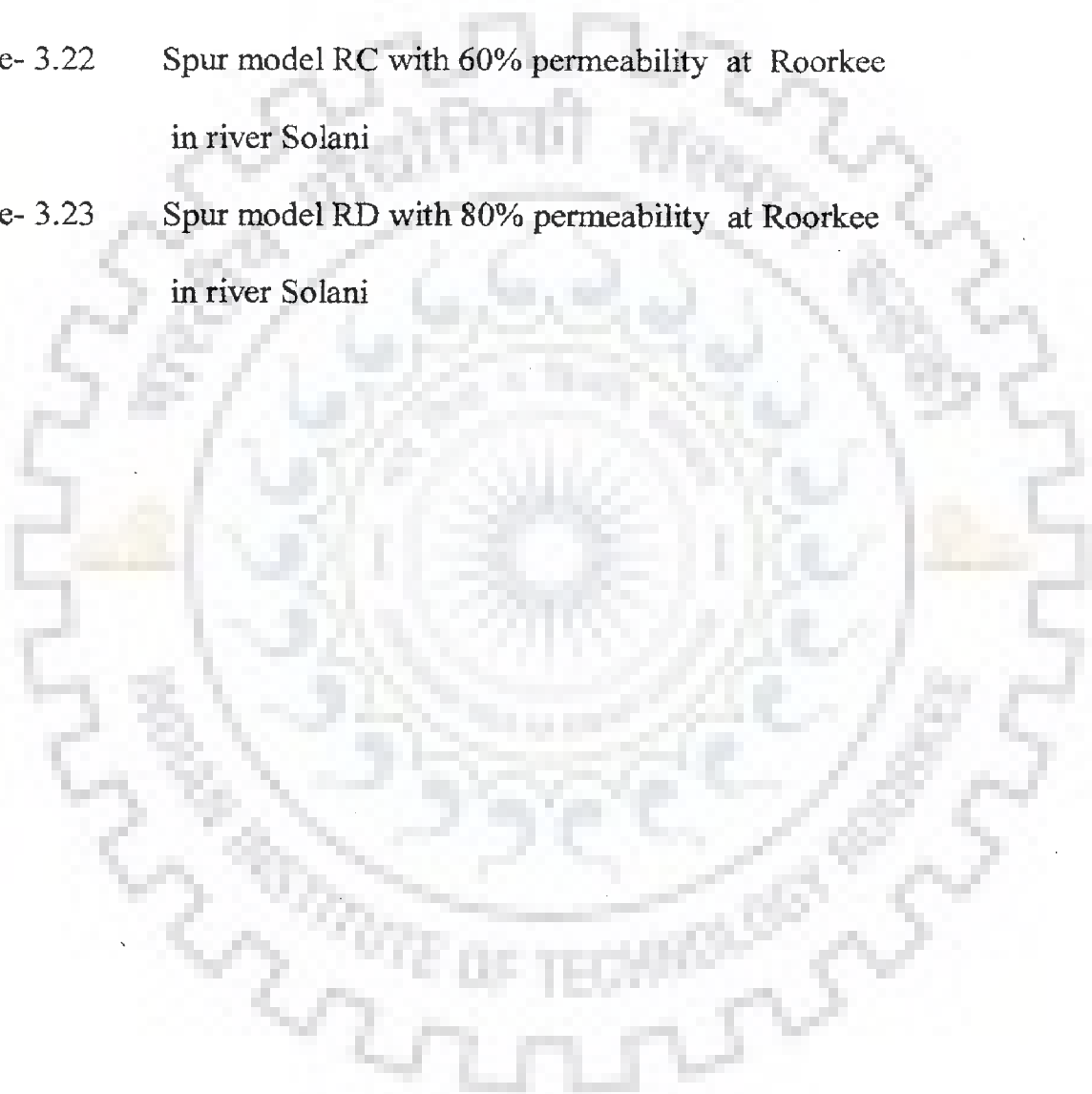
	for RB type permeable spurs	140
Fig. 7.2c	Agreement between observed and computed scour for RC type permeable spurs	141
Fig. 7.2d	Agreement between observed and computed scour for RD type permeable spurs	141
Fig. 7.3	Agreement between computed (eq.7.1) and observed scour/ width for experiments having bed particle size of 2.8 mm	142
Fig.7.4	Performance evaluation of equation 7.2 for experimental data of phase II	144
Fig.7.5	Steady state scour prediction using equation 7.2 for Solani river experiments	145



LIST OF PLATES

Plate No.	Description	Page No.
Plate- 1.1	Permeable spurs at Gumi Assam in river Brahamaputra	2
Plate- 1.2	Permeable spurs at Gurmukhteshver Muradabad in river Ganga	2
Plate- 3.1	Scour around experimental run no. A-3	54
Plate- 3.2	Scour around experimental run no. B-2	54
Plate- 3.3	Scour around experimental run no. B-6	55
Plate- 3.4	Scour around experimental run no. CA-2	56
Plate- 3.5	Scour around experimental run no. CB-3	57
Plate- 3.6	Scour around experimental run no. DA-1	57
Plate- 3.7	Scour around experimental run no. DA-8	58
Plate- 3.8	Scour around experimental run no. DA-9	58
Plate- 3.9	Scour around experimental run no. DB-4	59
Plate- 3.10	Scour around experimental run no. DB-8	59
Plate- 3.11	Scour around experimental run no. DB-10	60
Plate- 3.12	Scour around experimental run no. DB-13	61
Plate- 3.13	Scour around experimental run no. EA-2	61
Plate- 3.14	Scour around experimental run no. EB-4	62
Plate- 3.15	Scour around experimental run no. FA-3	62
Plate- 3.16	Scour around experimental run no. FB-2	63
Plate- 3.17	Scour around experimental run no. FB-3	63

Plate- 3.18	Scour around experimental run no. P2A-3	66
Plate- 3.19	Scour around experimental run no. PS2C - 3	66
Plate- 3.20	Spur model RA with 20% permeability at Roorkee in river Solani experimental	69
Plate- 3.21	Spur model RB with 40% permeability at Roorkee in river Solani	69
Plate- 3.22	Spur model RC with 60% permeability at Roorkee in river Solani	70
Plate- 3.23	Spur model RD with 80% permeability at Roorkee in river Solani	70



NOTATIONS

A	Constant
a	Model parameter
a_1	Grain size of smaller sieve available in close vicinity of required d_{50}
a_2	Grain size of larger sieve available in close vicinity of required d_{50}
a'	Empirical constant
a''	Constant depending on dia of sand grains
B	Flume/channel width
B_1	$B-b$
b	Length of spur
b'	Model parameter
b'_1, \dots, b'_n	Model parameter corresponding to different equilibrium time period
b''	Constant depending on setting velocity of sand grains
C_D	Coefficient of drag
C_d	Coefficient of discharge
C_v	Coefficient of velocity
D_t	Depth of scour below water after a time period t
D_1	$= y + d_s =$ total scour depth from water surface
d	Median grain size usually taken equal to d_{50}
d_p	Dia of pile
d_s	Depth of scour hole at any time below bed surface
d_{sc}	Calculated equilibrium scour depth for any spur

d_{scm}	Computed scour depth of permeable spur treating it as solid spur using Melville's approach
d_{se}	Equilibrium scour depth
d_{se1}, \dots, d_{sen}	Equilibrium scour depths due to discharges Q_1, \dots, Q_n
d_{so}	Observed equilibrium scour depth for spur in consideration
d_{st}	Depth of scour at any time
d_{50}	Median grain size of sediment
d_{90}	Grain diameter of the bed material at which 90% of the mixture by mass is finer
E	Error metric
F_r	Froude number
F_{r1}, \dots, F_{rn}	Froude number corresponding to different discharges Q_1, \dots, Q_n
g	Acceleration due to gravity
H	$= d_s / y$
H'	$= D_1 / y$
f	Lacey's silt factor
h	height of model above bed surface less by free board
h'	time period (hr.)
K	Function of coefficient of drag
K_d	Empirical coefficient for sediment grain size
K_F	Coefficient of scouring capacity of flow
K_g	Empirical coefficient for channel geometry
K_p	Coefficient dependent on sediment concentration
K_{qc}	Coefficient of the effect of increase in the specific water discharge at

the pile groyne head

K_s	Empirical coefficient for spur shape
K_t	Empirical coefficient for time ratio
K_v	Empirical coefficient for flow intensity
K_{yb}	Empirical coefficient for depth of flow and length of spurs
K_θ	Empirical coefficient for spur orientation
K'	Constant depending upon θ and position of spur dyke on curved bank
K'_2	$= 1.75/(d_{50} \text{ in mm})$
k	Model coefficient
k_1, k_2, \dots, k_n	Model coefficients
k'_m	Factor dependent upon shank slope
$k'_{\beta 1}$	Factor dependent upon contraction ratio
$k'_{\alpha'}$	Factor depending upon angle of groyne inclination
L_s	Width of scour hole
m'	Shank slope
m	meters
N	Number of runs
n	Model parameter
n'	Function of coefficient of drag (C_D)
n''	Function of fall velocity Reynold's no
n_1	Numerical exponent
p	Porosity
Q	Discharge cumecs
$Q_1 \text{ to } Q_n$	Different discharges which last for different time periods, in cumecs
q	Unit discharge/discharge intensity

q_a	Specific discharge of approaching flow
q_1	Discharge intensity at spur constriction
R^2	Co-relation coefficient
R_e	Reynolds number
r	Model parameter
r_b	Blockage ratio of piles and clear space between them
S	Slope of channel
S_p	Spacing of spur in series
S'_p	Clear distance between consecutive piles
t	Time at any stage of scour hole development
$t_{d1}, -t_{d2}, -t_{dn}$	Different time periods
t_e	Equilibrium time
$t_{e1}, -t_{en}$	Different equilibrium times corresponding to different discharges
t_{run}	Run time of the experiment
V	Mean approach velocity in m/sec
V_c	Threshold velocity for bed sediment entainment
w	Pier width or thickness of spur model
y	Mean depth of approach flow
$\alpha = \frac{B-b}{b}$	Opening ratio
α'	Angle which spur makes with the bank on downstream side
α''	A coefficient which is dependent upon the flow depth and size of the bed material

$$\beta = \frac{B-b}{.01b.p}$$

$\beta_1 = \frac{b}{B}$	Block ratio
γ_s	Specific weight of sediment
η	Function of fall velocity Reynolds no.
η_1	Function of coefficient of drag
η_2	Function of (w/b, F_r)
η_3	Function of (C_D , F_r)
μ	Dynamic viscosity
ν	Kinematic viscosity of water
θ	Inclination of spur to the direction of flow
ρ_f	Density of water
σ	Standard deviation
τ_c	Critical shear stress of bed material
$\tau_1 = \tau_b$	Bed shear stress
ω	Fall velocity of sediment
ξ	Shape parameter describing geometry of pier cross-section
$\Delta\gamma_s$	Difference in specific weights between sediment and water
$\Delta\gamma$	Difference in specific weight
Δy	Back water effect

INTRODUCTION

1.1 GENERAL

Rivers in alluvial plains are highly variable in their behaviour, due to which a considerable damage to their banks occurs, which in turn damages the property and human life situated near the riverbank. To avoid such damages, engineers have successfully used river training works. Among the river training measures, use of spurs or groynes is very common. These spurs may be impermeable or permeable in nature. Impermeable or solid spurs have found applications in different part of India, particularly in Indo-Gangatic plain. The work on solid spurs is extensively reported in literature as briefly described in Chapter 2. In fact, the Bureau of Indian Standard Code no. IS 8404-1976, IS 1808-1976 provide detailed design of solid spurs as per Indian practice. Contrary to a lot of literature on solid spurs, work on permeable spur has been limited. In recent years, due to economic consideration the emphasis has been placed for the construction of low cost spurs. In certain stretches of river Ganges as well as river Brahmaputra, such types of low cost spurs (Plates 1.1 and 1.2) have served the purpose satisfactorily and their use is thus gaining momentum. Based on the interaction with the field engineers, it was observed that the design of such spurs is very arbitrary and therefore, understanding of certain processes including the variation of scour around such spurs is highly desirable. Literature indicates that permeable spur are most effective on

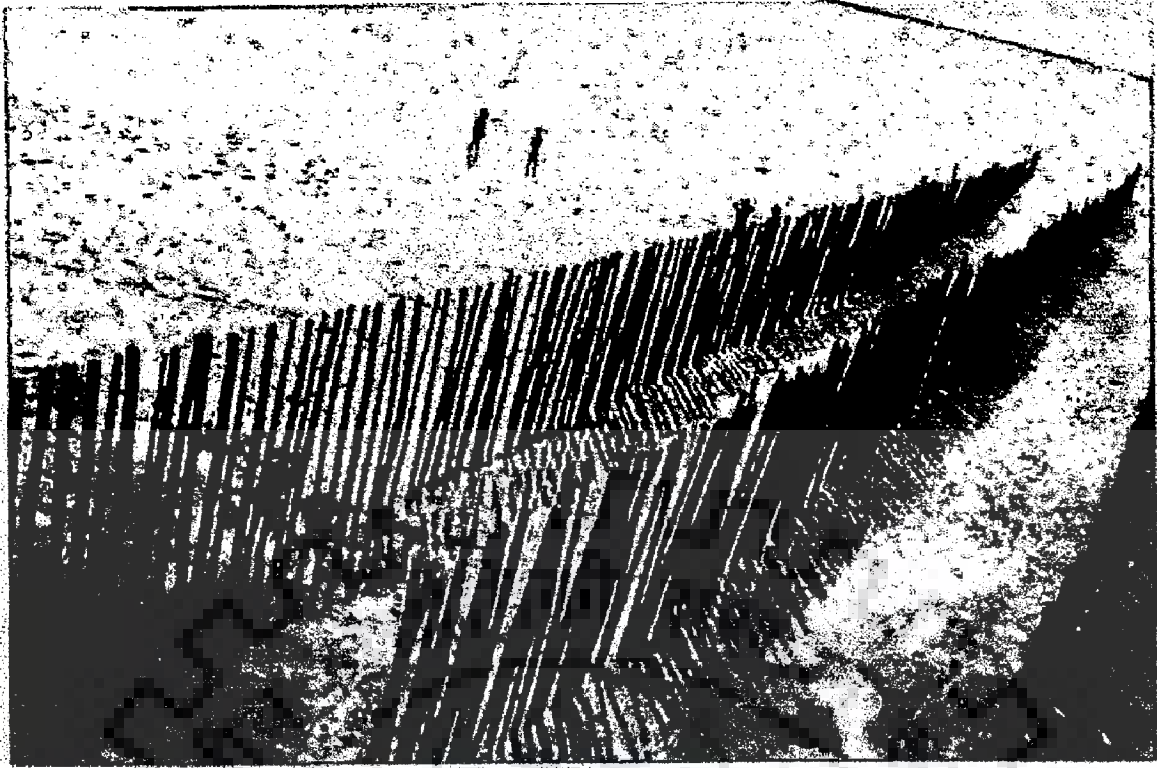


**PLATE- 1.1: PERMEABLE SPURS AT GUMI ASSAM
IN RIVER BRAHAMAPUTRA**

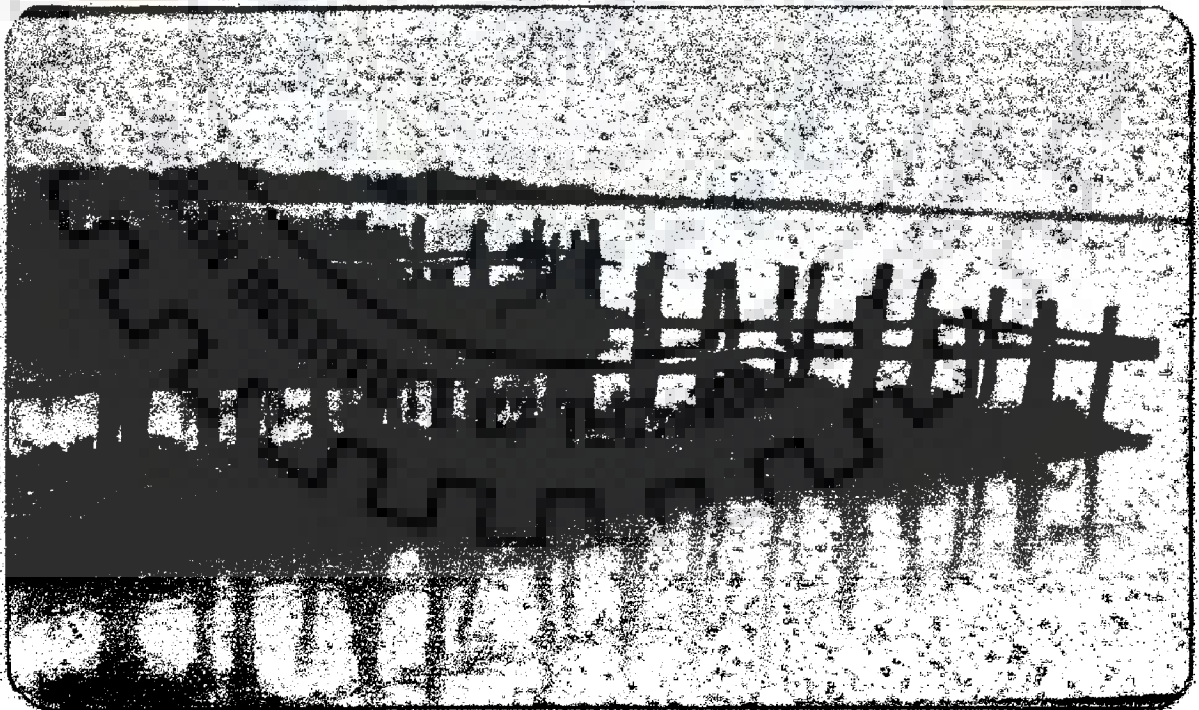


**PLATE- 1.2: PERMEABLE SPURS AT GURMUKHTESHVER
MURADABAD IN RIVER GANGA**

alluvial streams with considerable bed load and high sediment concentration (Przedwojski et al., 1995). Common type of permeable spurs are timber spurs, bamboo spurs, slotted spurs, etc. Some of these spurs are also filled with stone, sand bags, shrubs, etc. Although the work on permeable spurs can be traced to studies by Orlov (1951), Altunin (1962) etc., as referred by Przedwojski et al. (1995), there is lack of extensive studies on permeable spurs. It also appears from review of literature that detailed investigations regarding to different type of permeable spurs lack in literature. With this in background, the following objectives are set for the present study.

1.2 OBJECTIVES OF THE STUDY

- (1) To perform trial runs on different type of permeable spurs including slotted and pile spurs and identify permeable spurs which experience lesser scour at their nose.
- (2) Based on the processing of experimental data, identification of a particular type of permeable spur is to be done. For such a permeable spur, it is also envisaged to perform a large number of experiments.
- (3) To compare different approaches for representing scour around permeable spurs. This also includes the case of widely used method of scour estimation around bridge piers and abutments as proposed by Melville and Chiew (1999), Melville (1997).

- (4) Based on the analysis of data, identification of key variables influencing the scour phenomena is to be achieved. Also, suitable relationships are to be evolved for describing scour at the spur nose.
- (5) To study the temporal variation of scour during steady and unsteady flows. Based on the quasi steady state approximation of unsteady flow, the objective is to assess the applicability of principle of superposition in describing the temporal scour. This also includes the assessment of using lab based steady state equation of scour against field data.

1.3 ORGANISATION OF THESIS

To meet the above objectives, the present study is organized as follows:

Chapter 1 : It introduces the topic of investigation, underlying objectives and the layout of the thesis.

Chapter 2 : The literature review relevant to river training measures including solid and permeable spurs is presented. Also, different formulae to compute scour around spurs are listed. Certain case studies are also included to highlight the practical aspects of these spurs.

Chapter 3 : It provides the details of experimental program. It also contains pictorial representation of experiments done in different phases of the study. Phase 1 of the study deals with the trial experiments with different type of permeable spurs, while phase 2 and phase 3 experiments refer to experiments in the laboratory and field, respectively, for a selected type of permeable spur having minimum scour at the nose.

Chapter 4 : It presents the pattern of deposition and erosion of the alluvial bed in case of permeable spurs for certain selected experiments. It also contains the evaluation of different permeable models. The experimental results are processed to study the scour and identify the suitable spur with the minimum scour. Melville's approach is first of all extended to certain data sets collected at Roorkee and subsequently this approach is applied to identify the permeable spur with minimum scour.

Chapter 5 : It studies the performance of certain existing relationships for predicting scour around spurs. In addition, it also outlines an approach for the development of appropriate scour relationship.

Chapter 6 : Based on the lab-based relationships, the possibilities of using superposition principle to estimate scour in case of unsteady flow is explored. Towards this, the results in respect of temporal variation of scour are presented and used subsequently in unsteady state modelling.

Chapter 7 : It includes the results and discussion pertinent to various issues identified for the present study.

Chapter 8 : It summarizes the results of present investigation and outlines the main findings and provides framework for future work.

REVIEW OF LITERATURE

2.1 GENERAL

Rivers in alluvial plains are highly variable in their behaviour and to an average man often unpredictable. A placid stream during low flows may attain a tremendous fury during high stages. It may develop unforeseen meander, break through embankments, may attack towns and important structures, by pass bridges. In general such river behavior perpetrate havoc. River training structure guides and forces a stream into achieving some definite objectives and protecting some defined area. River training implies various measures adopted on a river to stabilize the river channel along a certain alignment with certain cross section so that consequently damage to and property adjacent to river banks is checked and river is stopped form altering its course. A variety of river training works including marginal embankment or levees, guide banks or guide bunds, groynes or spurs, submerged vanes, cut offs, pitching of banks, pitched islands, sills, closing dykes, longitudinal dikes, etc, have come into existence. Considering the huge costs involved in the construction of the river training works and their increasing demand in many reaches of rivers have focussed attention on permeable spurs. Due to its relatively lesser cost involvement and simple construction, permeable spur can be a cheaper method of bank protection. Therefore, present work deals with permeable spurs, a review of the same is considered in detail. Also, to assist the modelling of scour in permeable spurs, it is likely to get benefit from the literature on solid spurs. For this reason, certain

insight into different models of scour depth estimation is also presented for solid spurs.

2.2 CERTAIN SCOUR DEPTH MODELS ON SOLID SPURS

According to Liu and Skinner (1960), the scour hole increases indefinitely in the absence of sediment supply to the scour hole from the upstream. Garde et al. (1961) found that for all practical purpose, the maximum scour depth was obtained within 3 to 5 hours. This limiting scour depth is termed as the maximum scour depth. However, Melville and Chiew (1999) consider this maximum scour depth to fully develop after a duration in the order of days.

In almost all cases, the investigators found that maximum scour depth occurs at the nose of the spur. The scour hole was conical in shape on upstream side and elongated and shallower on downstream side (Garde et al., 1961). Based on review of literature on scour, sediment transport and flow resistance (Bathurst, 1978; Jain, 1981; Barbe et al., 1992; Ab. Ghani and Nalluri, 1996) associated variables with the scour depth can be summarized as

- (i) Variables describing geometry of the channel and spur dike, i.e., the width of channel (B), length of the spur dike (b) and angle of spur dike (θ)
- (ii) Variables describing the flow, i.e., mean velocity (V), depth of flow (y), total scour depth (D_1) and depth of scour hole, d_s , width/length of hole L_s .

- (iii) Variables describing fluid flow, i.e., mass density of water (ρ_f), difference in specific weight of water and sediment size ($\Delta\gamma_s$), dynamic viscosity (μ) and kinematic viscosity (ν).
- (iv) Variables describing sediment, i.e., median size (d).

Single solid spurs have been studied by several researchers giving relationships for scour depths, lengths of the spurs, spacing etc. These attempts have been made with the help of small-scale hydraulic model studies but these models do not have the same efficacy against the field observations. These formulae are poorly verified because they deal with simple form of groyne, i.e., a thin rectangular obstacle. Some of these formulae as well salient features of certain studies are described below.

Lacey (1920) gave approximate values of maximum depth of scour at a channel bend by relating these to the depth formula for regime conditions in a straight channel, i.e.

$$D_1 = 0.473 \left(\frac{Q}{f} \right)^{1/3} \quad (2.1)$$

where, D_1 = Lacey's regime depth (inclusive of scour) for a straight channel, Q = total discharge, f = Lacey's silt factor $= 1.76 \sqrt{d}$, where d = median diameter of bed material in mm. Lacey used a straight channels of regime condition which are not actually present in nature, also "d" taken is only median diameter, of a particle. He has not included other important parameters.

Khosla (1936) gave the following equation for the scour depth, D_1 in terms of discharge intensity q , and the silt factor f .

$$D_1 = 0.9 \left[\frac{q^{2/3}}{f^{1/3}} \right] \quad (2.2)$$

Inglis (1949) conducted experiments on bridge piers at Central Water Institute and Research Station (CWPRS, Poona), in an alluvial bed of sand with median diameter of d equal to 0.29 mm. He suggested that the effect of bridge piers, is to deflect current like a bend and therefore, proposed that maximum depth of scour, for a bridge pier, is also proportional to Lacey's regime depth.

He related maximum scour depth, D_1 , below water surface to the unit discharge q and pier width b , akin to spur length across flow as follows:

$$\frac{D_1}{b} = 1.70 \left[\frac{q^{2/3}}{b} \right]^{0.78} \quad (2.3)$$

He suggested a coefficient to be used with Lacey's regime depth D_1 for scour at the nose of spur dikes. He gave the value of scour at the nose of spur ranging from $1.7D_1$ to $3.8 D_1$, the coefficient depending upon the severity of river curvature. Besides, he suggested the value of coefficient depends on the length, angle and the position of the spur with respect to the river curvature. His basic study was on bridge piers and it assumed the same to be valid for spur dikes. But the shape and structure of spur is all together different from piers.

Ahmad (1951 part-1, 11) showed that a single spur can protect length between 3 to 5 times the spur projections. But when lengths longer than these are required to be protected, a combination of spurs has to be employed at such distances apart that the scour formed at the nose gives a continuous channel and the bank between the spur is protected from the main flow. He concluded after a series of experiments on channels with different radii of curvature, that S_p/b should have a value of about 5 where $S_p =$

spacing of spur in series and b = length of spur. He also concluded that for protecting larger lengths than two spurs can protect, the additional spur with $S_p/b = 5$ is efficacious.

Kilner (1952) conducted experiments in laboratory. Using two sizes of sand (0.19 mm and 1.68mm), he observed that the total depth of scour for fine sand is twice the total depth of scour for coarse sand.

Ahmad (1953) investigated the problem of scour with dimensional analysis approach . He conducted experiments with 0.354 mm and 0.695 mm sediment sizes to study the effect of discharge intensity, sediment size, flow concentration and the angle of spur dike on the scour depth and scour pattern around spur dikes. His limited study lead him to get the expression as:

$$y + d_s = D_1 = K'q_1^{2/3} \quad (2.4)$$

Where, y = depth of flow, d_s = depth of scour below bed level, q_1 = discharge intensity at the spur constriction, K' = constant depending upon angle of inclination of the spur and the position/location of the spur dyke on the curved bank.

For the rate of development of scour he gave an exponential relationship as follows:

$$\frac{D_t}{y} = (1 - b'' e^{-a''t}) \quad (2.5)$$

where: D_t = depth of scour below water after a time period t , a'' and b'' = constants depending on the diameter of sand grains and its settlement velocity respectively, t = time period of forming of scour.

He observed that the rate was much more in finer sediment than in coarser sediment. His studies were more explicit than initial studies but only two sizes of the sediment were taken into consideration. He did not consider secondary flows due to the bank curvatures and other parameters like Froude number, Reynolds number, drag coefficient, etc. His equation is valid for particle size range of 0.2 mm to 0.7 mm and depth of flow exceeding 0.06 m.

Altunin and Buzunov (1953) gave the following equation for maximum scour D_1 for a single spur

$$D_1 = k'_{\alpha'} k'_{\beta_1} k'_{m'} y \quad (2.6)$$

In this equation, $k'_{\alpha'}$ = factor dependent upon angle of groyne inclination, α' , where α' is the angle which spur makes with the bank on downstream side, k'_{β_1} = factor dependent upon contraction ratio, $\beta_1 = b/B$, b being the length of the spur and B channel width, $k'_{m'}$ = factor dependent upon shank slope, m' . His equation is valid for : (i) $30^\circ \leq \alpha' \leq 150^\circ$ (ii) $0 \leq m' \leq 3$, (iii) $0.1 \leq \beta_1 \leq 0.8$.

Garde (1953) and Garde and Subramanya (1960) studied the problem of scour around spur-dikes and piers. These investigations were conducted with 0.29 mm and 0.45 mm bed material. Spur dikes with different opening ratio, i.e. α , and piers of different shapes were under consideration. In case of spur dikes, their experimental data indicated the adequacy of Froude number and the opening ratio to define the flow parameter and the geometry of the spur respectively. They also studied the scour and its geometry. i.e., geometry of scour hole around the spur dikes.

Garde et al. (1961) conducted experiments on scour studies with sediment size of 0.29mm., 0.45mm., 1.00 mm and 2.25mm and opening ration of 0.9, 0.835, 0.667

and 0.530 to study the effect of sediment characteristics on scour. According to them, in almost all the cases the maximum scour depth occurred at the nose of spur dike.

The spur hole upstream of the spur dike was conical in shape, whereas downstream it was elongated and had a shallower slope. A deposition bar was formed adjacent to spur dikes on the downstream side in all cases. It was found that the width of the scour hole, L_s in front of spur dike has no consistent correlation with the maximum scour depth d_s . The ratio of $\frac{L_s}{d_s}$ varied from 1.8 to 5.00 and no systematic correlation existed either with the opening ratio, α , or with the size of the bed material, d . The dimensionless scour depth obtained was

$$\frac{y + d_s}{y} = K \frac{1}{\alpha} F_r^{n'} \quad (2.7)$$

in which K and n' are functions of C_D . They also presented curves for variation of K and n' with respect to C_D .

Neill and Chaplin (1962) in a discussion on above studies of Garde et al. (1961) has indicated that drag coefficient C_D is not a satisfactory measure of sediment property. He argued that C_D is constant for material larger than 1.5mm size. If C_D were a valid criterion, it would follow that above 1.5 mm size of sediment, scour depth would be independent of size which cannot be true.

Laursen and Toch (1953, 1956) and Laursen (1963) observed that the equilibrium depth of scour mainly depends on the flow depth for a given size of flow obstruction, e.g, bridge pier or abutment and that the flow velocity does not have any significant effect on scour depth.

Sastry (1962) studied the effects of spur dike inclination on scour characteristics. He used a spur dike with inclination θ varying from 30° to 150° with

upstream side. He used a bed material of 1mm with a constant opening ratio of 0.833. He proposed a dimensionless relationship for scour depth similar to equation given by Garde (1961) and found the scour depth to increase with angle of inclination of spur dikes.

Ramu (1964) studied the effects of sediment size on scour. He found that the effect of sediment characteristics can be better expressed by the fall velocity Reynolds number, $R_e = \frac{\omega d}{\nu}$, where ω = fall velocity of sediment, ν = kinematics viscosity of the fluid and d = median diameter of the sediment. Ramu gave a dimensionless equation in the form as

$$\frac{D_1}{y} = A \eta \frac{1}{\alpha} F_r^{n''} \quad (2.8)$$

where A = constant, having value of 4.

He presented curves showing relationship of η and exponent n'' respectively with Reynolds number as a function of fall velocity Reynolds number. He also confirmed the previous notion of Garde et. al. (1961) of the Froude number of flow to be a more suitable parameter for defining scour depth and the geometry of scour hole, as well, that of spur dike, than discharge intensity q_1 at the constriction as an adequate parameter for describing scour. Further, Ramu found that maximum scour shifted to the root of the spur on the upstream. This must be due to the presence of secondary vortex on the upstream, which may prove dangerous to the stability of spur itself.

Paintal and Garde (1965) worked on the effects of inclination and shape of obstruction on local scour. They concluded that maximum scour depth around an obstruction increased with the increase in coefficient of drag of its nose as well as

with the increase of angle of inclination of obstruction to the direction of flow, which was in tune with the findings of Sastry (1962).

Tyagi (1967) studied the effects of specific gravity of sediment on scour. He varied the constriction ratio from 0.10 to 0.47 and used sediments in the replacement as plastic and coke having median diameter of 2.48 mm and 4.05mm. Tyagi proposed the following relationship

$$\frac{V}{\left[\frac{\Delta\gamma_s d_s}{\rho_f} \right]^{1/2}} = 2\beta_1^{-1/6} \left[\frac{y}{d} \right]^{-1/2} \quad (2.9)$$

where the symbols have their usual meaning. $\beta_1 = b/B =$ block ratio

Garde and Chandra (1969) suggested the value of b/B to be fairly small so as to cause as little interference with regime of river as possible. They also recommended that the spur should make an angle of 95° to 110° with the bank on upstream side. They also proposed curves for determination of protected bank length due to single spur. In case more than one spur is required, they proposed to adopt Ahmad's recommendation (1951).

Komura (1971) tried to find general scour at a live bed, i.e., dynamic equilibrium state using continuity equation for flowing water, the equation for sediment transport, the continuity equation for sediment transport and Bernoulli's equation of energy. As a result he developed following equation for relative depth of scour along the constricted portion

$$\frac{d_s}{y} = (1 + 1.2F_r^2) \left[\left(\frac{B}{B_1} \right)^{2/3} - 1 \right] \quad (2.10)$$

where $B_1 = B - b$

Gill (1972) highlighted various significant points related to scour, e.g, the effect of the size of bed material on equilibrium depth of scour and on the rate of development of scour. He also suggested whether it is necessary to distinguish the scour caused by clear water flows from that caused by flows involving general bed load. He showed how the rate of scour depth is different in the two cases. He showed that total scour depth D_1 is independent of flow depth y . He gave the following modified form for local erosion around spurs.

$$\frac{D_1}{y} = \alpha'' \left(\frac{B}{B_1} \right)^{6/n_1} \left\{ \frac{1}{\left(\frac{B}{B_1} \right)^{1/n_1} \left(1 - \frac{\tau_c}{\tau_1} \right) + \frac{\tau_c}{\tau_1}} \right\}^{3/7} \quad \text{where } B_1 = B - b \quad (2.12)$$

$$1 - \frac{\tau_c}{\tau_1} = 0 \quad \text{for } \frac{\tau_c}{\tau_1} \geq 1 \quad (2.13)$$

where τ_c = critical shear stress of bed material. τ_1 = bed shear stress upstream of constriction. n_1 = numerical exponent, α'' = a coefficient which is dependent upon the flow depth and size of bed material, where

$$\alpha'' = 8.375 \left(\frac{d}{y} \right)^{0.25} \quad (2.14)$$

In this equation, d = particle size or grain size in meter and y is flow depth in meter.

It was also observed that the rate of scour development for fine sand remains higher than that of the coarse sand. Depth of equilibrium scour is affected by the depth of uniform flow upstream of spur location. The combined effect of the bed material and flow depth has been empirically formulated as described above. The depth of maximum scour is at the threshold of movement.

Neill (1973, 1980) gave the equation for maximum scour depth D_1 for a single spur.

$$D_1 = 2.1 \text{ to } 2.75 \left[\frac{2.5q^2}{d^{0.318}} \right]^{0.333} \quad (2.15)$$

The above equation is valid for particle range size of $0.1 \leq d_{50} \leq 200$ mm.

Todten (1975) (after Bogmar et al., 1988) wanted to find the basic characteristics of the flow pattern around groynes in order to use them in mathematical models. Two factors were considered very important: first the geometry of the field of separation and second the dissipation of energy. The basis of his theory was the laws of stream flow in the plane.

Michiue et. al (1984) used the Meyer- Peter and Muller's formulae for finding general scour at a live bed, i.e. dynamic state when the rate of sediment supply into contracted region is greater than zero, which is dynamic equilibrium state. He came out with the formula

$$\frac{d_s}{y} = \left[\left(\frac{B_1}{B} \right)^{-4/7} - 1 \right] + (0.5F_r^2) \left[\left(\frac{B_1}{B} \right)^{-6/7} - 1 \right] \quad (2.16)$$

Przedwojski et at. (1995) have compiled various formulae for scour depth estimation at a single spur in terms of two dimensionless terms, i.e.

$$H' = \frac{y + d_s}{y} = \frac{D_1}{y} = \frac{\text{Total depth of scour from the water surface}}{\text{Depth of flow}} \quad (2.17)$$

and relative maximum depth of scour hole

$$H = d_s / y = \frac{\text{Depth of scour hole from the bed of river}}{\text{Depth of flow upto the initial bed of river}} \quad (2.18)$$

It is not considered appropriate to describe all these formulae. However, it has been intended here to provide some information related to functional form of scour relationships.

In addition to the above studies, significant work on scour has been done by Melville and coworkers (1999). As Melville's approach is used in this study, details of this are given in Chapter 4.

2.3 PERMEABLE GROYNES

These allow some restricted flow of water to pass through them. These types of spur groynes partially obstruct the flow and slacken it to cause deposition of sediment carried by the river. Therefore permeable spurs are classified as sedimenting or silting spurs. They are best suited for the type of rivers which carry considerable amount of sediment in suspension, e.g., alluvial rivers in plains. Permeable groynes are most effective on alluvial streams with considerable bed load and high sediment concentration, which favours rapid deposition around the groynes (Beckstead, 1975; Alam and Faruque, 1986).

As the sediment accumulates between the groynes/spurs in series, the foreshore becomes more or less permanent soil such that there is no need to use any other material for its protection. However, in the rivers which carry relatively clear water, the action of such permeable spurs is to slow down the flow, thereby dampen the erosive strength of the current and thus also to prevent the local bank erosion upto some distance upstream and downstream. Due to above mentioned factors, United

Nations Economic Commission For Asia And The Far East (1953) recommends permeable type of groynes to be spaced further apart than the solid types.

Common types of permeable groynes/spur dikes are

- 1) Tree types of permeable, i.e. timber groynes/ bamboo groynes. Fig. 2.1 shows typical section of permeable bamboo groyne used in Bangladesh after Alam and Faruque (1986).
- 2) Pile groynes with wooden piles, RCC piles or sheet piles
- 3) Stone filling in balli crates. Stone filling in brushwood and stone filling in wire crates.
- 4) Slotted spurs.

When closely packed and tempered, there is generally no tendency for scour around the nose of the groyne or for undermining of piles with properly designed, constructed permeable spur/groynes. However, the limitation is that when debris gets collected upstream and the groyne becomes sand bound, it may function almost like an impermeable groyne. To guard against excessive scour occurring under such conditions, it is desirable to protect the bed both upstream and downstream of the groyne and around the nose with a 0.9 m thick stone apron over a width of 3m along the shanks and 6 m along the nose.

2.3.1 Slotted Spur

A slotted spur is a gabion construction with gaps in its length projecting from the river bank. Stone masonry check or piles has also been used. It is claimed that whereas an ordinary spur protects a river bank of about 3 times the spur length, a slotted spur protects 10 to 20 times its length. This type of spur was used with success on Ingury river in Georgia and Darya at Charzhro in the USSR (manual CBIP-204).

The dimensions adopted for spur length were 18 m, angle of spur to bank line 90° , angle of slots 30° to 45° , ratio of length of slot to its width in direction of flow 3 to 5. The flow velocity was 2 to 6 m/s.

2.3.2 Advantages And Disadvantages of Permeable Groynes

The advantages of permeable groynes may be summarized as below

- 1) They are relatively cheap because they need only temporary or semi permanent construction.
- 2) As small quantity of stones are required for construction of permeable groynes, they are specially suited for places where stones are scarce.
- 3) Permeable groynes are more effective in the regulation of river courses or in the protection of banks especially in a silt laden river than the impermeable spurs.
- 4) There are no serious eddies or scour holes in case of permeable spurs as in the case of solid spurs because the flow discharge does not change abruptly like in solid spurs.
- 5) In case of deep and narrow rivers, where depth are considerable, solid spurs become expensive and may cause undesirable flow conditions. But when permeable spurs are employed, they do provide necessary bank protection without much cost and serious eddy and scour formation.
- 6) The permeable spurs may be spaced farther apart than solid spurs.

For bank protection and training of rivers usually non-submerged spurs are used. But sometimes submerged groynes are also to be used. Usually in case of deep

rivers with considerable depth, submerged spurs are employed. Submerged spurs may be solid or permeable spurs. However, submerged permeable spurs are preferred to submerged solid spurs because submerged solid spurs create lot of turbulence and eddy formation whereas former does not create any of the two of so much intensity. Under submerged conditions, solid groynes are susceptible to severe erosion along the shanks resulting from flow over the top of the groyne. Permeable groynes are better suited to submerged conditions. Where deep scour has occurred in the river bed, submerged spurs are used as curative measures. Generally such submerged groynes are known as submerged sills or submerged dikes and are considered as a separate type of river training works.

The main disadvantage of permeable groynes is that they are not strong enough to resist shocks and pressure from debris, floating ice and logs. They are, therefore, unsuitable for upper reaches of rivers.

2.4 STUDIES ON PERMEABLE SPURS

Orlov (1951), on the basis of model tests with fine sand of $d_{50} = 0.14$ mm, formulated an expression for maximum depth of local scour at the head of a pile groyne.

$$d_s = 50r_b^{1.5} \frac{V^2}{2g} \quad (2.19)$$

where $r_b = \frac{d_p}{(S'_p + d_p)}$ = blockage ratio of piles and clear space between them;

d_p = diameter of piles, S'_p = clear distance between consecutive piles; V = mean cross-sectional velocity in river before construction of groyne. The definition sketch of a

pile Groyne after Orlov (1951) is given in Fig. (2.1). Orlov formula is valid for the first permeable groyne on a straight reach.

Altunin (1962) stated that

$$d_s = K'_2 \Delta y \quad (2.20)$$

where $K'_2 = 1.75 / d_{50}$, with d_{50} in mm and Δy is the back water effect of groyne.

The final equation proposed was as follows

$$d_s = \frac{8.75}{d_{50}} \cdot \frac{b}{B} r_b^{1/2} \frac{V^2}{2g} \quad (2.21)$$

Mukhamedov, et al. (1971) suggested that maximum depth of scour at the head of a pile groyne (D_1) can be calculated using

$$D_1 = K_F \left[\frac{K_{qc} q_a}{3.7 K_p d_{90}^{0.25}} \right]^{0.8} \quad (2.22)$$

where K_F the coefficient of scouring capacity of flow, K_{qc} = the coefficient for the effect of increase in the specific water discharge at the groyne head : K_p = the coefficient dependent on sediment concentration , d_{90} = grain diameter of the bed material at which 90% of the mixture by mass is finer, q_a = specific discharge of approaching flow.

Gole et al. (1975) conducted experiments on single solid and slotted spurs with mobile bed of sand of median size 0.30 mm in both straight as well as curved reaches. They concluded the following

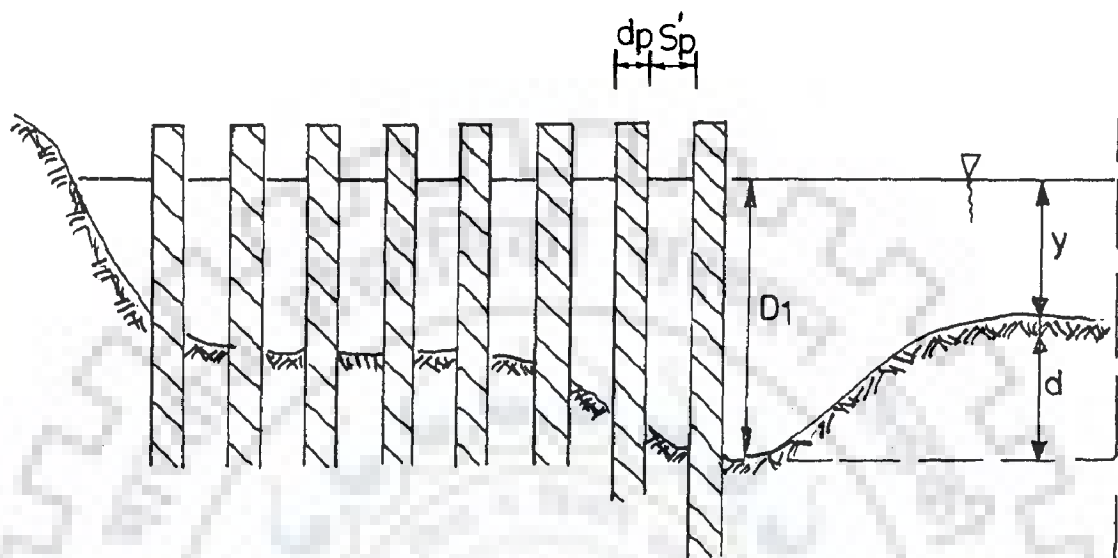


FIG. 2.1 DESCRIPTIVE SKETCH OF SCOUR AT PERMEABLE (PILE) GROUYNE

- (i) In a straight reach the length of bank protected by a slotted spur on the upstream side was 31.5% longer and on downstream side 37.5% longer than those of solid spurs.
- (ii) In the case of curved channel, the length of bank protected was however 33% shorter with slotted spurs than the length protected by solid impermeable spurs. On the other hand on the downstream side, the length protected was 107% longer giving an overall performance superior to that of solid conventional spur, the total length of bank protected being 68% longer than that with the solid impermeable spur that is with the help of slotted spurs.
- (iii) In a straight reach maximum scour depth at the nose of slotted spur is 34.38% and in curved banked reach 27% less than that obtained with solid spur.
- (iv) Visual observation regarding the flow pattern in case of both the spurs revealed that the eddies downstream of the solid spur were stronger than the eddies observed with the slotted spur.

Subramanya and Gangadharaiah (1989) studied solid and slotted spurs for scour in mobile bed and for imprint flow pattern in rigid bed. Their conclusions were as follows:

- (i) Slotted spurs have favourable downstream deposit pattern for both coarse and fine sands.
- (ii) The slotted spur in coarse sand causes smaller magnitude of the maximum depth of scour than a corresponding solid spur. An optimum permeability $p=0.40$ is suggested for such slotted spurs.

- (iii) In fine sands the presence of slots does not have any influence on the maximum depth of scour.
- (iv) In coarse sand bed rivers, the slotted spurs used in multiple configurations appear to have specific advantages over a corresponding solid spur dike arrangement.

Sharma (1991) conducted wind tunnel experiments on solid and porous fences fixed on the tunnel floor. These are akin to spurs across rivers. His measurements included the turbulence intensities in the longitudinal direction. His results indicate that the turbulence level in the wake behind porous fence is less than that in the wake behind solid fence. This supports the earlier concepts that permeable spurs function better in the presence of fine suspended sediment because of the lower level of turbulence behind them.

Singh (1993) studied the comparison of solid and permeable spur in series. In his study, he kept blockage ratio of spurs and their angle of inclination with the bank same in all cases, but the permeability and the spacing of the spurs were varied about 50% and 4 to 8 times the spur lengths, respectively.

He carried his experiment in a tilting flume, 0.6 m wide 0.5 m deep and 8m long at a slope of 1 in 1000. A sediment of 0.525 mm median size and 1.18 standard deviation was used under live bed condition of approach flow. Sediment was supplied manually into the flume at the transport capacity of the flow.

He has further tested the formula given by Ramu (1964) for prediction of scour and recommended it for further use. He confirmed that the surface flow velocity near the bank varied very gradually in case of single permeable spurs, thus, protecting longer lengths of the bank which suggests their possible better performance in alluvial

river with fine sediment load. Also in his studies he found for the spurs in series, that the scour depth around the first spur is almost equal to that of the single isolated spur, that means the presence of down stream spurs has little effect on the first spur.

He suggested that three spurs in series behave as a single unit, if the scour around the third spur is less than or equal to that around the second spur. And if the scour around 3rd is more than that at 2nd spur then they behave independently. He suggested that a spacing of $> 4b$ has been found suitable for all spurs. This notion is also an old one and needs more study for different conditions of bed load flow and discharge.

2.5 CERTAIN OBSERVATIONS FROM FIELD

CBIP Manual (1989) contains case studies illustrating the application of permeable spurs at various locations in India and abroad. As per this report, the left bank of the Ganga river near Mansi railway station was protected by crated stone spurs. Similarly, permeable bund was used to achieve diversion of Beas river at Govindwal in Punjab. Also timber pile permeable spurs have been practiced for protection of Dibrugarh town in Assam. Similarly, pile spurs have been used for the protection of Dhubri town in Assam. Thus, it is obvious that use of permeable spurs is not new in Indian context.

2.6 CONCLUDING REMARKS

From the preceding review of the literature, it could be seen that good deal of research was devoted to solid spurs which had been widely deployed in the past

decades. However, of late the construction costs of these solid spurs and groynes have registered a sharp hike due to corresponding rise in the material costs of stones, wire nets and earth fill especially in the Indian context, where numerous areas are awaiting bank protection measures. In sharp contrast to the solid groynes, the permeable spurs are highly cost-effective as borne out by the actual field experiences in India and in many other countries. While solid spurs function by deflection of flow away from the affected bank, permeable spurs primarily operate by slowing down and dissipating the erosive currents including sedimentation.

So far not much research has been conducted on the various aspects of permeable spur notwithstanding its deployment in many real life situations with considerable degree of success. In the above context, it could be realized that in-depth research needs to be undertaken on the permeable spur notably with regard to the extent of scour magnitude and its impact with regard to varying spur permeability.

In this work it is envisaged that, the above two important aspects having a close bearing on the effective design of a permeable spur, be taken up for intensive research endeavour involving both lab and field experiments in a compatible manner.

EXPERIMENTAL PROGRAMME

3.1 INTRODUCTION

From the preceding Chapter, it is apparent that a variety of permeable spurs have come into existence. It is obvious that certain preliminary studies on the performance of permeable spurs are necessary in order to identify the spurs with minimum scour at the pier nose. With this in view, the experimental programme was organised in three phases. In the first phase, experiments were performed in a 50cm wide mobile bed flume using 21 nos. of different physical models of permeable spurs of two blockage ratios with varying degrees of permeability. In this phase of laboratory experiments, primarily it was endeavoured to gain an insight into the physical behaviour of different types of models for assessment of a suitable one for the intensive lab experiments to be followed subsequently. In the second phase of experiments conducted in a 50cm wide mobile bed flume of 11m length, detailed experimentations were undertaken on the pile model configurations which were decided on the basis of results in the preceding phase. The flow conditions, bed material, degree of spur permeability and the channel blockage ratios were realistically varied in the second phase of experiments which yielded the desired experimental data for undertaking the required analysis of data. In the third phase of experimental study, the chosen configurations of laboratory models of pile spurs were faithfully reconstructed with identical permeabilities in the Solani river near Roorkee to elicit actual field informations on their behaviour.

The main aim of this study is to investigate the scour depth and deposition patterns around spur models considering permeable spurs with different percentages of permeabilities which are founded in uniform sediment and subjected to clear water conditions. Therefore, experiments were conducted to examine the effects on scour depth and deposition pattern of a number of parameters including flow velocity, flow depth, discharge intensity, spur length and their shape and sediment size, in clear water conditions. Some of the experiments were conducted to supplement existing data for particular effects, e.g. on solid spurs, while other experiments were designed to produce comprehensive data sets for the effect of parameters either not previously investigated or for which only very limited data were available. The experiments were accomplished using two different laboratory flumes which are described in the subsequent sections. With this background, the details of the experimental programme are presented below.

3.2 LABORATORY FLUMES AND OTHER ACCESSORIES

3.2.1 Flume Used In First Phase

This 50 cm wide, 350 cm long flume is fitted with an inbuilt upstream tank along with a separate down stream tank. All three parts of the flume are made up of painted mild steel. The down stream tank is attached with a pump which is 10HP (horse power) in capacity. 10cm diameter pipes connect this pump to the upstream tank of the flume which is deeper than the flume in 1st 30 cm length. The width and depth of the upstream tank are 50 cm and 100 cm respectively while the width and depth of the flume are 50 cm x 50 cm respectively. This flume has side walls made up of transparent perspex sheet in 240 cm length up to 25 cm before the tail gate.

An evenly perforated perspex sheet of one cm dia holes and 1cm thickness separates the upper tank from the channel portion of flume at 50 cm distance from the upstream face of the up stream tank. The purpose of this sheet is to stabilize the flow and make it uniform. The upstream pipe drops the water right at the base of the upstream tank to minimize all disturbances.

A V-notch is fixed in the down stream tank for discharge measurements. The down steam tank is 90 cm wide, 90 cm deep, 250 cm long internally. The tail end of the flume is placed roughly 15 cm above the top of the upstream end of the tank. This tank is bifurcated into two stories in first 160cm length on the flume end side, the depth of the upper portion being 40 cm. A V-notch is fixed at the end of upper storey with its vertex placed 15 cm from the base of upper portion at the end of upper portion. A baffle wall is placed to curb all the disturbances of the water falling from the flume into the tank. It is 90cm away from upstream end of the tank. In the bottom portion is placed the opening of the pump close the base of tank, 5 cm above it.

The flume is mounted on two R.C.C. blocks 65 cm in height from the floor, 66 cm wide and 39 cm in length. A threaded rod is grouted in the lower-end block. The lower end of the flume is mounted over this threaded rod with the help of a very strong nut with handles in such away that the lower portion of flume could be moved up or down max. of 4% for creating the desired slope. The plan of this flume is given in Fig. 3.1

Two railings are mounted on the top edges, i.e. left and right sides of the flume over which are placed all the required equipment for measurement of velocity, depths, and levels, etc. Pitot tubes and pointer gauges are placed on separate graduated trolleys. Both the railings were graduated in cm with permanent marker pens and with paint.

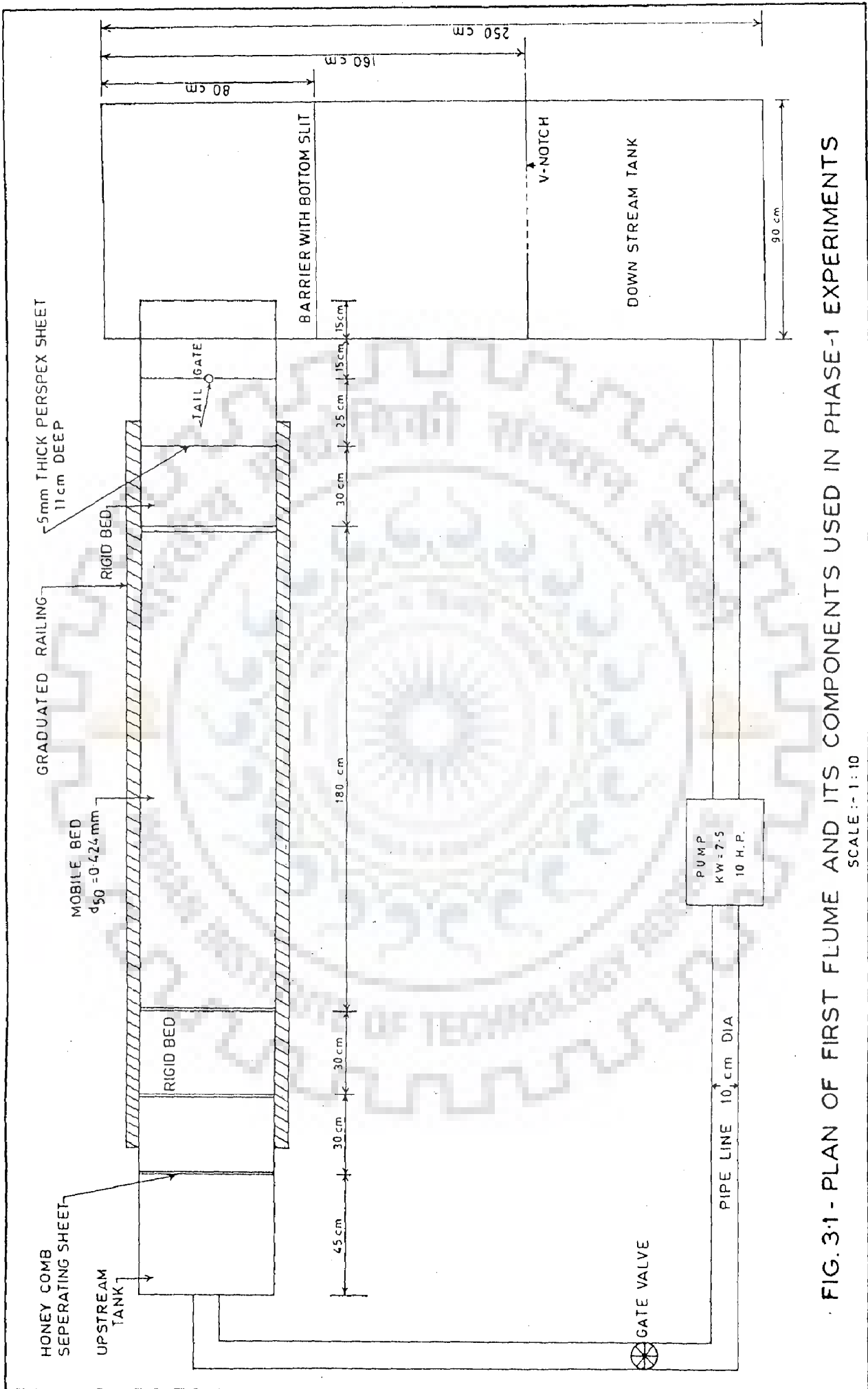


FIG. 3.1 - PLAN OF FIRST FLUME AND ITS COMPONENTS USED IN PHASE-1 EXPERIMENTS
SCALE :- 1 : 10

For clear water experiments, the working section of the flume commenced 30 cm away from the evenly perforated perspex sheet. Three energy dissipaters were placed a little distance from the sheet in a triangular fashion in this 30cm distance, to make the flow more evenly distributed and break its turbulence and extra energy.

After that 30cm long and 11cm thick, bed of bricks and gravel are placed. This brick bed is covered with coarse sand which is glued to it with cement slurry in order to make the roughness coefficient of this section same as that of subsequent test bed section. This bed was bounded by 11 cm solid perspex sheets on both upstream face and down stream faces.

Subsequent to this section, was introduced the test section of uniform sand bed of grain size $d_{50} = 0.424$ mm, 180 cm in length and 11cm in depth. The depth of the section was calculated on the basis of the method given by Melville (1997) for calculating equilibrium scour depth. Subsequent to this section was placed same arrangement of bricks, gravel with the sand cover over 30 cm length, as was placed prior to sand bed section

3.2.2 Flume Used In Second Phase

The second flume used was eleven meter long tilting flume, made of mild steel with side walls made of transparent perspex sheet. Flume has an in-built up stream tank of 40cm x 90 cm x 115cm dimensions. The depth of flume is 50 cm and the width is 50 cm. Diagrammatic scheme is given in Fig. 3.2. The bed of flume is supported on angle iron sections the lower ends of which are connected to a shaft, placed lengthwise parallel to the central portion of flume below it. Shaft is movable horizontally backwards and forwards with the help of a gearbox and electric motor such that if the shaft moves towards the direction of flow the front portion of flume

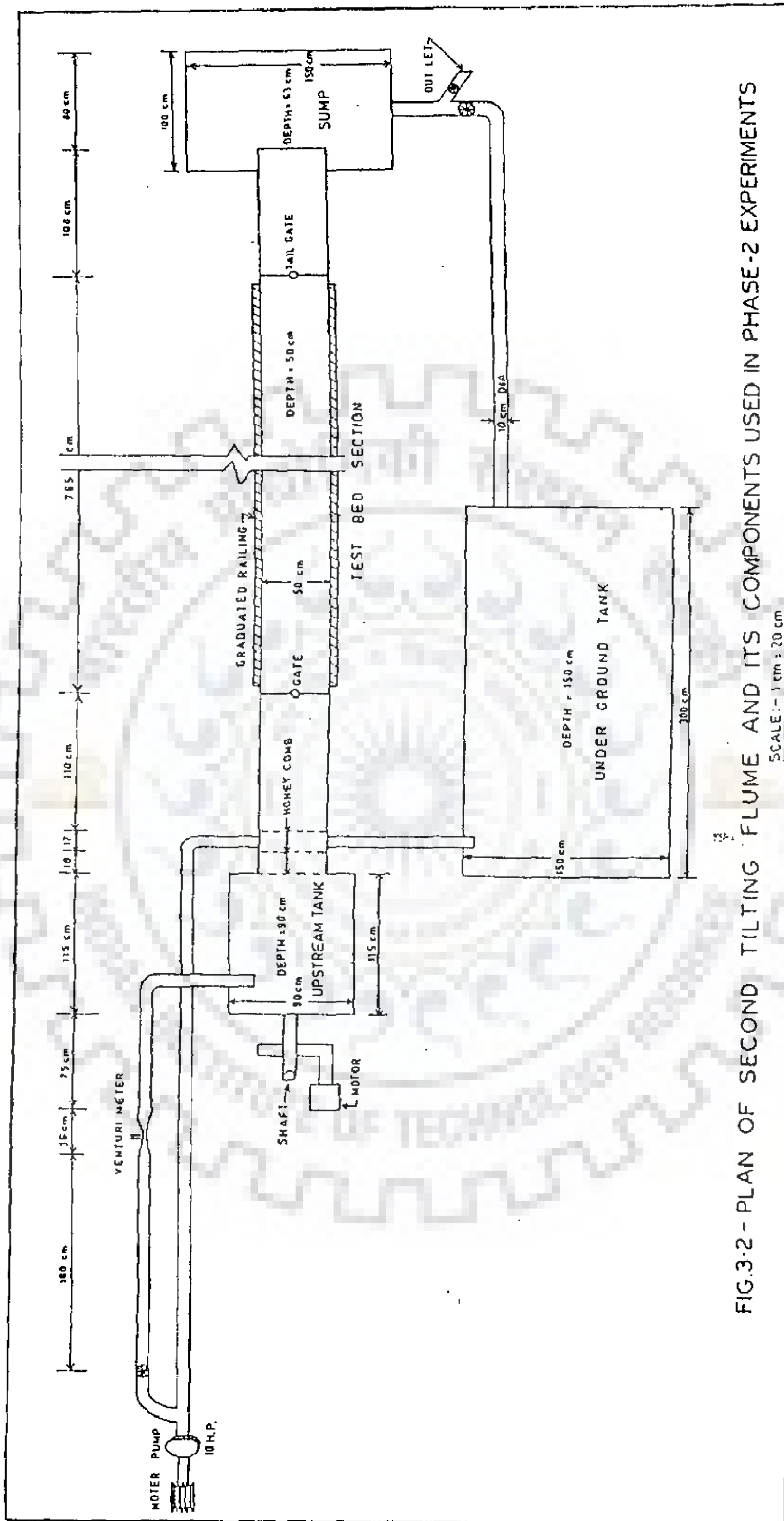


FIG.3.2 - PLAN OF SECOND TILTING FLUME AND ITS COMPONENTS USED IN PHASE-2 EXPERIMENTS

SCALE :- 1 cm = 20 cm

moves upwards and lower portion moves downwards and vice versa. This is the mechanism of changing the required slope. The water flowing in the flume falls into a sump which is connected to an underground tank of 1.50 m x 1.5 m x 3 m dimensions. From the under ground tank water is lifted with the help of a pump of 10 HP capacity. 10 cm diameter pipes carry water from the underground tank to the up stream tank. The discharge is regulated with the help of a gate valve placed after the pump. A venturimeter is placed at a distance of 180 cm from the gate value and 70 cm before the bend of pipe leading to the top of upstream tank. The venturimeter is attached to the mercury manometer.

3.2.3 Materials Used

The required sand of $d_{50} = 0.4\text{mm}$ grain size was available from quite far off places. Therefore raw material was procured from a crusher at Bahadurabad. This raw mixture was sieved through sieves of 0.6mm size and 0.3mm sieve. The coarse sand retained on 300 micron gave uniform coarse sand material. The fine gravel of $d_{50} = 2.8\text{mm}$ was procured by sieving the material through 4mm and retained it on 2mm sieves. Their d_{50} was calculated as follows, i.e.

$$d_{50} = \sqrt{a_1 a_2}$$

where, a_1 = grain size of smaller sieve available in close vicinity of required d_{50} , and a_2 = grain size of larger sieve available in close vicinity of required d_{50} .

For coarse sand sieving was done in between sieves of 0.3 mm and 0.6 mm. For sieve analysis the weight of coarse sand taken was equal to 1000 gm. Sieve analysis of the sediment material of $d_{50} = 0.424$ mm is given in Table 3.1.

Table 3.1 :The Sieve Analysis of the Sediment Material of $d_{50} = 0.424$ mm.

S.No.	Size of sieve in mm	Weight retained on this sieve in gm.	% weight retained in gm.	Cumulative finer in gm.	% finer in gm.
1	0.6	Nil	Zero	1000	100
2.	0.5	295	29.5	705	70.5
3.	0.425	160	16	545	54.5
4.	0.400	70	7	475	47.5
5.	0.355	275	27.5	200	20
6.	0.300	200	20	Zero	0

The cumulative frequency curve for this coarse sand sediment with $d_{50} = 0.424$ mm are given in Fig. 3.3. Fine gravel was sieved in between sieves of 2mm and 4mm. The weight of this material taken for sieve analysis was equal to 1000 gm. The results are shown in Table 3.2.

Table 3.2: Sieve Analysis of the Sediment Material of $d_{50} = 2.8$ mm.

S.No.	Size of sieve in mm	Weight retained on this sieve gm	% weight rationed in gm	Cumulative finer in gm	% finer or gm
1	4	Nil	0	1000	100
2.	3.35	130	13	870	87
3.	2.8	365	36.5	505	50.5
4.	2.6	430	43	75	7.5
5.	2.4	40	4	35	3.5
6.	2.36	10	1	25	2.5
7.	2	25	2.5	Zero	Zero

The cumulative frequency curve for this fine gravel sediment with $d_{50} = 2.8$ mm is given in Fig. 3.4.

3.3 EXPERIMENTAL PROCEDURE

Experiments were conducted in the following steps

- (I) First flume was adjusted to required slope.

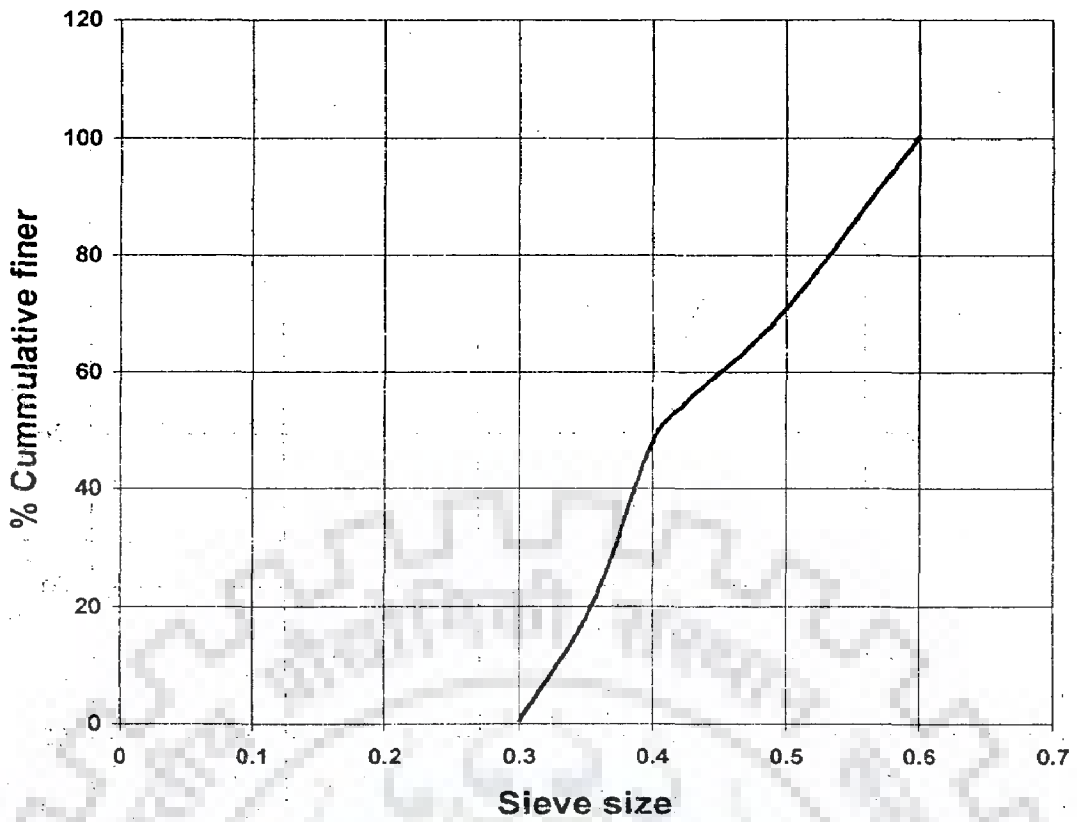


FIG 3.3 : CUMMULATIVE FREQUENCY CURVE FOR SAND $d_{50}=0.424\text{mm}$, RANGING FROM 0.3mm TO 0.6mm

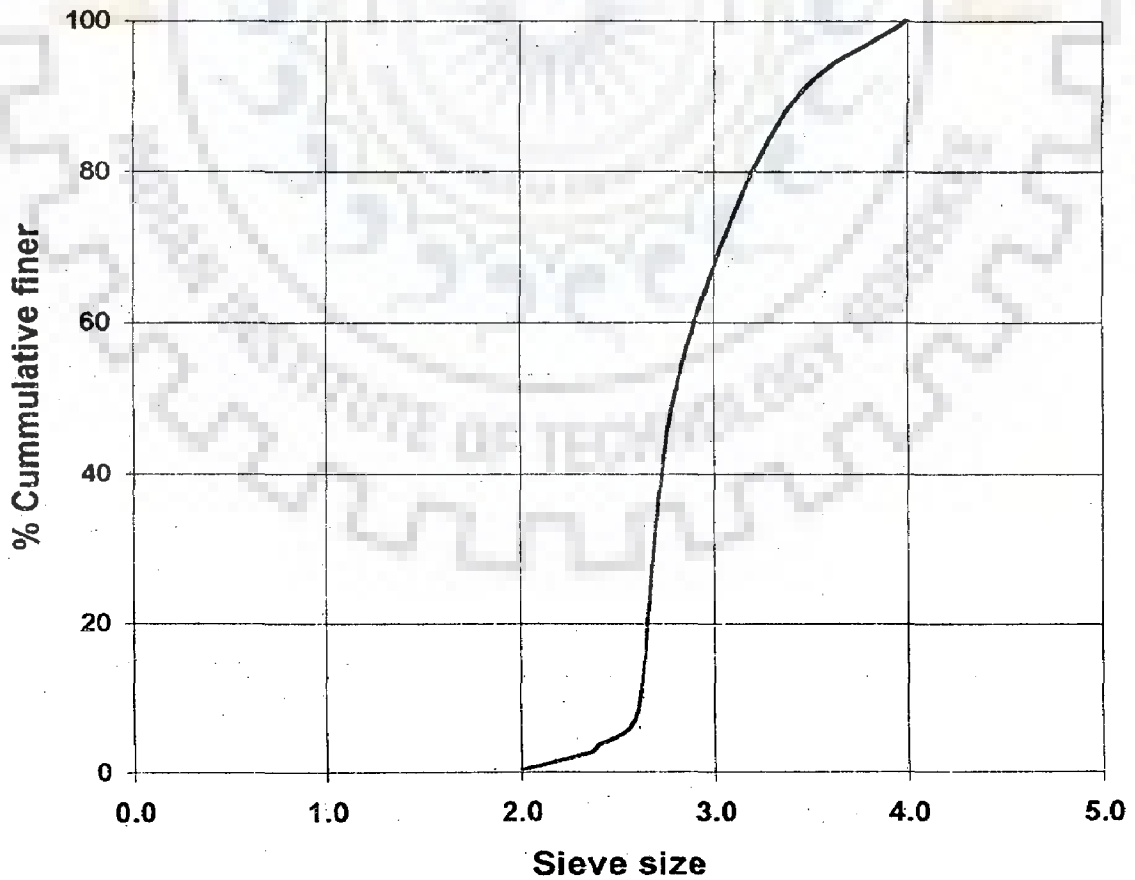


FIG 3.4 : CUMMULATIVE FREQUENCY CURVE FOR GRAVEL $d_{50}=2.8\text{mm}$, RANGING FROM 2mm TO 4mm

- (II) The depths of sediment test bed layers were fixed as per already calculated depths at 11cm .
- (III) Pitot tubes, V-notch and the venturimeter were calibrated by the standard procedures and their C_v and C_d were 0.918, 0.6885, 0.99 respectively. Calibration chart for V-notch is given in Fig 3.5. The calibration chart for pitot tube is given in Fig. 3.6.
- (IV) The models were fixed in the layer of sand bed at right angle to the side wall of the flume.
- (V) The required discharges were adjusted against required depth by hit and trial adjustment of the tail-gate of flume and the gate valve of pump and readings of venturimeter or V-notch, as the case used to be.
- (VI) Prior to conducting of each experimental run, the test bed section was leveled with the help of spirit level and the plastic leveling instruments.
- (VII) Velocities were measured at 8 different cross-sections for each experiment. Those locations in x-axis were at:
- (a) spur location itself, i.e. zero cm from spur model,
 - (a) 5cm, 10 cm, 20 cm both up stream and down stream of spur, and
 - (b) 30cm down stream of spur models also at any other sections if the need arose.

At each section following grid points, Fig 3.7 were chosen for taking measurements of velocities.

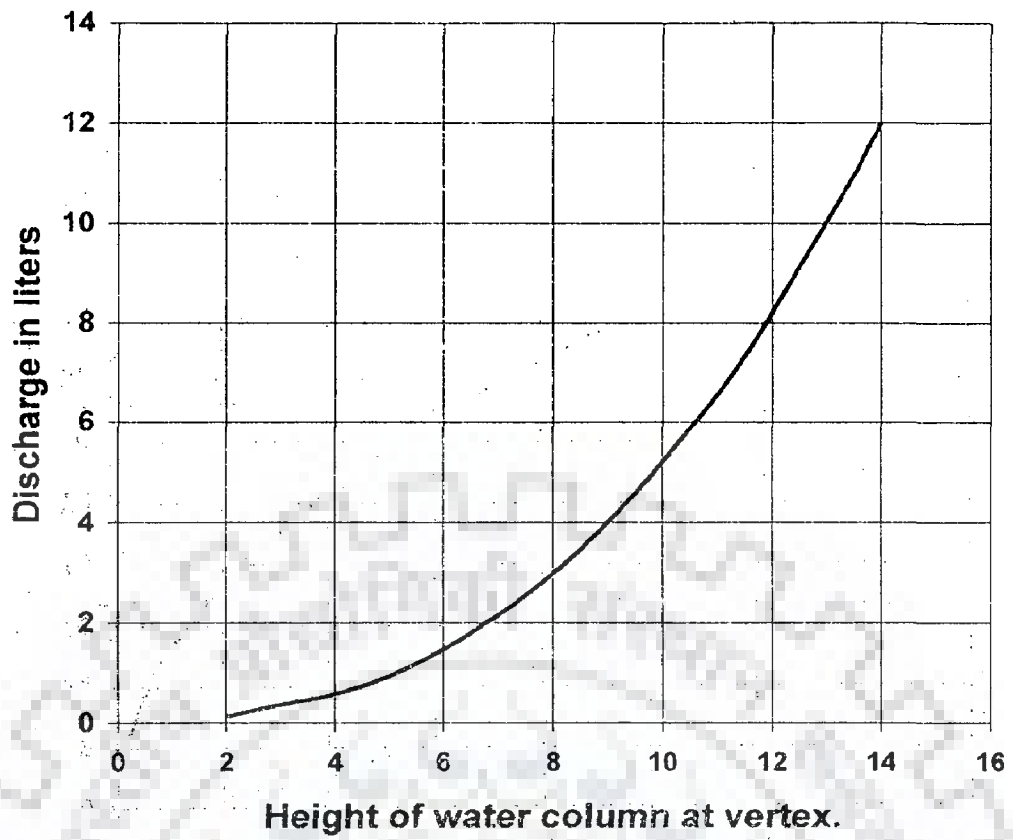


FIG. 3.5 : CALIBRATION OF V-NOTCH

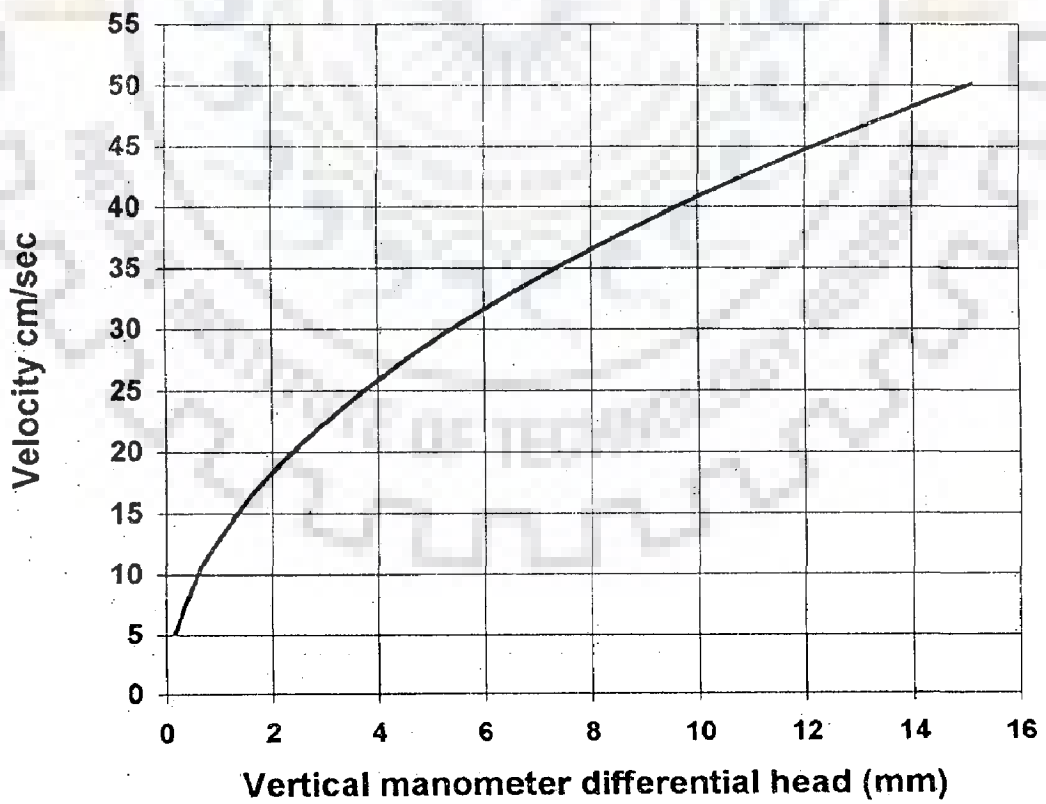


FIG 3.6 : CALIBRATION CHART FOR PITOT TUBE

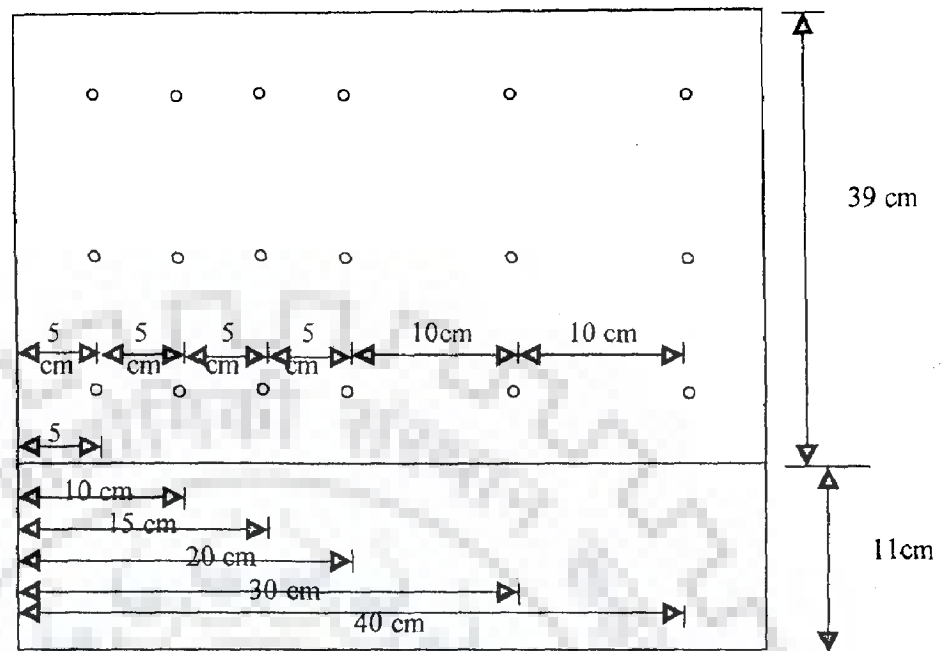


FIG. NO. 3.7: GRID POINTS IN CROSS-SECTIONAL LOCATIONS ACROSS THE FLUME FOR MEASUREMENTS OF VELOCITIES

- (VIII) Maximum scour depths along the nose and shank of the spur model were noted during the flow conditions after every 5min, 10min, 15min, 30min, 45min, 1hrs, then after every half an hour till 4hrs. Afterwards regularly after every hour as long as the experiment was run.
- (IX) After equilibrium scour had reached, the flow was stopped and the profile of whole scour hole and the deposition bar so developed were taken with the help of levels measured by the pointer gauge at every 1cm or 2cm grid in x and y directions.
- (X) In order to trace the flow pattern of flow lines with the help of floats, either wax balls or aluminum foil chips were used. The trajectory of wax balls mostly in close vicinity of spur, around its nose and through its slits and slots

were observed. Flow lines traced with the help of floats were used to see and judge the protected distance on downstream of the spur model.

- (XI) Photographs were taken of the developed profiles from both upstream side view and from downstream side view, after the termination of the run. Diagrams were also drawn by visual inspection and actual dimensions in x, y and z direction were measured. This was done to ascertain the geometry of the scour hole and the deposition bar.

3.4 PHASE ONE MODEL EXPERIMENTS

It was intended at the first instance to try out various permeable spur models of different types and shapes for the first phase of the study. Different models used in the Phase 1st experiments are shown in Fig.3.8 a to n. Some of the relevant statistics of these models are given in the Table 3.3 a to k. In these Tables b = length of spur, y = depth of flow, h = the height of spur above bed level, %p = percentage porosity of the models, w = width or thickness of the models. All the models were nonsubmerged. Models were made up of perspex sheets painted with oil paint, except some pile structures, which were of wooden pencils. The first model was of zero permeability, representing solid spur. After first model of zero permeability, plate models of different permeability were introduced with different shapes of slots, slits or holes in them. Among them are:

- (a) Model plates with round holes. Round holes started either from test bed section or 1 cm above it.
- (b) Plate models with horizontal and vertical slots. Slots started from test bed section. Number of horizontal and vertical slots were either 2 or 3 in each

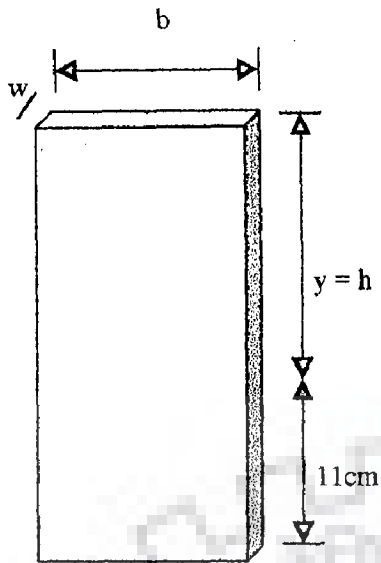


FIG. 3.8 a : MODEL OF ZERO PERMEABILITY

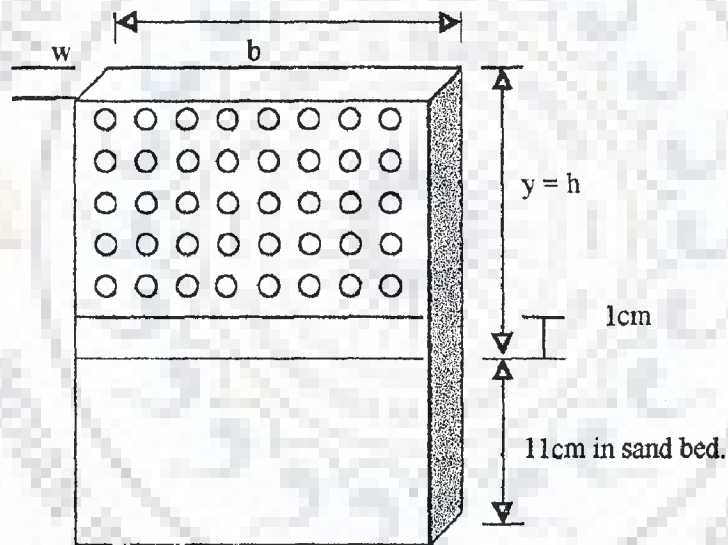


FIG. 3.8 b : MODEL WITH ONLY ONE DIMENSIONAL HOLES

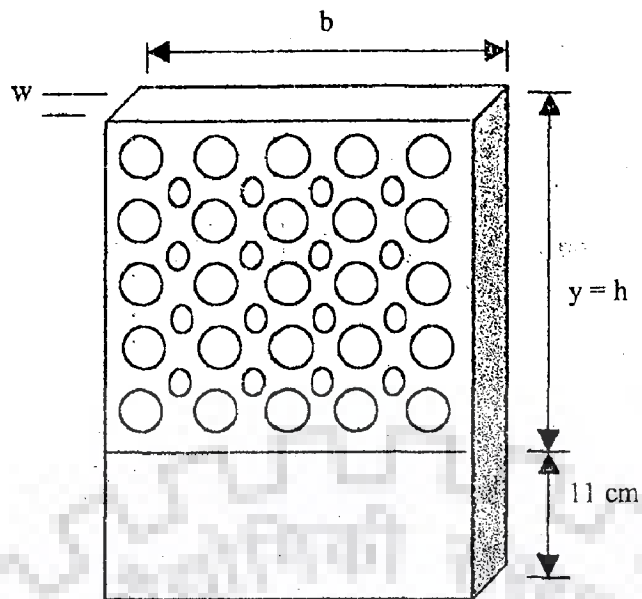


FIG. 3.8 c : MODEL WITH ROUND HOLES OF TWO DIFFERENT DIAMETERS

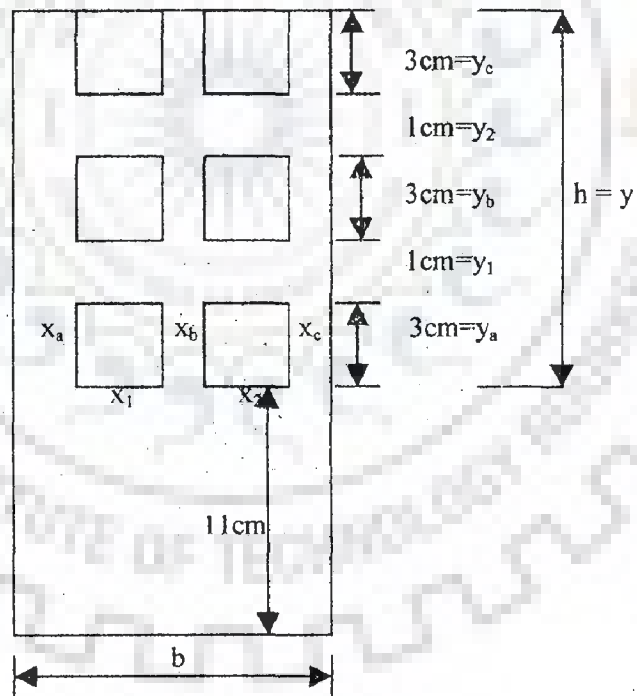


FIG. 3.8 d : MODEL WITH TWO SQUARE / RECTANGULAR SLITS IN EACH ROW

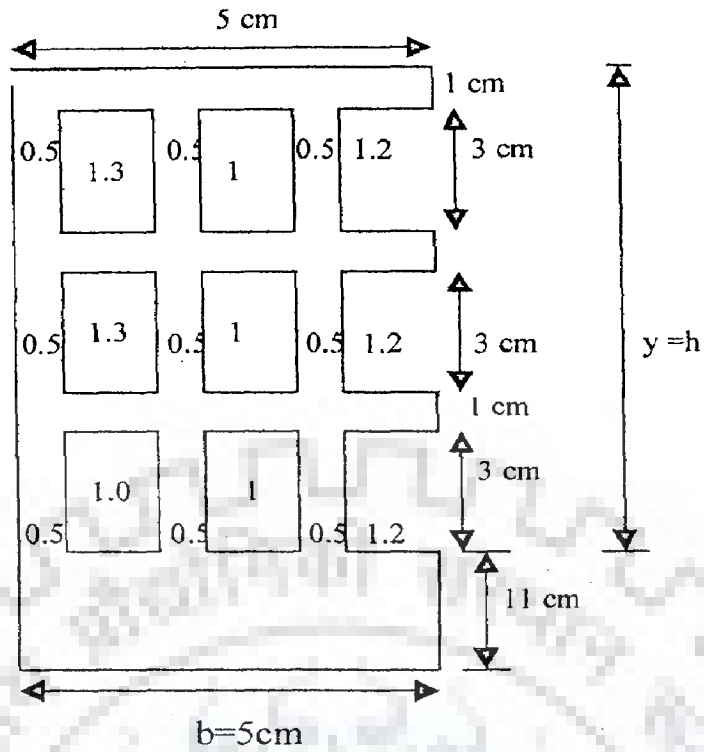


FIG.3.8 e : MODEL WITH THREE SLITS IN EACH ROW

(SLITS OPPOSITE TO SPUR-SIDE-WALL ARE OPEN)

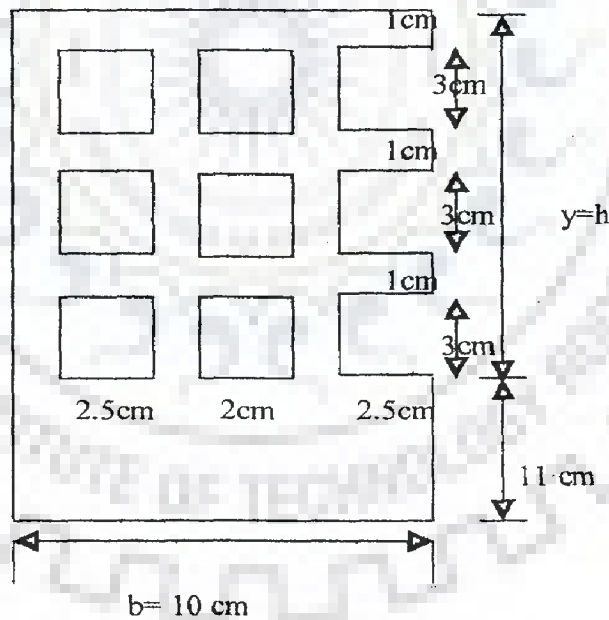
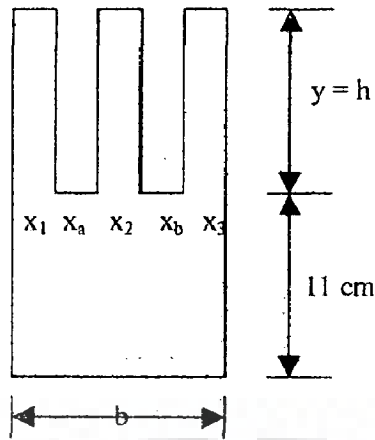


FIG. 3.8 f : MODEL WITH THREE RECTANGULAR SLITS

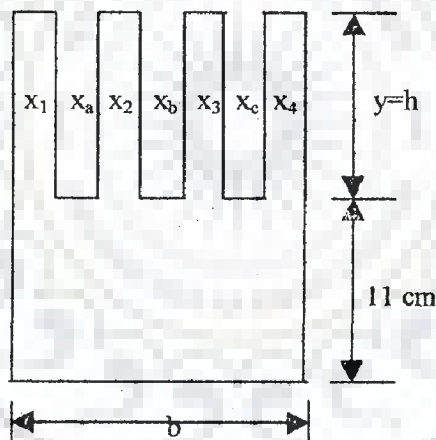
(SLITS IN MID STREAM ARE OPEN ON EXTREME EDGE)



$x_{1 \text{ to } 3}$ = length of solid portion in y-axis of the flume

$x_{a \text{ to } b}$ = length of vertical slot portion in y-axis

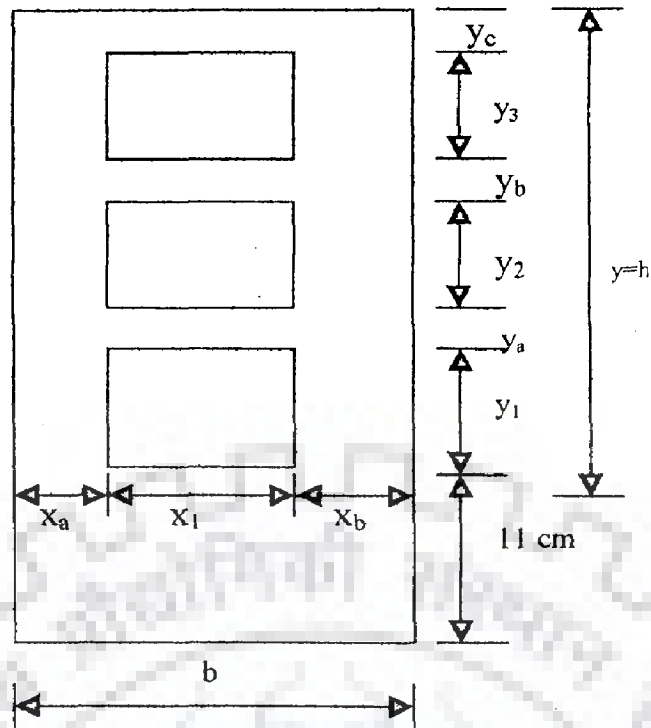
**FIG-3.8 g : MODEL WITH 2 VERTICAL SLOTS THROUGH
OUT THE DEPTH OF FLOW**



$x_{1 \text{ to } 4}$ = length of solid portion in y-axis of the flume

$x_{a \text{ to } c}$ = length of vertical slot portion in y-axis of the flume

**FIG. 3.8 h : MODEL WITH 3 VERTICAL SLOTS THROUGH
OUT THE DEPTH OF FLOW**



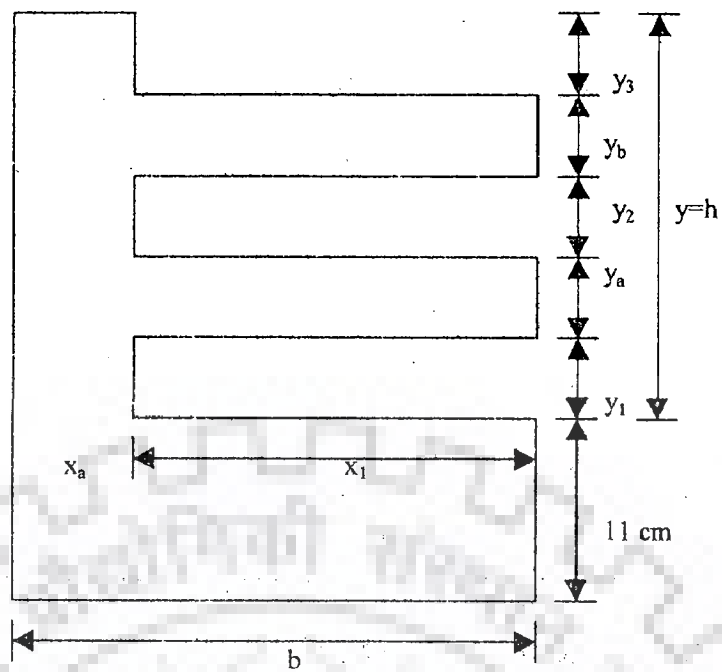
The length of the openings along y - axis = x_1

The length of the solid portions along y -axis $x_a = x_b$

The heights of solid portions along z -axis = $y_a = y_b = y_c$

the heights of openings along z -axis = $y_1 = y_2 = y_3$.

**FIG3.8 i: MODEL WITH ONLY ONE RECTANGULAR SLOT
IN EACH ROW THROUGH OUT ITS LENGTH (THE SLITS
ARE CLOSED ON TOP, BOTTOM, LEFT AND RIGHT)**



The length of the openings along x - axis = x_1

The length of the solid portion along x - axis = x_a

Heights of solid portions along z-axis $y_a = y_b \dots\dots = y_n$.

Heights of solid portions along z-axis $y_1 = y_2 \dots\dots = y_n$.

FIG 3.8 j : MODEL WITH ONLY ONE HORIZONTAL RECTANGULAR SLOT IN EACH ROW WHICH ARE OPEN ON MID STREAM SIDE

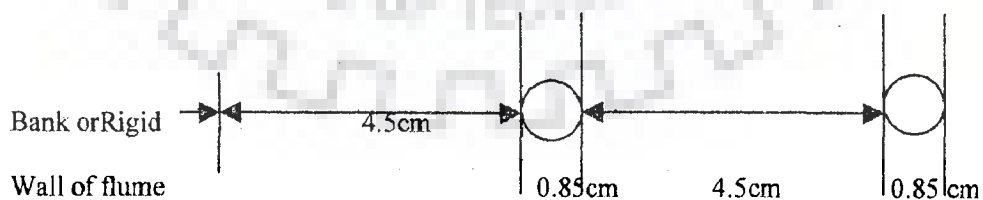


FIG. 3.8 k : SINGLE ROW PILE SPUR MODEL MADE WITH TWO WOODEN PENCILS

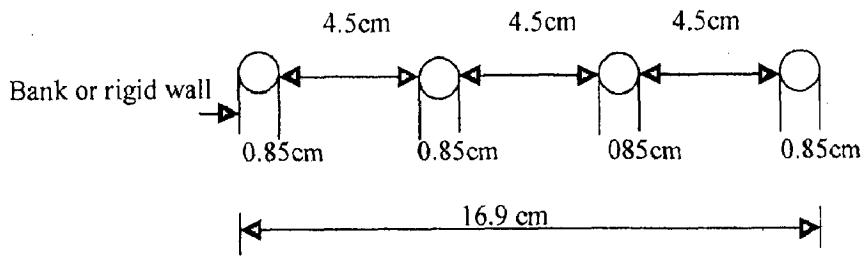


FIG. 3.8 1 : SINGLE ROW PILE SPUR MODEL MADE WITH FOUR WOODEN PENCILS

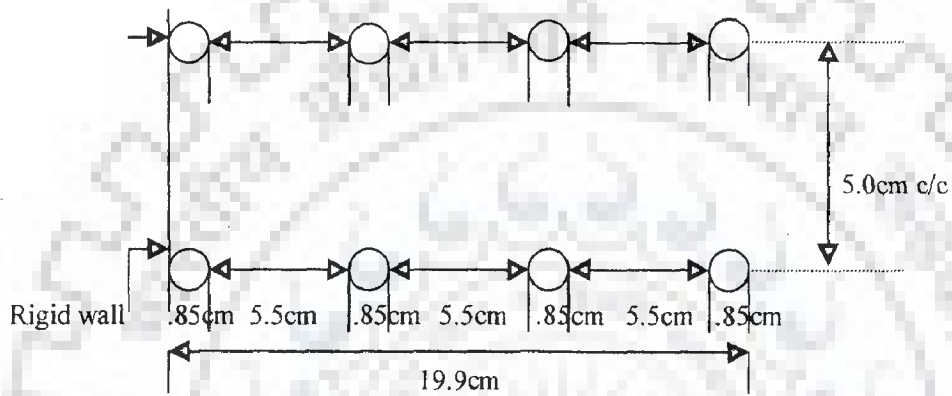
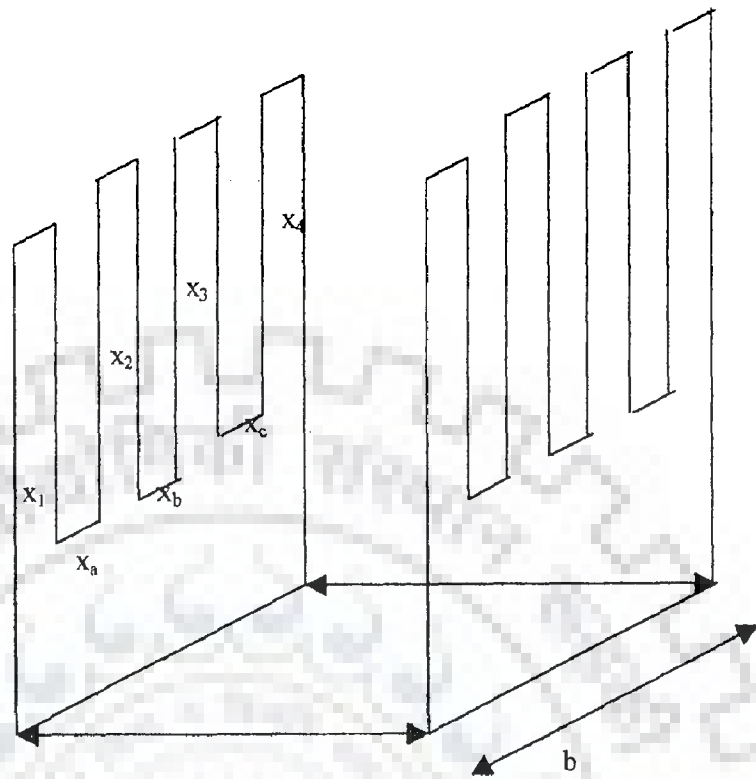


FIG-3.8 m : TWO PARALLEL ROWS PILE SPUR MODEL MADE WITH EIGHT WOODEN PENCILS



Length of solid portion = x_1 to x_4

Length of vertical slot portion = x_a to x_c

**FIG-3.8 n : TWO PARALLEL PLATES WITH 3
VERTICAL SLOTS MODEL**

Table 3.3 a : Pertinent data related to experiment on solid spur (fig. 3.8a)

Case	b cm	h cm	% p -obtained
A-1	5	8	0
A-2	10	8	0
A-3	10	10	0
A-4	5	10	0

Table 3.3 b : Pertinent data related to experiment on spur model with round holes of 6 mm dia. (fig. 3.8 b)

Case	b cm	h cm	% p -obtained
B-1	5	8	31
B-2	10	8	31
B-3	10	10	31
B-4	5	10	31

Table 3.3 c : Pertinent data related to experiment on spur model with alternate rows of round holes of dia. 1cm and 4mm (fig. 3.8 c)

Case	b cm	h = y cm	% p -obtained
B-1	5	8	58
B-2	10	8	58
B-3	10	10	58
B-4	5	10	58

Table 3.3 d : Pertinent data related to experiment on spur model with two rectangular holes in each rows. Two row in 8cm depth & three rows in 10 cm depth (Fig. 3.8 d)

Case	b cm	x ₁ to x ₂ cm	x _a to x _c cm	h = y cm	y _a to y _c cm	y ₁ to y ₂ cm	% p obtained
CA-1	5	1.75	0.5	10	3	1	57
CA-2	10	3.5	1	10	3	1	58
CA-3	5	1.75	0.5	8	3	1	55
CA-4	10	3.5	1	8	3	1	55

Table 3.3 e : Pertinent data related to experiment on spur model with three rectangular holes in each row. The holes in the mid stream are open in mid stream side. Two rows in 8cm depth & three rows in 10 cm depth (fig. 3.8 e - 3.8 f)

Case	b cm	x_1 to x_3 cm	x_a to x_c cm	h =y cm	y_a to y_c cm	y_1 to y_2 cm	% p obtained
CB-1	5	1	0.5	8	3	1	57
CB-2	10	2.5/2	1	10	3	1	58
CB-3	5	1	0.5	10	3	1	55
CB-4	10	2.5/2	1	8	3	1	55

Table 3.3 f : Pertinent data related to experiment on spur model with two vertical slots. Slots start from the test bed surface and are open on top (fig. 3.8 g)

Case	b cm	x_1 to x_3 cm	x_a to x_b cm	h =y	% p obtained
DA-1	10	2	2	10	42
DA-2	5	1	1	10	40
DA-3	10	2	2	8	42
DA-4	5	1	1	8	40
DA-5	5	0.83	1.25	8	51
DA-6	10	1.67	2.5	8	50
DA-7	5	0.83	1.25	10	51
DA-8	10	1.67	2.5	10	50
DA-9	10	2.33	1.5	10	31
DA-10	5	1.16	0.75	10	33
DA-11	5	1.16	0.75	8	33
DA-12	10	2.33	1.5	8	31

Table 3.3 g : Pertinent data related to experiments on spur model with three vertical slots. Slots start from the test bed surface and are open on top (Fig. 3.8 h)

Case	b cm	x_1 to x_4 cm	x_a to x_c cm	$h = y$	% p obtained
DB-1	10	1.25	1.67	8	54
DB-2	5	0.625	0.83	8	51
DB-3	10	1.25	1.67	10	54
DB-4	5	0.625	0.83	10	51
DB-5	5	0.75	0.66	8	42
DB-6	10	1.5	1.34	8	42
DB-7	5	0.75	0.66	10	42
DB-8	10	1.5	1.34	10	42
DB-9	10	1.75	1	10	36
DB-10	5	0.87	0.5	10	33
DB-11	5	0.87	0.5	8	36
DB-12	10	1.75	1	8	33

Table 3.3 h : Pertinent data related to experiments on spur model with horizontal slots. Three rectangular, horizontally placed slots in 10 cm depth & two slots in 8cm depth. Slots are closed on mid stream side. 1st slot starts from bed level (Fig. 3.8i)

Case	b cm	x_1 cm	x_a to x_b cm	$h = y$	y_1 to y_3 cm	y_a to y_c cm	% p obtained
EA-1	5	4	0.5	10	2	2	50
EA-2	10	8	1	10	2	2	49
EA-3	5	4	0.5	8	2	2	43
EA-4	10	8	1	8	2	2	41

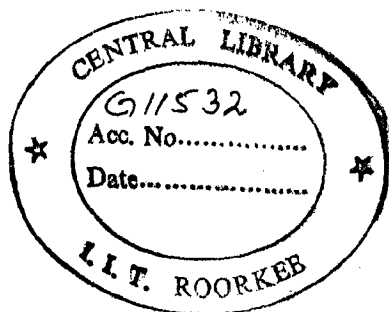


Table 3.3 i : Pertinent data related to experiments on spur model with horizontal slots open on mid stream side. Three rectangular, horizontally placed slots in 10 cm depth & two slots in 8cm depth. 1st slot starts from bed level (Fig. 3.8 j)

Case	b cm	x ₁ cm	x _a cm	h =y	y ₁ to y ₃ cm	y _a to y _c cm	% p obtained
EB-1	5	4	1	8	2	2	40
EB-2	10	9	1	8	2	2	45
EB-3	5	4	1	10	2	2	48
EB-4	10	9	1	10	2	2	54

Table 3.3 j: Pertinent data related to experiments on pile spur model in form of pencils dia 0.85 cm each (Fig. 3.8 k to 3.8 l)

Case	b cm	Spacing edge to edge cm	h =y	% p obtained
FA-1	10.7	4.5	10	84
FA-2	10.7	4.5	8	84
FA-3	16.9	4.5	10	78
FA-4	15.8	4.5	8	78

Table 3.3 k : pertinent data related to experiments on two parallel rows of pile spur model in form of plate and pencils dia 0.85 cm each (fig. 3.8m to 3.8.n)

Case	b cm	Spacing with in row edge to edge cm	Spacing in between two rows cm	h =y	%p obtained
FB-1	19.5	5.5	5	10	80
FB-2	17	5.5	5	8	76
FB-3	10	5.5	5	10	51
FB-4	10	5.5	5	8	51

plate, with different % of permeabilities in each type, intended to be around 30%, 40% and 50% range.

- (c) Bamboo piles were modeled with wooden pencils of 0.85cm diameter and the spacing between the pencils in each row were created according to thumb rules employed in the field and similarly spacing in between the rows too was established proportional to the spacing employed in the field on the basis of some thumb rules.
- (d) Besides above mentioned ones, other group of 8 models all 10cm in length, had 60% porosity. But differed in terms of model types with shapes of slits, slots and holes.

Thickness of 5mm was maintained for all plate models. All the models had free board above total water depth. Their exact % of permeabilities are mentioned in tables along with each experimental description.

In this phase of experiments, simulation runs in a 50cm wide and 350cm long, tilting & mobile bed flume, as shown in Fig. 3.1, were made with 21 nos. of different physical spur models. The permeable spur models of two blockage ratios with varying degrees of permeability from 0% to 84% were used. 68 no. of experiments were conducted. The varying lengths of the spur models taken were 5cm and 10cm, discharges were 0.00625 cumecs and 0.00992 cumecs, and the depths of flow were maintained at 8cm and 10cm. All these experiments were conducted with same uniform bed material of d_{50} equal to 0.424 mm. The bed slope was kept constant at 1 in 5000. τ_b , the bed shear stress calculated was 0.216 N/m^3 while as the critical bed shear stress calculated was 0.233 N/m^3 . The experiments were run for maximum of 12hrs. to min of 4 hrs. as per the development of the equilibrium scour. Two Froude

nos., i.e. 0.176 and 0.20027 were maintained. All the experiments were conducted in clear water conditions.

In first set of 30 lab experiments, flow was adjusted to be less than critical conditions for particle movement on the approach bed, so the average approach velocity established was 0.156m/sec. In second set of 38 experiments, again in clear water conditions, the discharge and the water depth of flow were adjusted near to but less than critical conditions, such that ripple bed features were created as a consequence of inducing the models. In this case, the average approach velocity established was 0.198m/sec. The Table related to details of experiments and experimental data of these experiments are given in the appendix in Tables A-1, A-A, A-B, A-CA, A-CB, A-DA, A-DB, A-EA, A-EB, A-FA, and A-FB.

The transverse and longitudinal velocities along three different depths, protected distance down stream of spur model, temporal variation of scour around the models, equilibrium scour depth and the bed profile on a close grid after the closure of discharge were the parameters which were measured for every experimental run. The ranges of equilibrium scour depth found for different models was from minimum of 12mm for pile spur model to maximum of 103mm for solid spur models. Similarly the ranges of protected distance down stream of spur model were found to be minimum of 5cm to maximum of 1.8m. Photo graphs from different angles were also taken after draining of all the water from the flume, for all the experiments. 17 of such photographs from the first phase have been attached in the thesis to highlight the scour profile of those particular spur models (Plate no. 3.1 to 3.17).

On the basis of above investigation the pile model developing least depth of scour was selected for extensive experimentation in second phase.

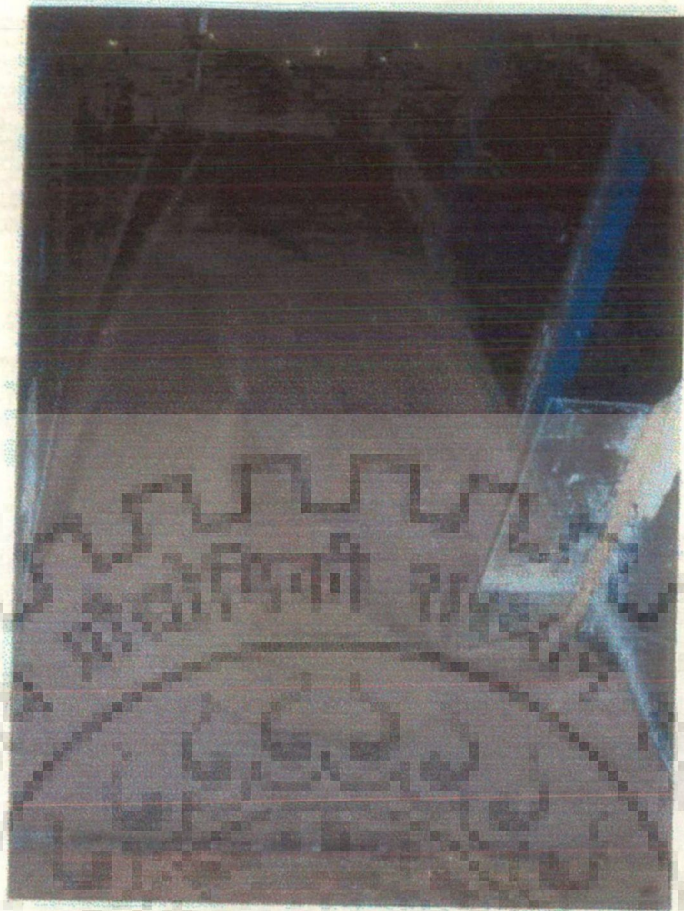


**PLATE- 3.1 : SCOUR AROUND EXPERIMENTAL
RUN NO. A - 3**

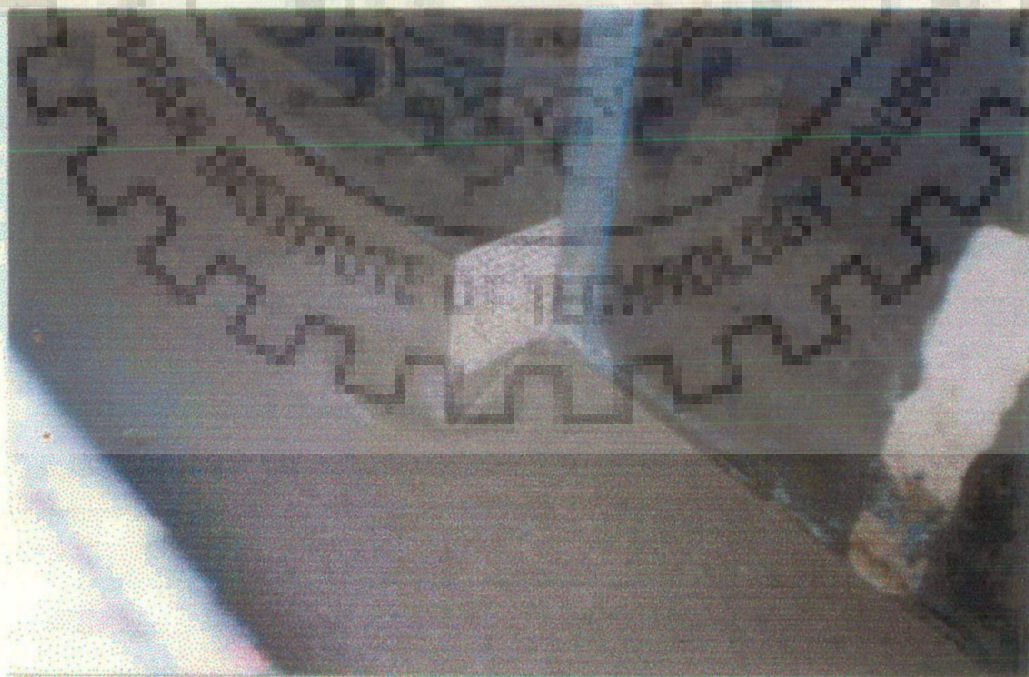


**PLATE- 3.2 : SCOUR AROUND EXPERIMENTAL
RUN NO. B - 2**



**PLATE- 3.3 : SCOUR AROUND EXPERIMENTAL
RUN NO. B-6**

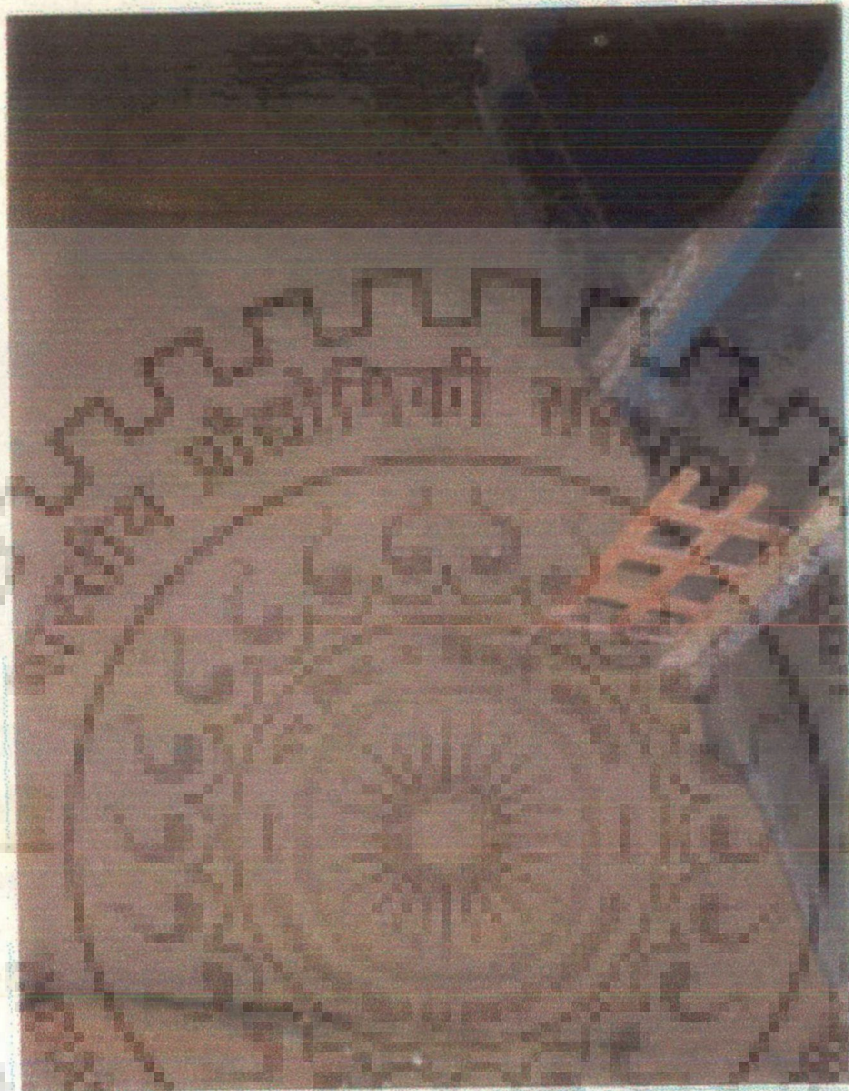


**PLATE- 3.4: SCOUR AROUND EXPERIMENTAL
RUN NO. CA-2**

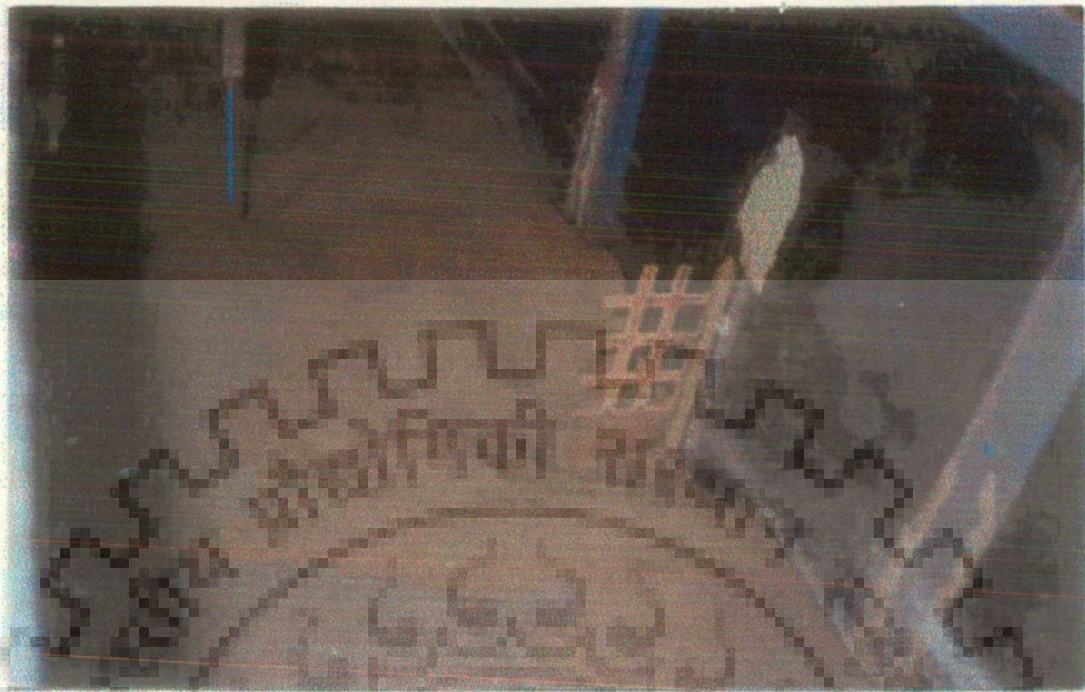


**PLATE- 3.5 : SCOUR AROUND EXPERIMENTAL
RUN NO. CB - 3**

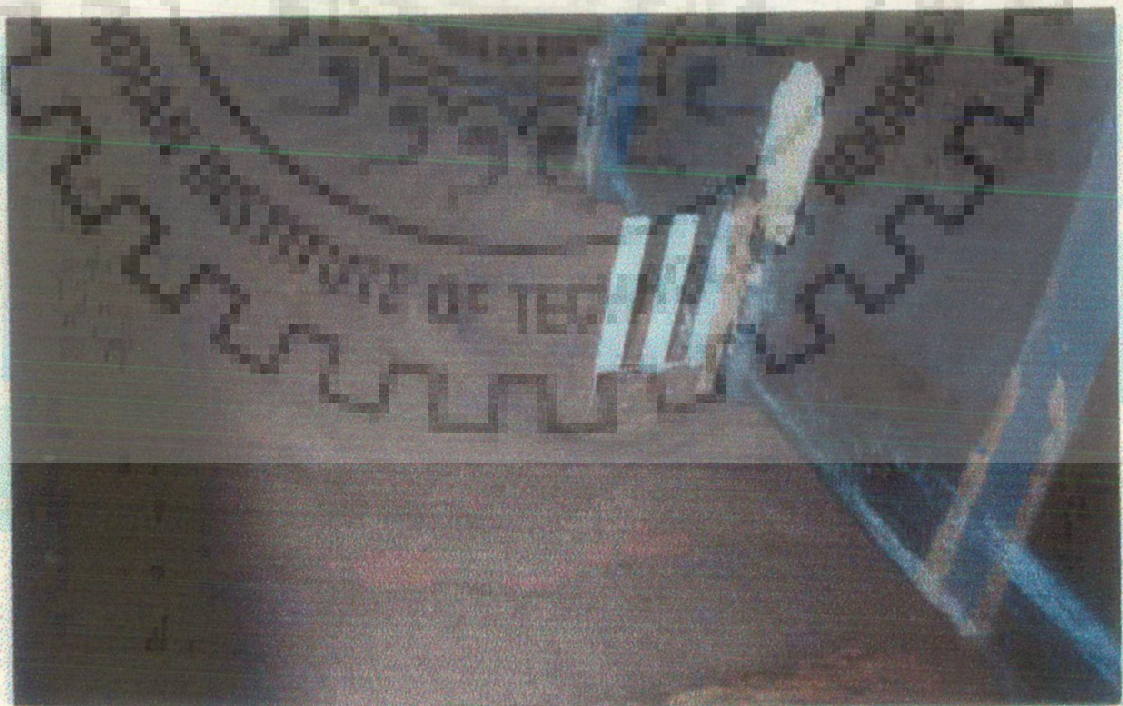


**PLATE- 3.6 : SCOUR AROUND EXPERIMENTAL
RUN NO. DA-1**



**PLATE- 3.7: SCOUR AROUND EXPERIMENTAL
RUN NO. DA-8**



**PLATE- 3.8: SCOUR AROUND EXPERIMENTAL
RUN NO. DA-9**



**PLATE- 3.9 : SCOUR AROUND EXPERIMENTAL
RUN NO. DB-4**



**PLATE- 3.10 : SCOUR AROUND EXPERIMENTAL
RUN NO. DB - 8**



**PLATE- 3.11 : SCOUR AROUND EXPERIMENTAL
RUN NO. DB - 10**



**PLATE- 3.12 : SCOUR AROUND EXPERIMENTAL
RUN NO. DB - 13**



**PLATE- 3.13 : SCOUR AROUND EXPERIMENTAL
RUN NO. EA -2**



**PLATE- 3.14 : SCOUR AROUND EXPERIMENTAL
RUN NO. EB- 4**



**PLATE- 3.15 : SCOUR AROUND EXPERIMENTAL
RUN NO. FA - 3**

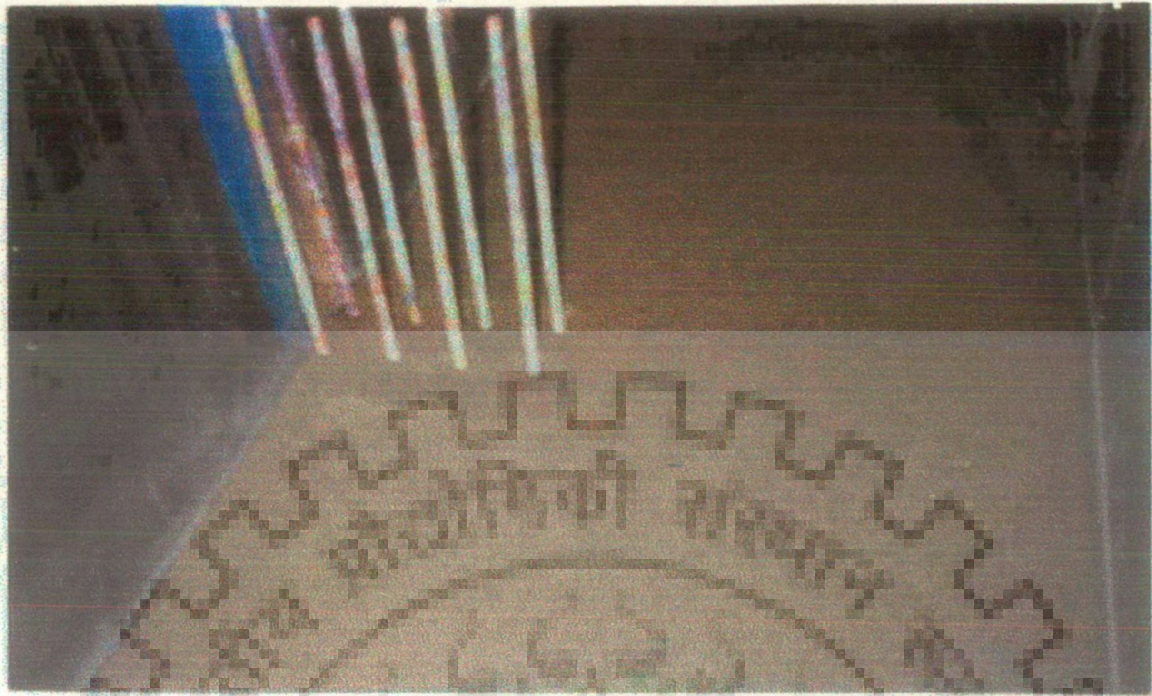


**PLATE- 3.16 : SCOUR AROUND EXPERIMENTAL
RUN NO. FB - 2**

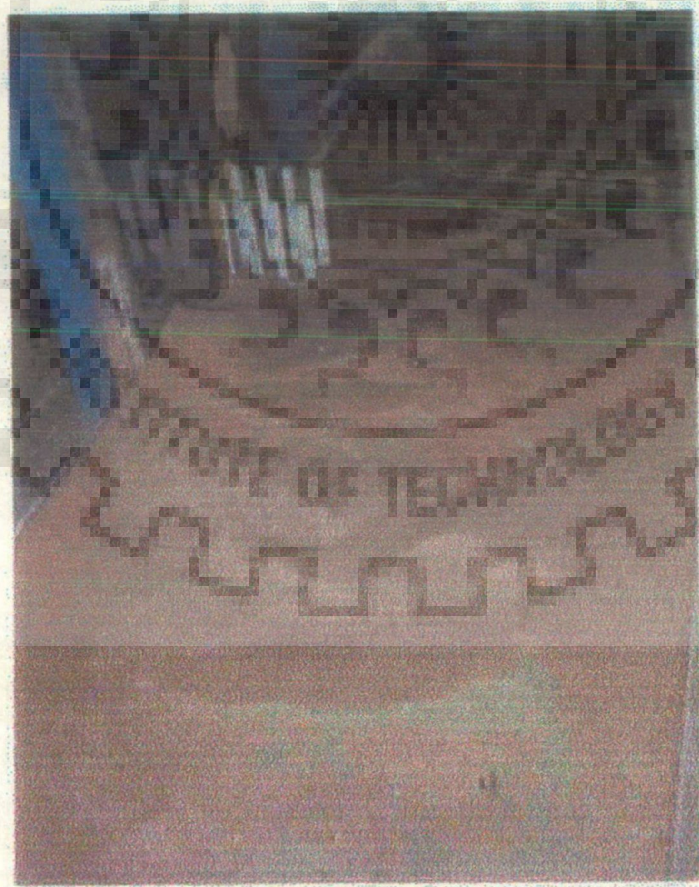


**PLATE- 3.17 : SCOUR AROUND EXPERIMENTAL
RUN NO. FB - 3**

3.5 PHASE TWO PILE SPUR EXPERIMENTS

In this phase of experiments, experimental runs were made in a longer, tilting flume i.e. 50cm wide and 11m long mobile bed flume, as shown in Fig. 3.2. The permeable pile spur models of two blockage ratios with 5 different percentages of permeabilities varying from 15% to 80% were made with 30cm long pencils of 0.85cm diameter. Total of 80 experiments were conducted in this phase in two sets. 1st set of 30 experiments were done with uniform coarse sand of d_{50} equal to 0.424mm and 2nd set of 50 experiments were done with uniform fine gravel of d_{50} equal to 2.8mm. The varying lengths of the spur models taken were 5cm and 10cm. Three different discharges were taken on uniform coarse sand bed ranging from 0.006 cumecs to 0.0149 cumecs and five different discharges were taken on uniform fine gravel bed ranging from 0.0067 cumecs to 0.027 cumecs, the depths of flow were maintained at 10cm and 11cm respectively in two bed materials. The bed slope were kept constant at 1 in 5000 and 1 in 2000 respectively in two bed materials. τ_b , the bed shear stress calculated was 0.37 N/m^2 where as the critical bed shear stress calculated was 2.27 N/m^2 for $d_{50}=2.8\text{mm}$. The experiments were run for maximum of 8 hrs. to min of 4 hrs. as per the development of the equilibrium scour. Three Froude nos. ranging from 0.12 to 0.3 were created for sand bed and five Froude nos. ranging from 0.12 to 0.48 were created for gravel bed. All the experiments were conducted in clear water conditions.

In first set of 30 lab experiments, in sand bed flow was adjusted to less than critical conditions for particle movement on the approach bed and also were adjusted equal to critical conditions, so the average approach velocity established was ranging from 0.119 m/sec to 0.298 m/sec. In second set of 50 experiments in gravel bed, again

in clear water conditions the discharge and the water depth of flow were adjusted less than critical conditions, so the average approach velocity established was ranging from 0.125 m/sec to 0.502 m/sec. The Table of classification and experimental data of these experiments are given in the appendix in Tables A-P, A-PS, A-PA, A-PB, A-PC, A-PD, A-PE, A-PSA, A-PSB, A-PSC, A-PSD and A-PSE.

The transverse and longitudinal velocities along three different depths, protected distance down stream of spur model, temporal variation of scour around the models, equilibrium scour depth and the bed profile on a close grid after the closure of discharge were the parameters which were measured for every experimental run. The ranges of equilibrium scour depth found for different models were from minimum of 9mm to maximum of 95mm in sand bed and from minimum of 4mm to maximum of 60mm in gravel bed were observed. Similarly, the ranges of protected distance down stream of spur model were found to be minimum of 2cm to maximum of 90cm. For all the experiments, photographs from different angles were also taken after draining of all the water from the flume. Two photographs from this second phase have been attached in the thesis to highlight the scour profile of these particular pile spur models (Plate no. 3.18 to 3.19).

In order to validate the model based on this phase of experimentation, third phase of experiments were taken up in Solani river.

3.6 PHASE THREE FIELD EXPERIMENTS

Four bamboo spurs were constructed in River Solani 7 Km away from the place of study. The permeabilities of these spurs varied from 20% to 80%. They were constructed 50 m apart from each other. After considering a blockage ratio of 10%,



**PLATE- 3.18 : SCOUR AROUND EXPERIMENTAL
RUN NO. P2A - 3**

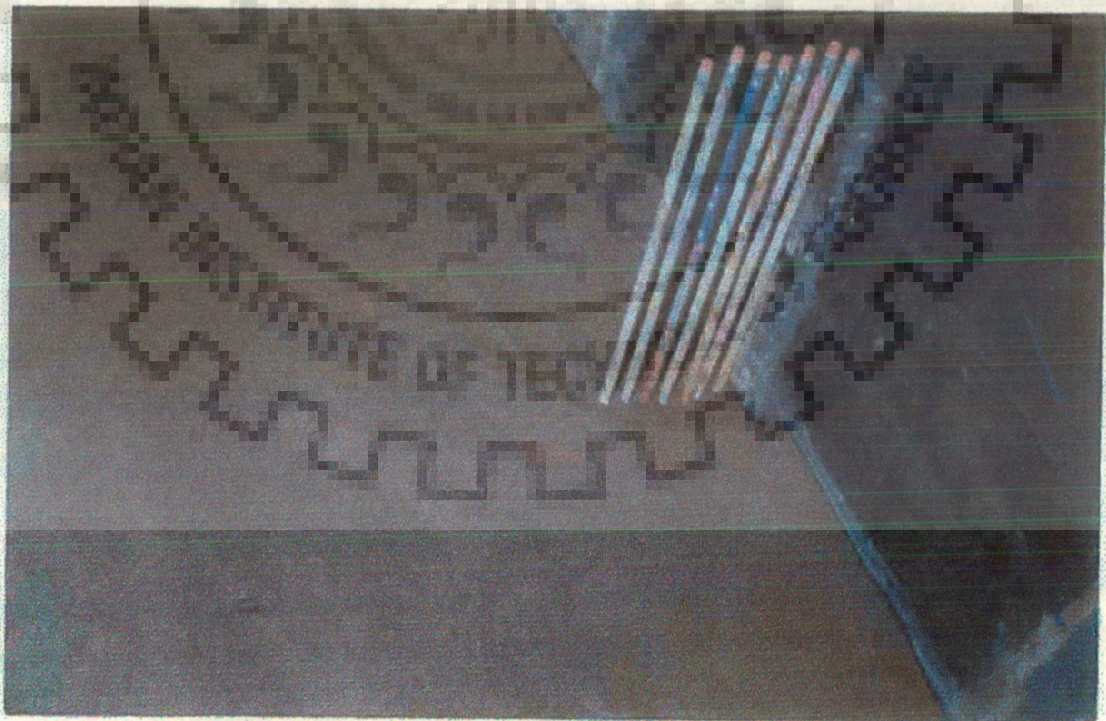


**PLATE- 3.19 : SCOUR AROUND EXPERIMENTAL
RUN NO. PS2C - 3**

bamboos of 6 cm diameter were driven into river bed from one bank towards the middle of river up to a length of 3m each. The river widths measured over the spur locations were 30m each. Four permeable spurs constructed were of 20% , 40% , 60% and 80% permeabilities. The bamboos were kept at equal spacing within each spur as per the % of permeability. Bamboos were driven 1m to 1.5m deep in to the river bed with the help of hammers according to the ease of driving. All the bamboos within each spur were tied among themselves with very thick ropes, which were anchored to the bank. The photograph of the each bamboo pile spur in river Solani are attached (Plate no.3.20 to 3.23).

3.6.1 Field Experimental Procedure

Maximum scour depth was measured around all permeable spurs vis a vis the discharge in the river; both parameters were measured regularly after every 24 hours. Following measurements were also taken.

- (1) The grain size distribution of the bed material was checked by the standard methods. Samples taken were dried in electrical oven for 5 days to 6 days. Every where around all spurs the river bed grains were found uniform of size

$$d_{50} = 0.21\text{mm with } \sigma \text{ ,standard deviation } \frac{d_{50}}{d_{16}} = \frac{0.21}{0.20} = 1. \text{ Table no. 3.4}$$

shows the sieve analysis of the bed material of this river at the construction spots.

Table No. 3.4: The Sieve Analysis Of The Bed Material Of River

Solani At The Spur Construction Spots.

Sl. No.	Size of sieves in mm	Wt retained on sieves in gm.	% wt. Retained	Cumulative finer in gm	Cummulative % finer in gms.
1.	0.85	3	0.6	497	99.4
2.	0.425	7	1.4	490	98
3.	0.3	30	6	460	92
4.	0.15	420	84	40	8
5.	0.75	30	6	10	2
6.	Pan	10	2	0	0

- (2) The initial bed levels of the river and the max scour depth after every 24hrs were measured against a bench mark with the help of dumpy level at all the spur locations.
- (3) Discharge variations were measured throughout this duration by the measurement of velocities and depths at every one meter distance along the river cross sections near the spurs. The discharges were calculated by integration of area velocity method.
- (4) The slope of the river was calculated with the help of Dumpy level by reading the difference in level of water surface at different sections over a distance of 500 m. which showed the slope of river as 1 in thousand.

The Table pertaining to details of experiments and experimental data of these experiments are given in the appendix in Tables A-R and A-RS.

3.7 SUMMARY

The details pertaining to experiments conducted in various phases are described to assess the findings of the present study. Details of flumes, although not necessary, are presented to highlight the fact the phase one experiments which are



PLATE- 3.20 : SPUR MODEL RA WITH 20% PERMEABILITY AT ROORKEE IN RIVER SOLANI

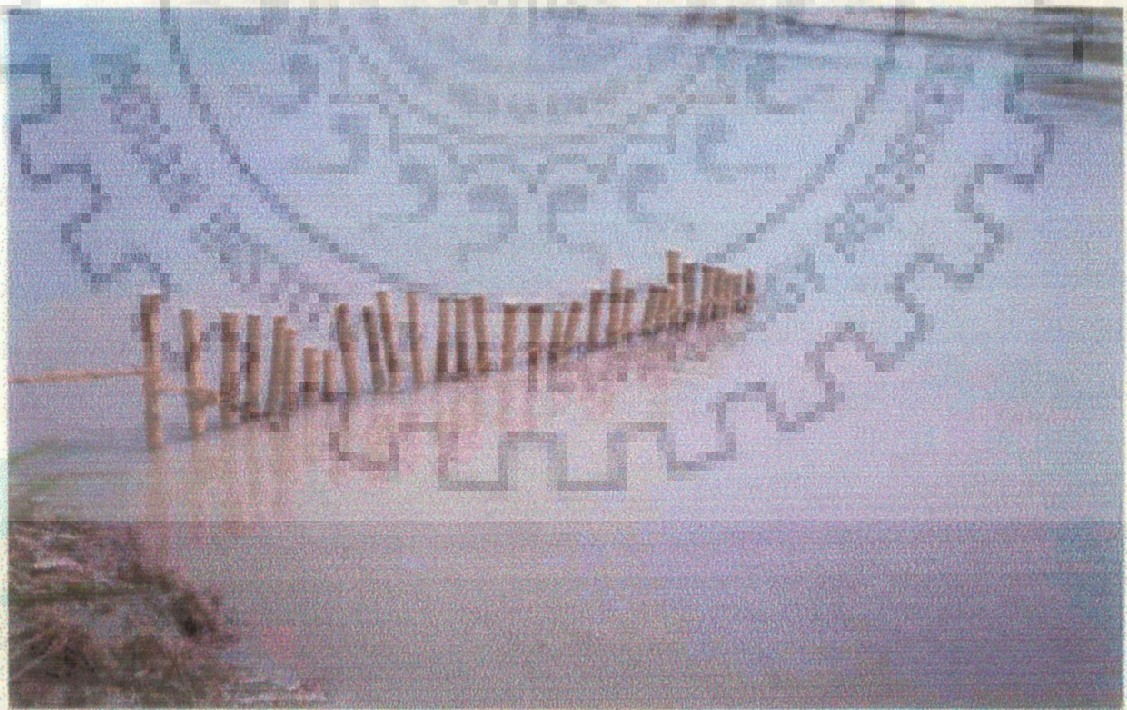


PLATE- 3.21 : SPUR MODEL RB WITH 40% PERMEABILITY AT ROORKEE IN RIVER SOLANI



PLATE- 3.22 : SPUR MODEL RC WITH 60% PERMEABILITY AT ROORKEE IN RIVER SOLANI



PLATE- 3.23 : SPUR MODEL RD WITH 80% PERMEABILITY AT ROORKEE IN RIVER SOLANI

conducted in a flume of smaller length, are only trial runs to identify the permeable spurs with minimum scour. No analysis of phase I is performed except the scour obtained in this phase has been used to ascertain the role of different parameters such as porosity and Froude number. Also it has indicated that pile spurs experience minimum scour. This fact led to the planning of second phase experiments.



PRELIMINARY ASSESSMENT OF SCOUR AROUND DIFFERENT PERMEABLE SPURS

4.1 INTRODUCTION

Considering the fact that in field conditions, permeable spurs of different type have been used, a set of 68 experiments were performed in phase I of this study to monitor behaviour of some of these spurs,. The objective of these experiments was to identify the permeable spur in which the minimum scour occurred at the nose of the pier. For identical conditions of flow and geometry of piers, the pattern of scour around the nose of spurs were compared to identify the permeable spur corresponding to minimum scour. It is also apparent from different plates, shown in Chapter 3, that the scour is minimum in case of permeable pile spurs. Thus, no explicit analysis for identification of the permeable spur with minimum scour is considered necessary. Rather for the modeling of scour around permeable pile spurs, certain analysis including use of existing models is considered relevant. Based on the review of literature on scour, it is considered to use Melville's approach because of its applicability to model scour around bridge piers as well as abutments. Prior to testing this approach, it was considered desirable to test this against the past experiments performed at Roorkee, and not tested so far using this approach. The chapter begins with the essentials of Melville's approach and its evaluation with a large number of solid spur experiments conducted at Roorkee in the past. The feasibility of using Melville's approach to permeable pile spurs is also examined. Later, some of the bed

profiles are shown in this chapter for case of permeable pile spurs to highlight the influence of porosity as well as Froude number on scour and this feature is utilized to develop a rigorous approach of steady state scour modeling in next Chapter.

4.2 ASSESSMENT OF MELVILLE'S APPROACH

Assuming constant density of sediment and the absence of viscous effects, an expression for d_{se} at a spur of length 'b' in a uniform sediment, can be written as follows

$$\frac{d_{se}}{b} = f \left(\frac{V}{V_c}, \frac{y}{b}, \frac{d_{50}}{b}, \frac{t}{t_e} \right) \quad (4.1)$$

where, d_{50} = median grain size of sediment, y = mean depth of approach flow:

t = time at any stage of scour hole development, V_c = threshold velocity for bed sediment entrainment,

$$\left(\frac{V}{V_c} \right) = \text{flow intensity}; \quad \left(\frac{y}{b} \right) = \text{flow shallowness}$$

$$\left(\frac{d_{50}}{b} \right) = \text{sediment coarseness}; \quad \text{and} \quad \frac{t}{t_e} = \text{time ratio.}$$

The scour depth changes with flow intensity can be explained in terms of the balance between sediment input to and output from the scour hole. For clear water scour there is no sediment input. Melville (1997), Shen et al. (1966), Ettema (1980) and Chiew (1984) have noticed such trends in case of bridge piers.

Rouse (1940) and Doddiah et al. (1953) stated that the scour depth is directly proportional to a geometric progression of time. According to Liu and Skinner (1960), the scour depth increases indefinitely in the absence of sediment supply to the scour hole from upstream. Because equilibrium clear water scour depth is reached

asymptotically with time, it can take a very long time for equilibrium scour hole to form. Melville and Chiew (1999) use t_e , as the time at which the scour hole develops to a depth (the equilibrium depth, d_{se}) at which the rate of increase of scour does not exceed 5% of the pier diameter in the succeeding 24 hour period, i.e.,

$$\frac{d(d_{se})}{dt} \leq \frac{0.05b}{24 h'} \quad (4.2)$$

The method with addition of time factor and simplified to apply to spurs found in uniform sediments can be written as (Melville 1997).

$$d_s = K_{yb} K_v K_d K_t K_\theta K_s K_g \quad (4.3)$$

These K's are empirical expressions, also called as effectiveness factors in the present study, account for the various influences on scour depth as follows: K_{yb} = empirical coefficient for depth of flow and length of spur, K_v = empirical coefficient for flow intensity, K_d = empirical coefficient for sediment grain size, K_t = empirical coefficient for time ratio, K_θ = empirical coefficient for spur orientation with θ being inclination of spur to the direction of flow, K_s = empirical coefficient for spur shape and K_g = empirical coefficient for channel geometry.

For estimations of scour depth d_s at any time, K's are given as follows, by Melville (1997).

$$K_{yb} = 2b \quad \text{for } b/y < 1 \quad (4.4a)$$

$$K_{yb} = 2\sqrt{yb} \quad \text{for } 1 < b/y < 25 \quad (4.4b)$$

$$K_{yb} = 10y \quad \text{for } b/y > 25 \quad (4.4c)$$

$$\left. \begin{aligned} K_v &= V/V_c \quad \text{for } V/V_c < 1 \\ K_v &= 1 \quad \text{for } V/V_c > 1 \end{aligned} \right\} \quad (4.5a)$$

$$V_c = U_{*c} 5.57 \log(5.53 \frac{y}{d_{50}}) \quad (4.5b)$$

$$U_{*c} = \sqrt{\frac{\tau_c}{\rho_f}} \quad (4.5c)$$

$$K_d = 0.57 \log(2.24 b/d_{50}) \quad \text{for } b/d_{50} \leq 25 \quad (4.6a)$$

$$K_d = 1 \quad \text{for } b/d_{50} > 25 \quad (4.6b)$$

In eq. 4.5, τ_c is the critical shear stress of sediment and ρ_f is the density of fluid.

Richardson et al. (1993) gave values for K_θ for abutments, which are consistent with the Laursen and Toch (1956) curve and are shown in Table 4.1.

Table 4.1 : K_θ versus θ after Richardson et al. (1993)

θ°	0	15	30	45	60	90	120	150
K_θ	--	--	0.9	--	0.97	1	1.06	1.08

Channel geometry effects are unimportant as long as the velocity and depth of flow used is represented by the flow shallowness y/b . K_g is included in K_{yb} for a rectangular channel, as seen in above equations for K_{yb} . However, it is to be calculated differently for compound channel comprising of flood plain and main channel (Melville 1997). Therefore, for rectangular channels $K_g = 1$.

For circular piers or vertical wall abutments oriented perpendicular to the flow, K_{yb} represents the maximum possible scour depth. Values of K_v , K_d , and K_g are always ≤ 1 and the effect of each of these factors is to reduce the scour depth given by

K_{yb} for abutments or spurs oriented obliquely to the channel. Slightly larger scour depth than given by K_{yb} can occur if K_θ lies between 1 to 1.1.

Melville (1997) has suggested the values of K_s for abutments as given in Table 4. 2.

Table 4.2 : K_s for abutments after Melville (1997)

For	Shape	H:V	K_s
Abutments	Vertical wall	--	1
	Wing wall		0.75
	Spill through	0.5:1	0.6
	Spill through	1:1	0.5
	Spill through	1.5:1	0.45

4.3 DATA ANALYSIS

Five different sets of data for scour depths as observed in laboratories were taken. These are by Garde and Subramanya (1960,1961), Nambudripad (1961), Ramu (1964), Tyagi (1967, 1973) and Singh (1993). The range of their data is given in Table 4.3 where in 'B' denotes the flume width.

The mean approach velocity was calculated using the continuity equation. The critical shear stress ' τ_c ' was calculated using Shields' diagram (Garde and Ranga Raju, 1985). V_c was calculated using equation (4.5b). The values of K_s , K_θ , K_g , happened to be 1 each in all the cases. K_t was assumed as 1 as different investigators termed their scour depth as equilibrium scour depth. Ranges of dimensionless parameters considered by different investigators are given in Table 4.4. The

Table 4. 3 : Range of parameters used by different investigators and the observed (d_{so}) and calculated (d_{scm}) scour depths

Author	t_e hr.	No. of Runs	B mm	b mm	Q m ³ /sec	d_{50} mm	σ	S^* 10 ⁴	γ_s gm/cc	y mm	D_{so} M m	d_{scm} mm
Garde & Subramanya (1960, 1961)	3 to 5	45	610	102 to 287	0.0040 to 0.0252	0.29	1.66	9 to 40	2.69	34 to 189	43 to 179	91.6 to 363.3
Nambud- ripad (1961)	3 to 5	33	610		0.0113 to 0.0510	0.29 to 2.25	1.38 to 2.08	11 to 50	2.69 to 2.75	64 to 244	6 to 155	73.4 to 201.3
Ramu 1st series (1964)	3 to 5	26	914	168 to 457	0.0425 to 0.0849	7.50 & 10.5	1.33 & 1.21	29.4	2.68 & 2.70	74 to 140	49 to 224	123.30 to 334.7
Ramu 2nd series (1964)	3 to 5	35	990	165 to 500	0.023 to 0.057	2.15 & 4.00	1.39 & 1.50	29.4	2.69 & 2.72	52 to 158	34 to 226	24.3 to 334.7
Tyagi (1967,1973)	2 to 4	42	610	61 to 207	0.004 to 0.125	2.48 & 4.05	1.15 & 1.31	0.00	1.05 & 1.50	21 to 151	17 to 267	84.87 to 353.93
Singh (1993)	3	3	600	120	0.008 to 0.014	0.525	1.18	10	2.65	36 to 55	115 to 143	131.45 to 162.48

Table 4.4 : Range of dimensionless parameters taken by different investigators.

Sl. No.	Authors	B/y	V/Vc	b/d ₅₀
1.	Garde and Subramanya. (1960, 1961)	0.66 to 7.52	0.397 to 1.25	351.27 to 988.61
2.	Nambudripad (1961)	0.41 to 2.19	0.365 to 1.467	44.73 to 347.069
3.(a)	Ramu 1st Series (1964)	1.34 to 5.78	0.438 to 0.953	22.423 to 59.1
(b)	Ramu 2nd Series (1964)	1.19 to 6.85	0.055 to 0.974	41.58 to 422.247
4.	Tyagi (1967, 1973)	0.47 to 9.02	0.622 to 2.019	15.062 to 83.63
5.	Singh (1993)	2.18 to 3.33	1.35 to 1.52	228.57

agreement between computed scour depth (using Melville's approach) and the observed scour depths in respect of the runs of different investigators are given in Figs. 4.1 - 4.5. The lines corresponding to ' $d_{scm} = 2d_{so}$ ', ' $d_{scm} = d_{so}$ ' and ' $d_{scm} = 0.5d_{so}$ ' are also shown in these figures to assess the performance of Melville's relationship for the data of different investigators.

4.4 RESULTS AND DISCUSSION

As many as 184 runs related to scour around single solid spur have been used in this study. The approach of Melville (1997), which has been found successful against a large number of available data in the literature does not hold good in the present analysis. One of the possible reasons for this may be that the relationships for piers and abutments are not suited to describe scour around solid spurs. However, this reasoning is ill founded as a lot of similarity exists between the flow around abutments and solid spur. Having accepted this, one can also question the use of K_t as one in the present analysis. As the run lengths for the data used in this study seldom exceed six hours, it is also possible to question these data as the representative of equilibrium scour depth as per Melville's criteria. This means that the data used in the present analysis are certain fraction (less than one) of the real equilibrium scour depth, which would have taken a much longer time to develop. On an average, it can be observed from Table 4.5 that for more than 90% of the data, calculated scour depth exceeds the observed scour depth. At present, no relationship exists to compute equilibrium scour time in case of flow around either abutments or spurs. Thus, a precise evaluation of scour around spurs at any time is currently not feasible and this requires further investigations.

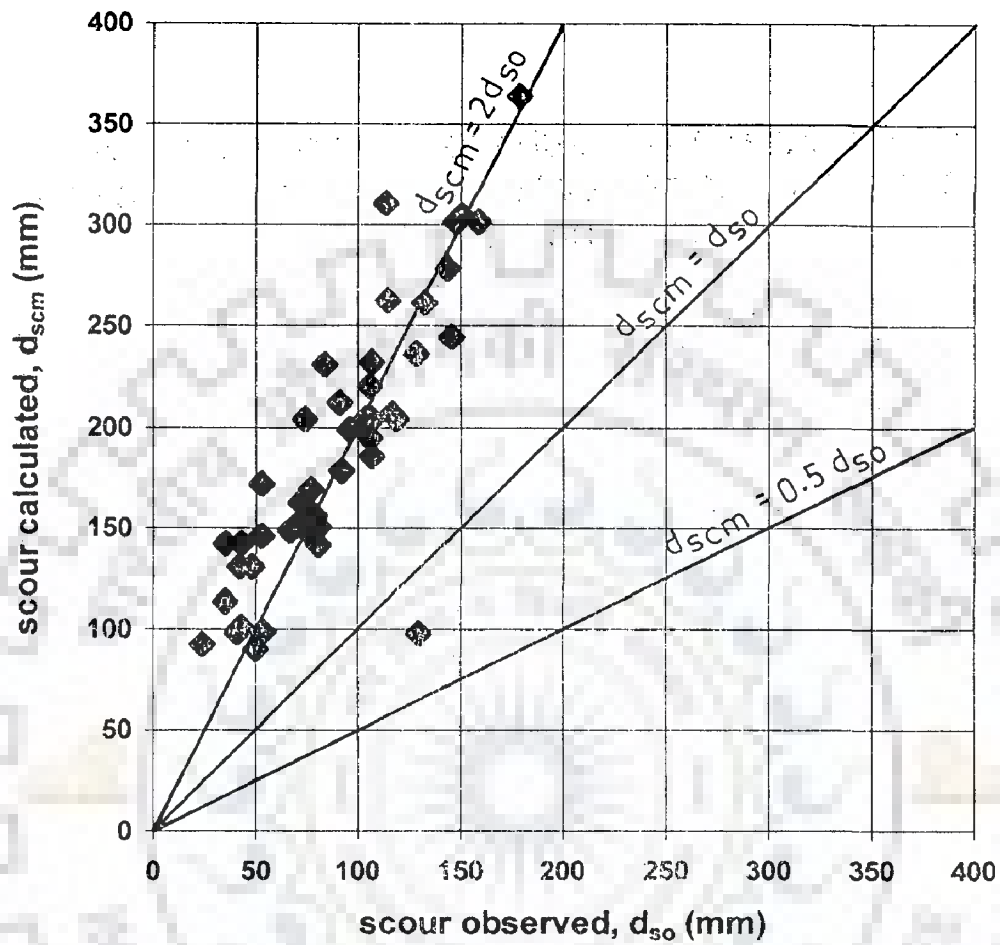


FIG 4.1; AGREEMENT BETWEEN COMPUTED (MELVILLE'S APPROACH 1999) AND OBSERVED SCOUR DEPTHS (GARDE & SUBRAMANYA1961)

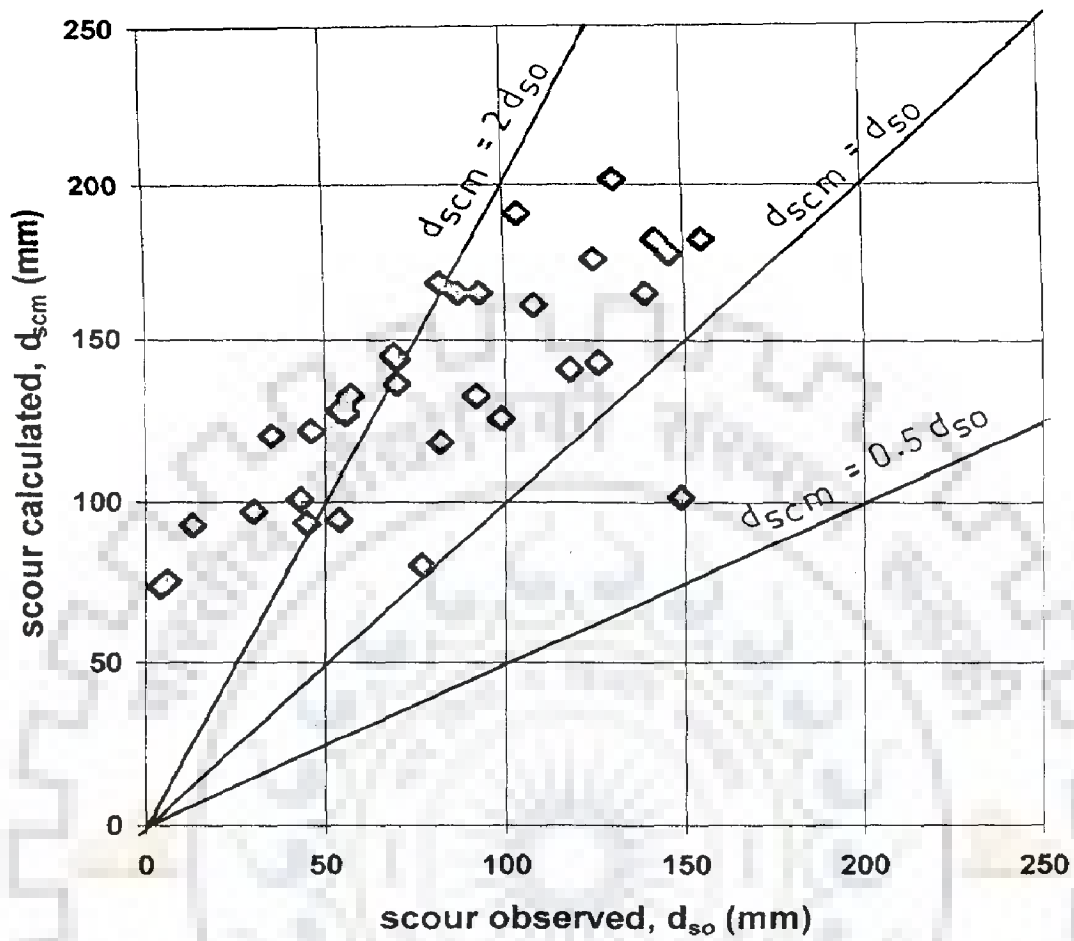


FIG 4.2: AGREEMENT BETWEEN COMPUTED (MELVILLE'S APPROACH 1999) AND OBSERVED SCOUR DEPTHS (NAMBUDRIPAD 1961)

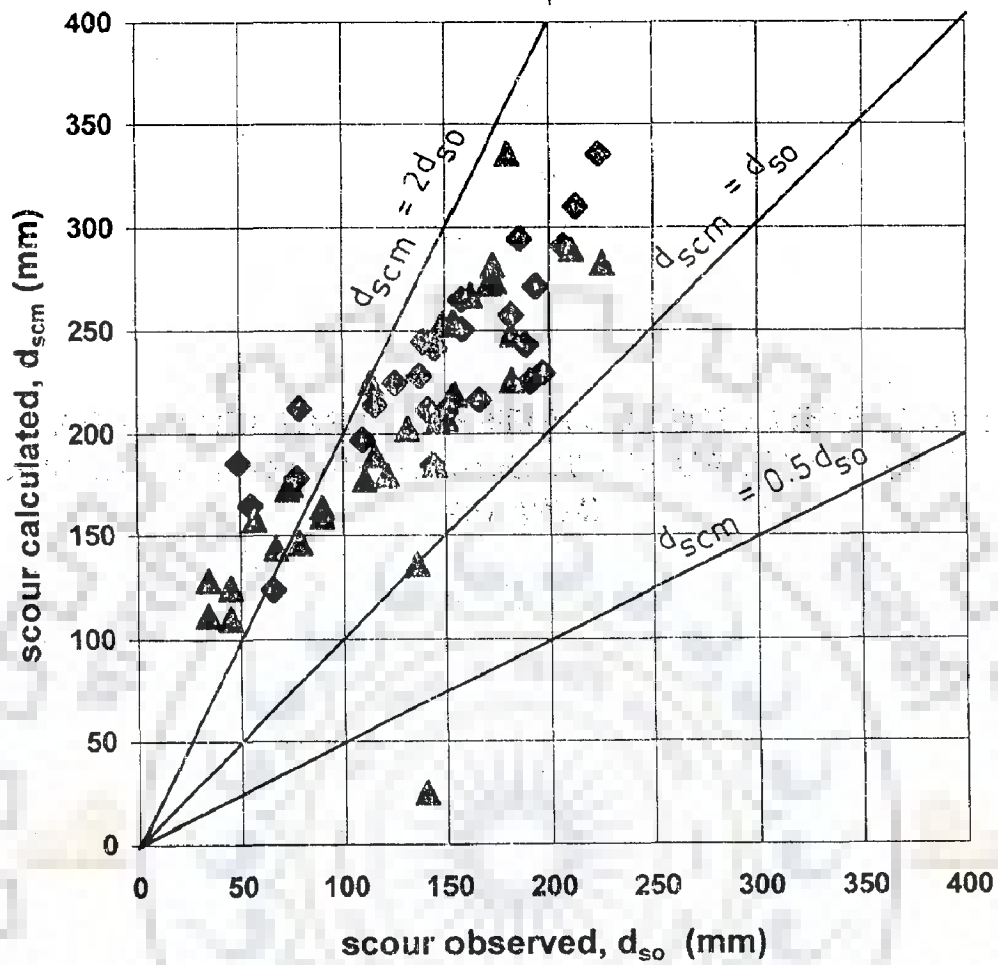


FIG 4.3: AGREEMENT BETWEEN COMPUTED (MELVILLE'S APPROACH 1999) AND OBSERVED SCOUR DEPTHS (RAMU (a) (b). 1964)

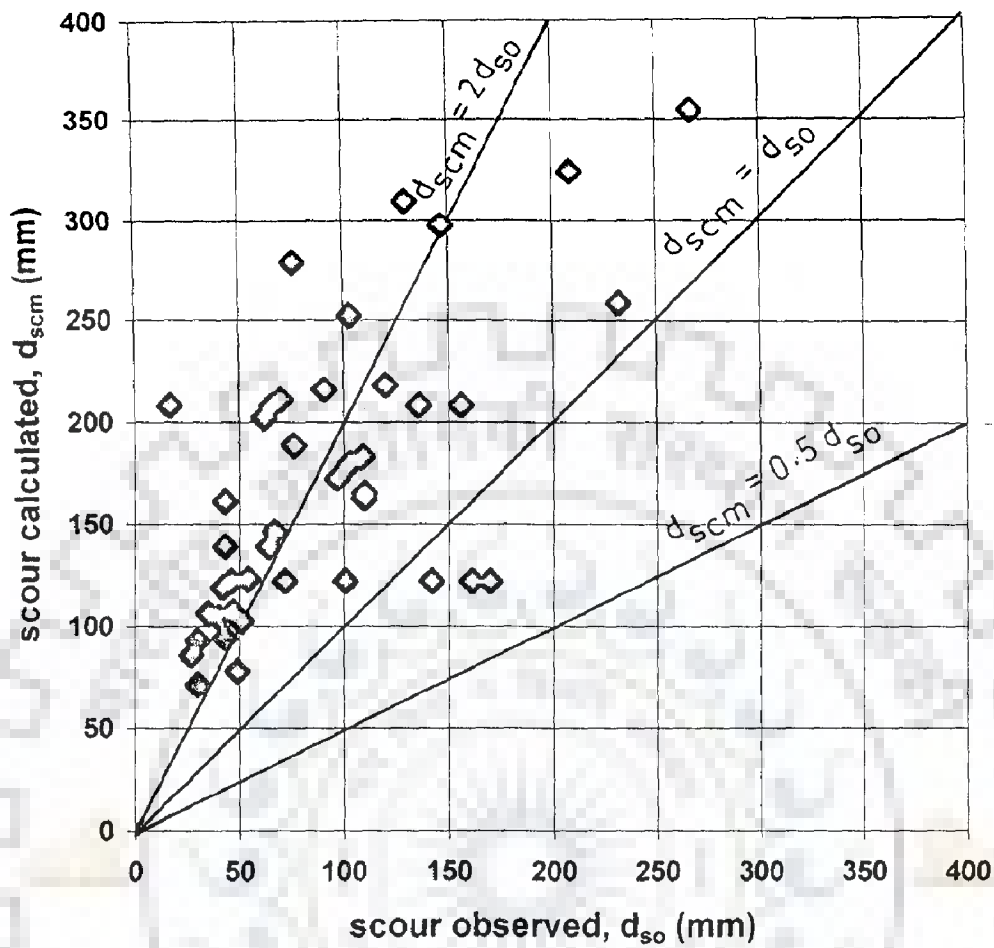


Fig 4.4: AGREEMENT BETWEEN COMPUTED (MELVILLE'S APPROACH 1999) AND OBSERVED SCOUR DEPTHS (TYAGI 1973)

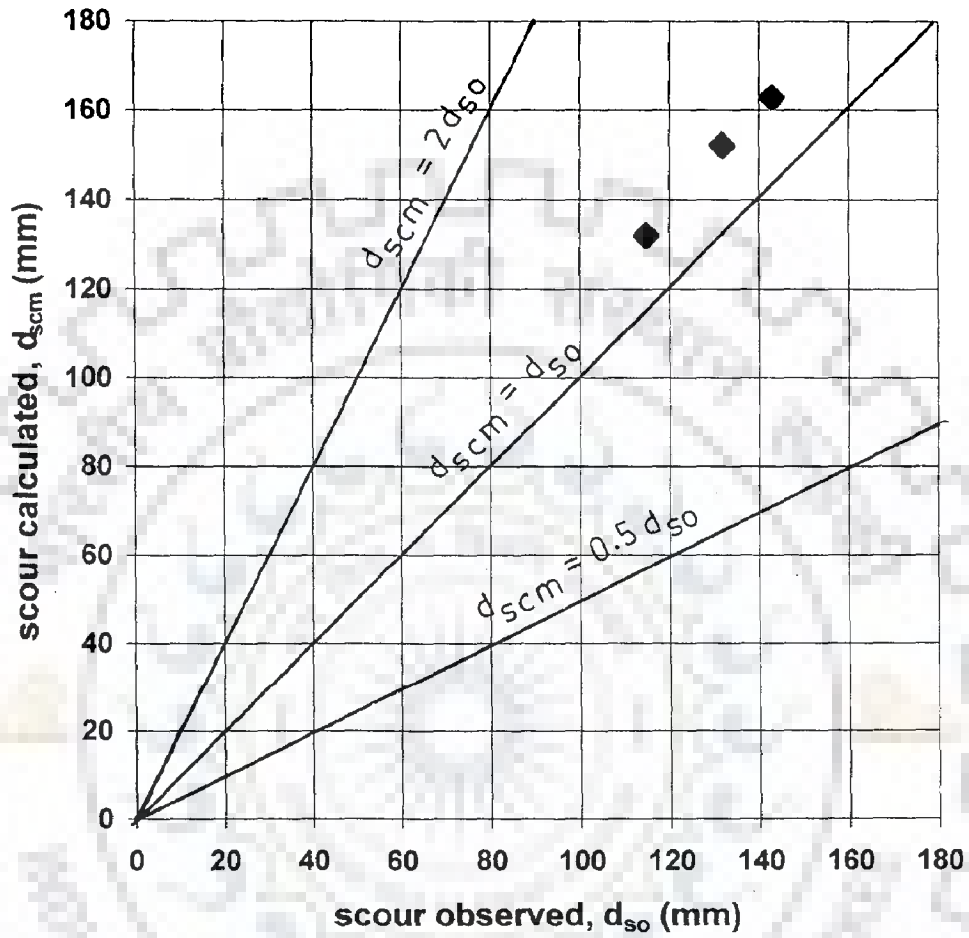


FIG 4.5: AGREEMENT BETWEEN COMPUTED (MELVILLE'S APPROACH 1999) AND OBSERVED SCOUR DEPTHS (SINGH, 1993)

Table 4.5 : Performance evaluation of Melville (1997) relationship.

Sl. No.	Source	No. of data	% of data with			% of data with	
			$d_{scm} > d_{so}$	$d_{scm} > 2d_{so}$	$d_{scm} = 2d_{so}$	$d_{scm} < 0.5d_{so}$	$d_{scm} < d_{so}$
1.	Garde and Subramanya (1960, 1961)	45	97.78	48.89	-	-	2.22
2.	Nambudripad (1961)	33	96.97	45.45	-	-	3.03
3.	Ramu 1st Series (1964)	26	100	15.38	3.85	-	-
	Ramu 2nd Series (1964)	35	94.29	22.85	2.86	2.86	2.86
4.	Tyagi (1967, 1973)	42	92.86	52.38	7.14	-	7.14
5.	Singh (1993)	3	100	-	-	-	-

If one agrees to the experimental findings of Melville (1997) that equilibrium time can be much larger than 3 to 6 hours, it is fair to say that the relationships based on the data used in this study require further retrospection in terms of their utility to equilibrium scour depth computations.

4.5 TESTING OF MELVILLE'S APPROACH USING PERMEABLE SPUR EXPERIMENTS

In order to study the feasibility of using Melville's approach for permeable spurs, one possible approach is to develop an effectiveness factor or K value corresponding to a given porosity. Let the scour depth computed by Melville's approach is d_{scm} by treating permeable spur as a solid spur. Thus, the effectiveness factor to account for the effect of porosity can be represented by the ratio d_{so}/d_{scm} .

Thus, attempts were made to develop plots between the ratio of d_{so}/d_{scm} with porosity for different sets of experiments. Fig. 4.6 a to d, shows some of these variations. It can be seen that the data do not collapse on a single curve, thus making it difficult to suggest a rational formula for the effectiveness factor. In view of Fig. 4.6 a to d, it was decided to develop another model for the experiments in phase II. A preliminary analysis towards this was also attempted to identify the important parameters with the help of visual interpretation of the bed profiles, as described next.

4.6 BED PROFILES IN CASE OF PERMEABLE SPURS

Study of bed profiles may be used to infer a lot. Indirectly, it reflects the intensity of flow at any point within the flow domain. If a point in the bed experiences

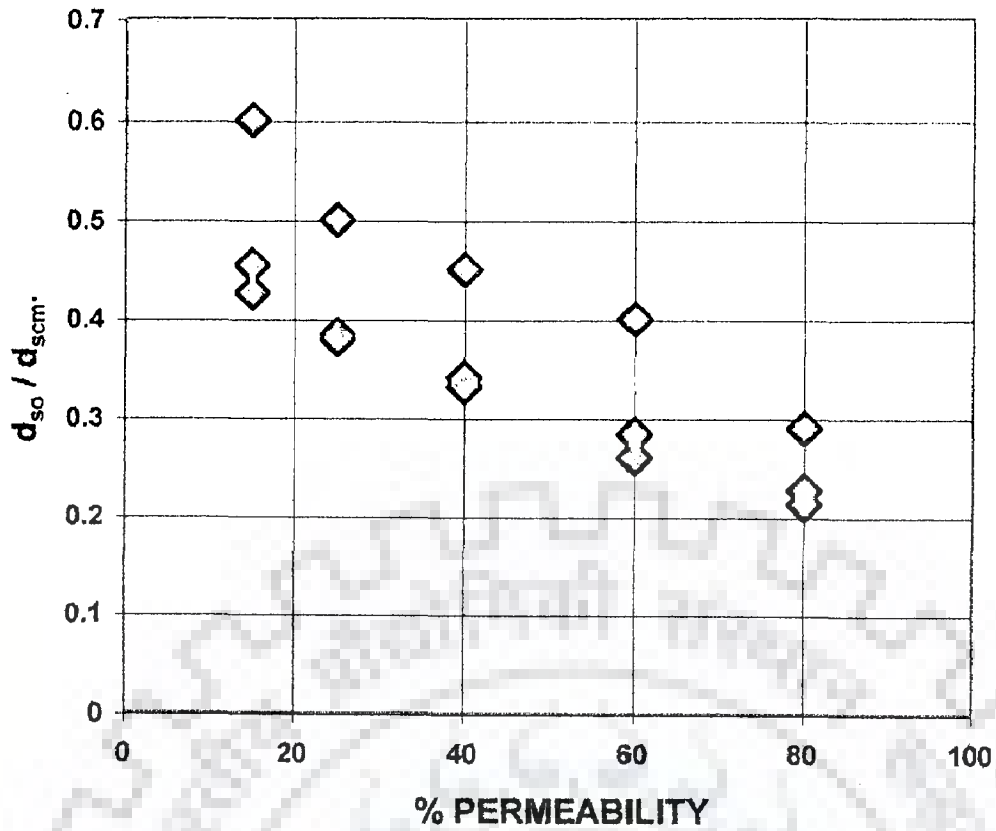


FIG. NO. 4. 6 a : VARIATION OF d_{50}/d_{scm} WITH PERMEABILITY IN $d_{50}=0.424\text{mm}$ GRAIN SIZE AND $b=5\text{cm}$.

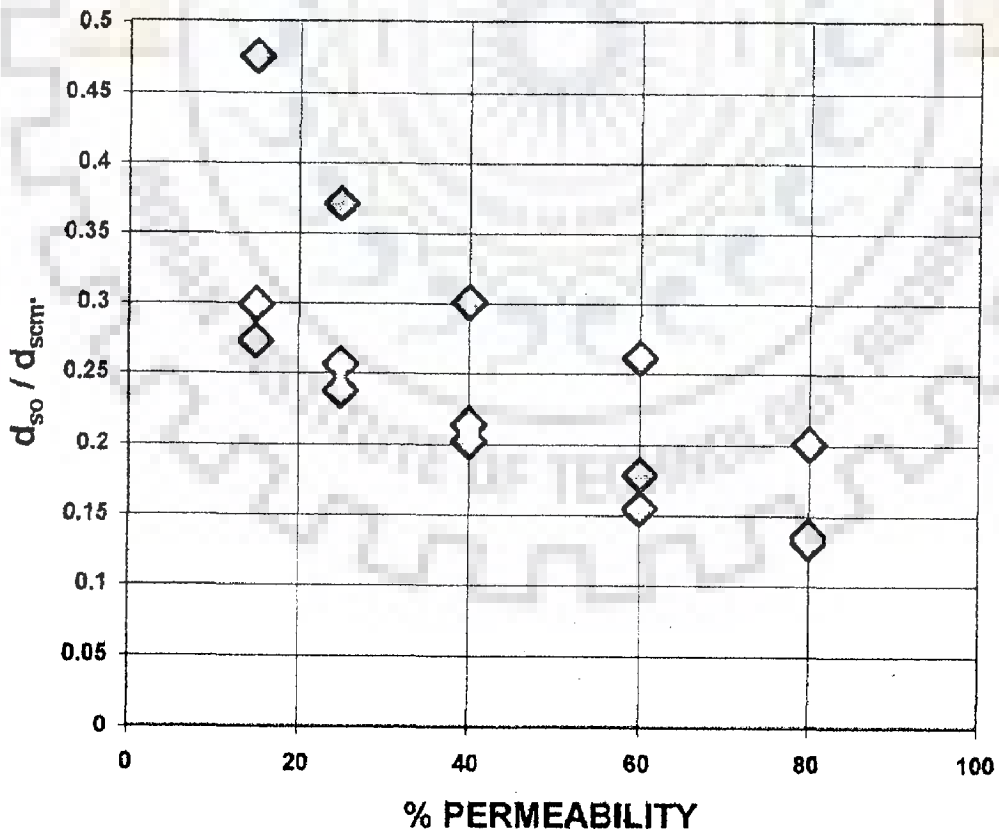


FIG. NO. 4. 6 b : VARIATION OF d_{50}/d_{scm} WITH PERMEABILITY IN $d_{50}=0.424\text{mm}$ GRAIN SIZE AND $b=10\text{cm}$.

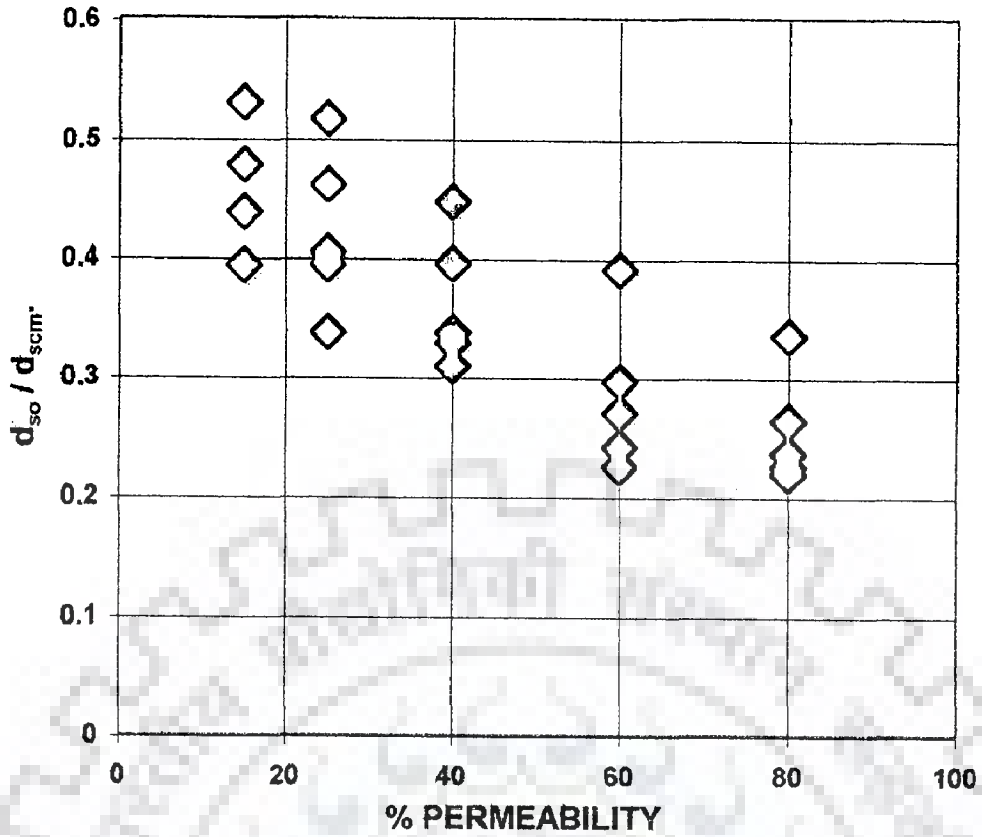


FIG. NO. 4. 6 c : VARIATION OF d_{50} / d_{scm} WITH PERMEABILITY IN $d_{50}=2.8\text{mm}$ GRAIN SIZE AND $b=5\text{cm}$.

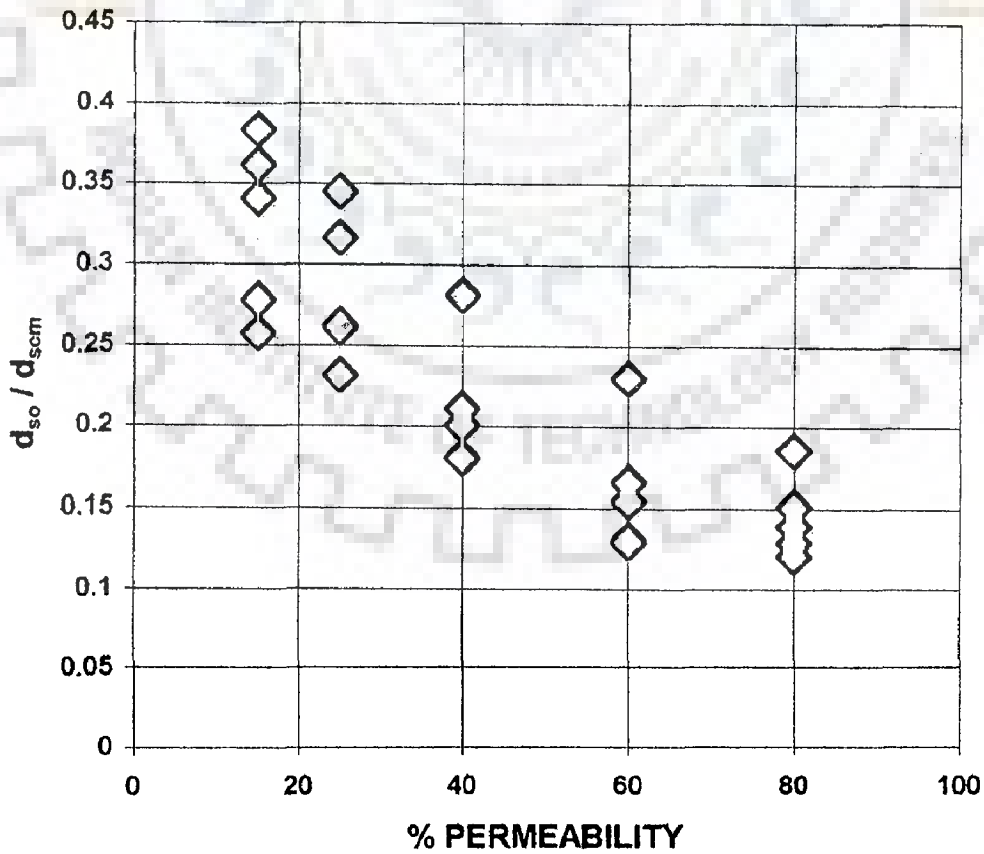


FIG. NO. 4. 6 d : VARIATION OF d_{50} / d_{scm} WITH PERMEABILITY IN $d_{50}=2.8\text{mm}$ GRAIN SIZE AND $b=10\text{cm}$.

scour, it means that the velocity is higher at that point in comparison to a point where deposition has taken place.

It is preferred to show interpolated bed profiles for experiment nos. P1E5 and P1A5 in Fig. 4.7 and Fig. 4.8 respectively. In each of these figures, the Froude number is 0.48 and the length of spur are 5cm with the porosity of the permeable pile spurs being 80% and 15% respectively. It can be seen that at high porosity, the tendency of scour is reduced significantly in comparison to that at lesser porosity.

4.7 SUMMARY

Assessment of Melville's approach is made Based on the analysis of 184 experiments on scour around solid spurs, it was observed that Melville's approach yielded higher values of calculated scour depths for more than 90% of data. These values would have been lower with the use of K-factor for the time. Development of K-factor for the time is necessary to model scour around solid spurs and it is advisable to conduct experiments for a longer time to see if Melville's observation of scour around bridge piers and abutments get fulfilled in case of solid spurs also. Feasibility of using Melville's approach to permeable spurs has been examined and the bed profiles are interpreted to identify the important variables influencing scour around permeable spurs.

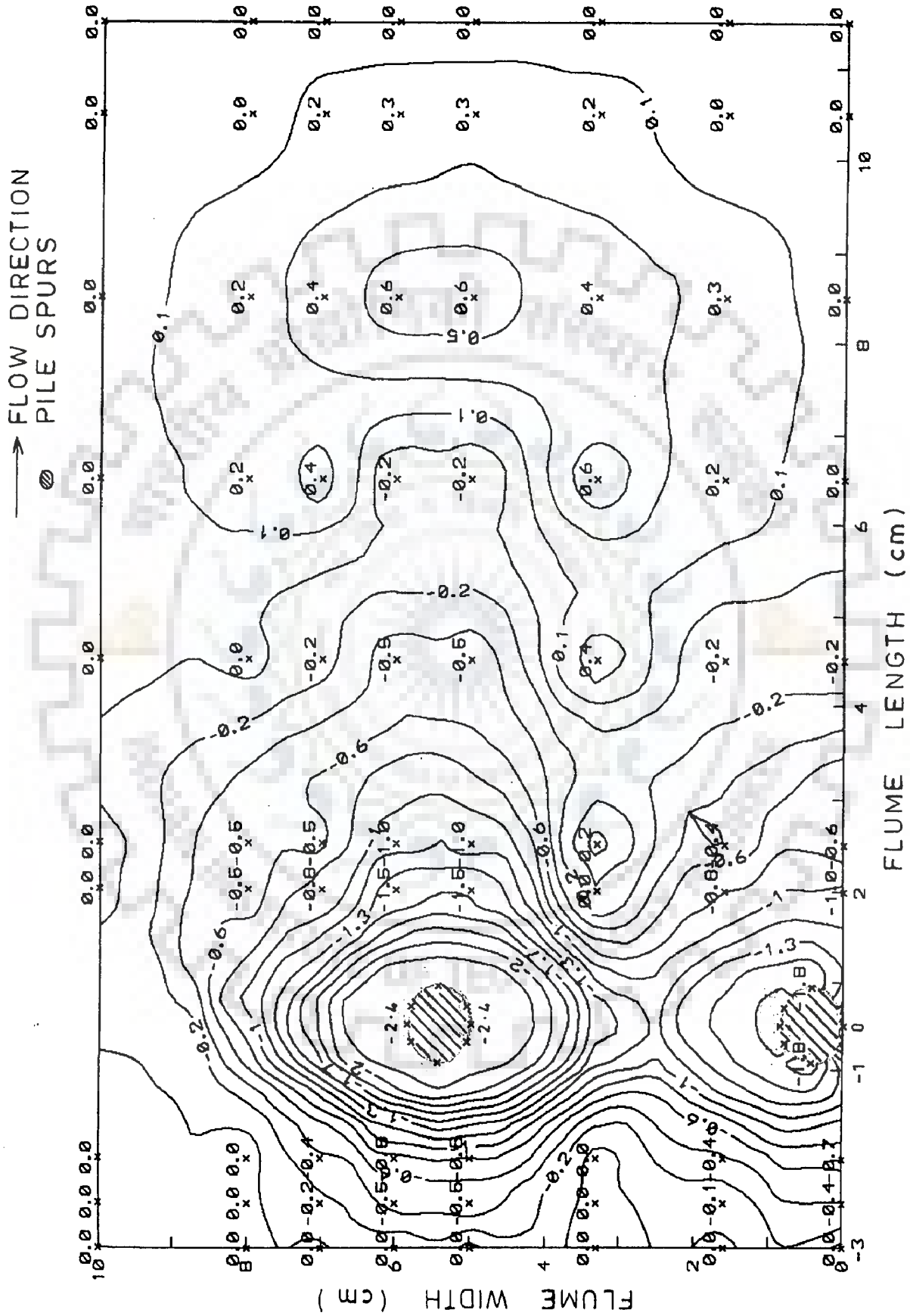


FIG. 4-7 INTERPOLATED BED PROFILES FOR EXPERIMENT NO. P1E5

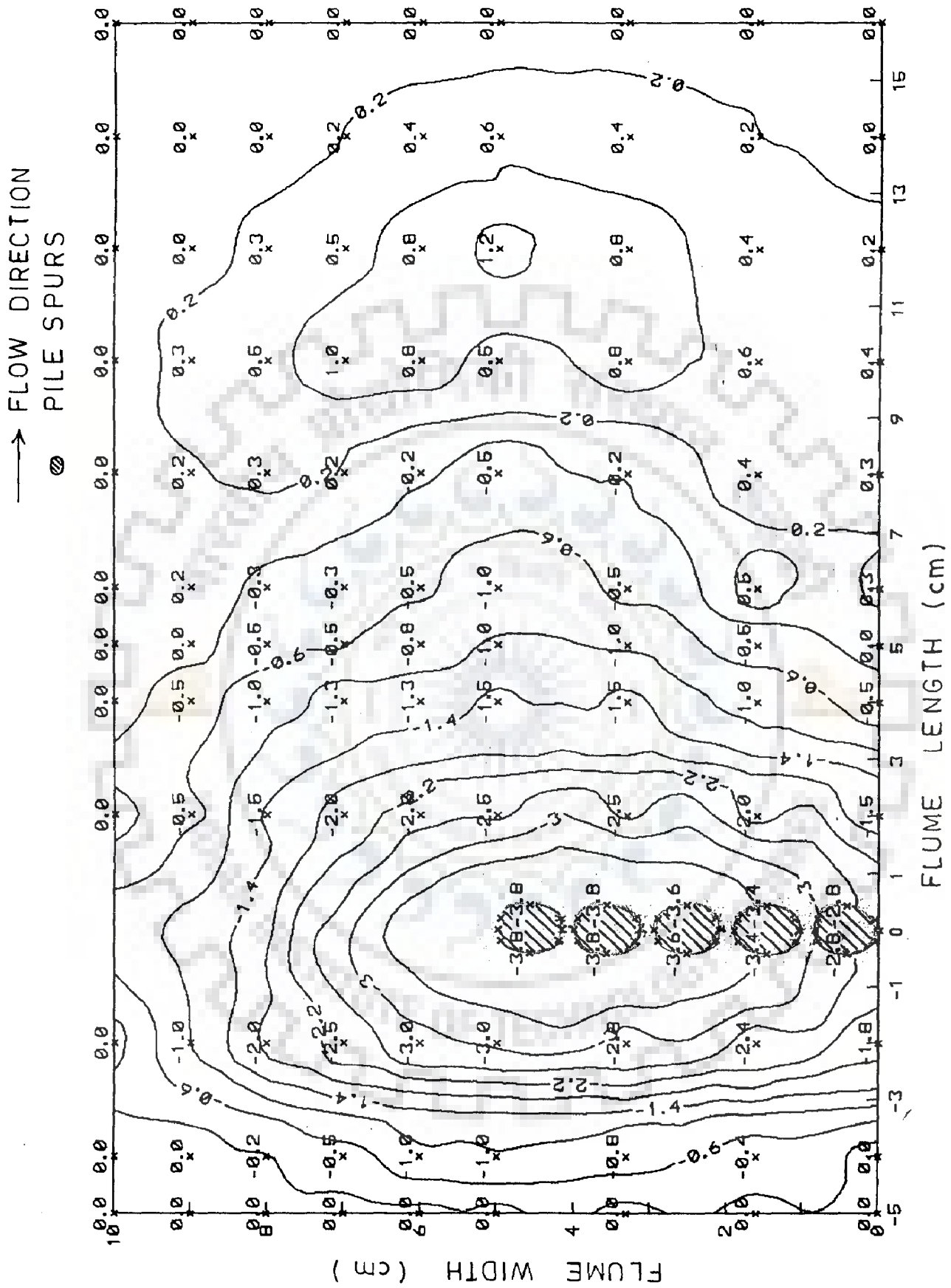


FIG. 4.8 INTERPOLATED BED PROFILES FOR EXPERIMENT NO. P1 A5

STEADY STATE MODELLING OF SCOUR

5.1 INTRODUCTION

In previous chapter, scour around different types of permeable spurs was described by subjecting these spurs to the action of steady flows. It was also observed that the minimum scour occurs around pile spurs. Considering the importance of these in Indian conditions, a large number of experiments were also performed and details of these experiments along with experimental data is included in Chapter 3. To get proper advantages of these experimental data, it is necessary to analyse these and develop some useful relationships for the estimation of equilibrium scour. The present chapter is an attempt in this direction.

5.2 FUNCTIONAL RELATIONSHIPS FOR SCOUR

Considering the fact that a large number of studies including those available to describe scour around bridge piers deal with a obstructed flow situation, it is logical to assume that the local scour around pile spurs will have similar dependency on variables describing flow, fluid, sediment and geometry .

For describing scour around spurs, Garde (1961) has identified the pertinent variables as follows: mean flow velocity V , average depth of flow y , mass density of water ρ_b , difference in specific wt. $\Delta\gamma$, dynamic viscosity μ , median size of sediment

d , standard deviation σ , difference in specific weight between sediment and water $\Delta\gamma_s$, channel width B , pier's width w , pier length b , shape parameters describing geometry of pier cross section ξ , and angle of inclination θ . In terms of these parameters, the following expression of scour depth, D_1 , relative to water surface was proposed by Garde (1961) as

$$D_1 = f(V, y, \rho_f, \Delta\gamma, \mu, d_{50}, \sigma, \Delta\gamma_s, B, b, w, \xi, \theta) \quad (5.1)$$

Using dimensionless analysis, equation (5.1) can be written as

$$\frac{D_1}{y} = f\left(\frac{B}{y}, \frac{d}{y}, \frac{B-b}{B}, \frac{\sigma}{y}, \frac{V}{\sqrt{gy}}, \theta, \frac{4 \Delta\gamma_s d}{3 \omega^2 \rho}, \frac{w}{b}, \xi\right) \quad (5.2)$$

In equation (5.2), ω is settling velocity of sediment particle. In equation (5.2), some of the dimensionless terms including $\left(\frac{B}{y}, \frac{d}{y} \text{ and } \frac{\sigma}{y}\right)$ have been found to be not very important and for these reasons they have been also ignored. A simplified form of the dimensionless relationship for the scour depth has been proposed as follows.

$$\frac{D_1}{y} = K \cdot \frac{1}{\alpha} \cdot F_r^m \quad (5.3)$$

In eq. (5.3),

$$\alpha = \frac{B-b}{B} \quad (5.4a)$$

and

$$F_r = \frac{V}{\sqrt{gy}} \quad (5.4b)$$

In eq. (5.3), K and n are functions of coefficient of drag. In the literature, K has been also expressed as

$$K = A.\eta_1 \eta_2 \eta_3 \quad (5.4c)$$

The coefficients η_1 , η_2 , and η_3 have been further related to $C_D, \frac{w}{b}, F_r, etc.$

As the present series of experiments have been performed under a limited state of conditions represented by two values of d and two values of b , it is not possible to perform a detailed investigation into variability of η_1 , η_2 , and η_3 . For these reasons, an attempt is made to calibrate a relationship of the following form.

$$\frac{d_{sc}}{d} = a' \cdot F_r^n \cdot \beta^r \quad (5.5)$$

In eq. (5.5), a' is an empirical constant. For the spur with certain porosity, p , the parameter β is defined as follows.

$$\beta = \frac{B - b}{0.01 \cdot b \cdot p} \quad (5.6)$$

In eq. (5.6), p is porosity in percentage. The use of parameter β is valid for the present experiments having variation of p between 20 to 80.

5.3 CALIBRATION OF THE SCOUR RELATIONSHIP

To calibrate the parameters a' , n , and r , the following error metric, E , is used.

$$E = \frac{100}{N} \sum \left| \frac{\text{observed scour depth} - \text{computed scour depth}}{\text{observed scour depth}} \right| \quad (5.7)$$

Equation (5.5) involves three unknown parameters. To have some idea about these parameters, one can process these scour observations in the following manner. Let us consider the experiment nos. P1A-1, P1A-2, P1A-3, P1A-4, and P1A-5. For these experiments, parameter beta is constant. Thus, if scour depth is plotted with respect to Froude number, one can have the following variation

$$d_{sc} = 153.77 F_r^{1.30} \quad (5.8)$$

The above variation is shown in Fig. 5.1. In eq. (5.8), the computed scour depth d_{sc} , is in mm. Similarly, for experiments no. P1A-1, P1B-1, P1C-1, P1D-1, and P1E-1, one can observe that in these experiments, F_r remains constant while the parameter beta varies in these experiments. Processing of scour data in these experiments leads to the following variation

$$d_{sc} = 1.5615 \beta^{0.467} \quad (5.9)$$

The plot of eq. (5.9) is shown in Fig. 5. 2. In eq. (5.9), the computed scour depth is in mm.

Equations (5.8) and (5.9) provide the basis for deciding the preliminary values/ranges of various model parameters. Using various combinations of these parameters, the relationships with minimum value of E were obtained for different sets of data.

For the experiments with $d_{50} = 2.8$ mm, flume width $B = 50$ cm and $b = 5$ cm, the following relationship has been calibrated

$$d_{sc} = 20.51 F_r^{1.2117} \beta^{.3649} \quad (5.10)$$

The error metric in obtaining eq. (5.10) was obtained as 7.93%.

Similarly for the experiments with $d_{50} = 2.8$ mm, $b = 10$ cm, the following relationship is calibrated as

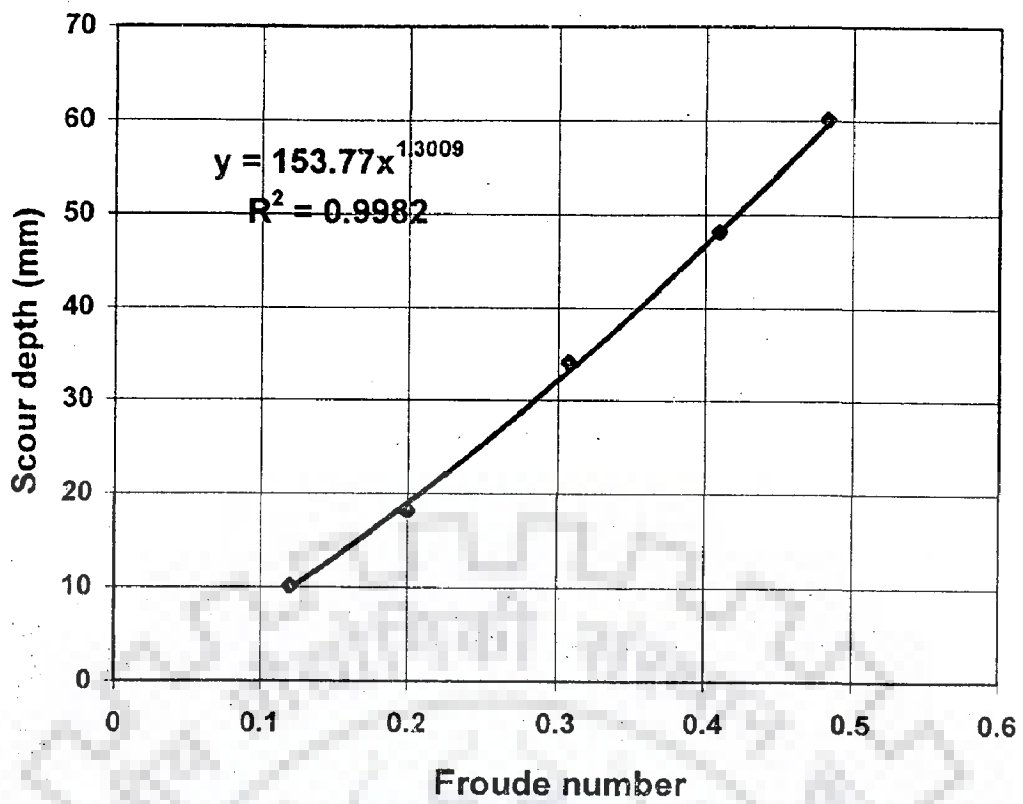


FIG. 5.1: SCOUR DEPTH IN RELATION TO F_r
($p = 15\%$, $b = 5\text{cm}$, $d = 2.8\text{mm}$)

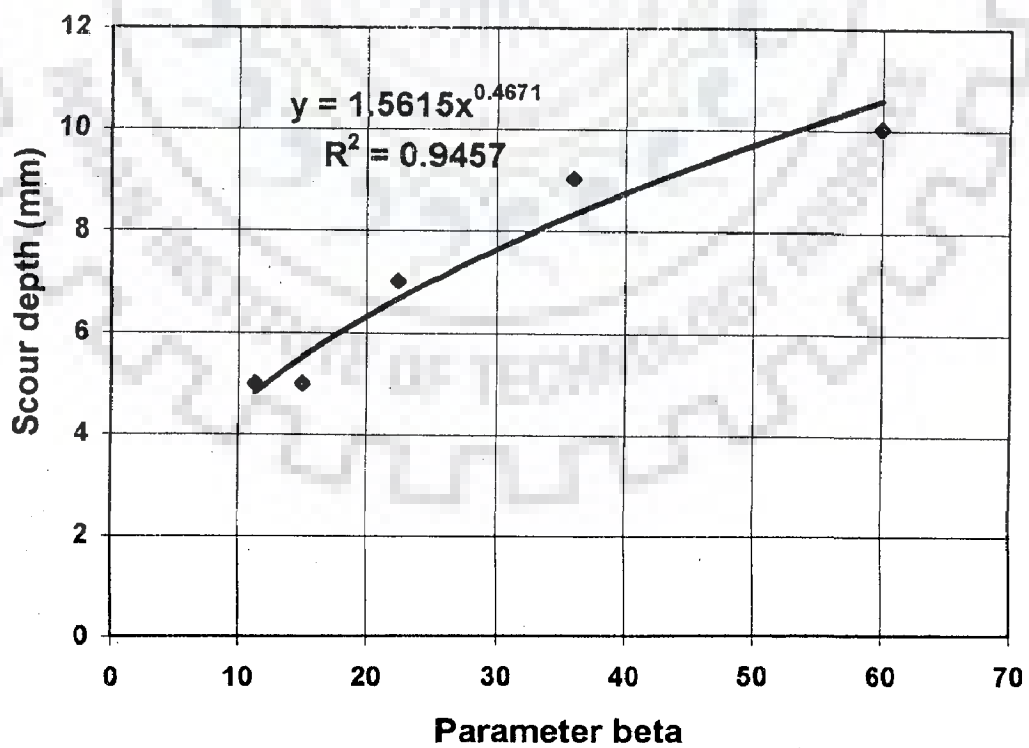


FIG. 5.2: SCOUR DEPTH IN RELATION TO BETA
($F_r = 0.12$, $b = 5\text{cm}$, $d = 2.8\text{mm}$)

$$d_{sc} = 20.51 F_r^{1.2117} \beta^{.605} \quad (5.11)$$

The error metric associated with eq. (5.9) is 5.32 %.

For experiments with d_{50} as 0.424 mm and $b = 5$ cm, the relationship of similar nature has been obtained as follows.

$$d_{sc} = 52.67 F_r^{1.2117} \beta^{.3649} \quad (5.12)$$

Average error in obtaining eq. (5.12) was 6.9%.

Similarly for $d_{50} = 0.424$ mm and $b = 10$ cm, the relationship was obtained as

$$d_{sc} = 52.67 F_r^{1.2117} \beta^{.6226} \quad (5.13)$$

Average error in obtaining eq. (5.13) has been 12.05%.

It is interesting to see from (5.10) to (5.13) that the exponent of β is 0.3649 for $b = 5$ cm and is around 0.6 for $b = 10$ cm. In eqs. (5.10) –(5.13), the scour depth is in mm.

The performance of the calibrated relationships is shown in Fig. 5.3a-5.3d. Also, the error lines are shown in these figures for assessing the merit of calibration in developing eqs. (5.10) to (5.13).

5.4 CALIBRATION OF DIMENSIONLESS RELATIONSHIPS

Eqs.(5.10)-(5.13) are not dimensionless in nature. These equations can be recast into a series of dimensionless relationships. For example, non-dimensionalizing d_{sc} as d_{sc}/w , where w is the width or diameter of a spur may lead to following form of eqs. 5.10-5.13, respectively.

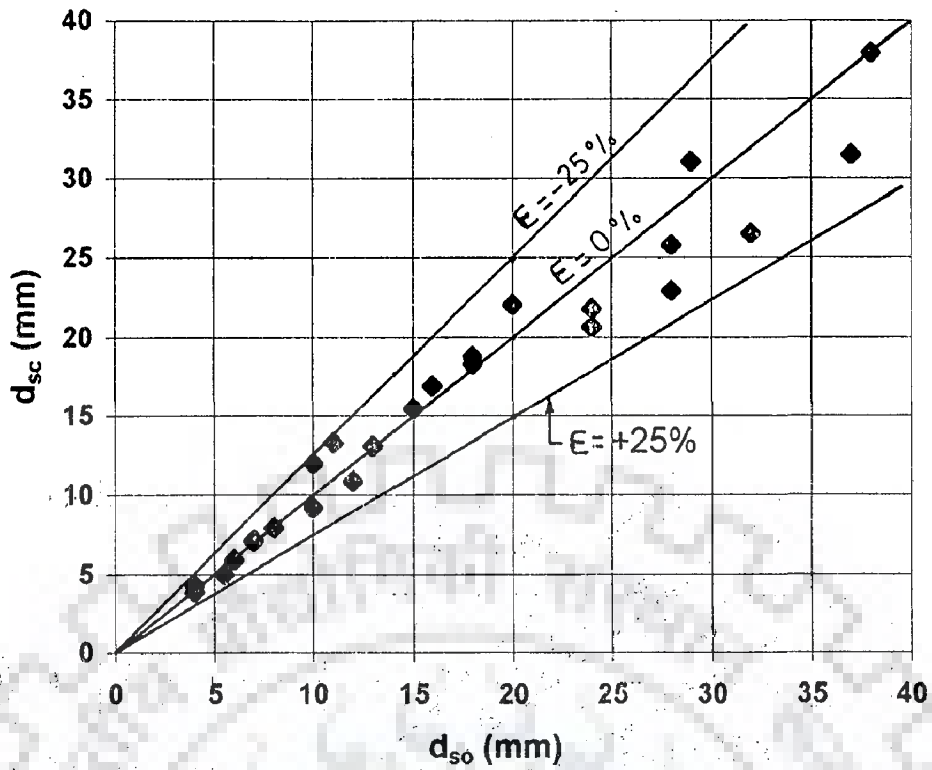


FIG. 5.3 a: AGREEMENT BETWEEN COMPUTED AND OBSERVED SCOUR DEPTH FOR PILE SPURS ($d = 2.8\text{mm}$, $b = 50\text{mm}$)

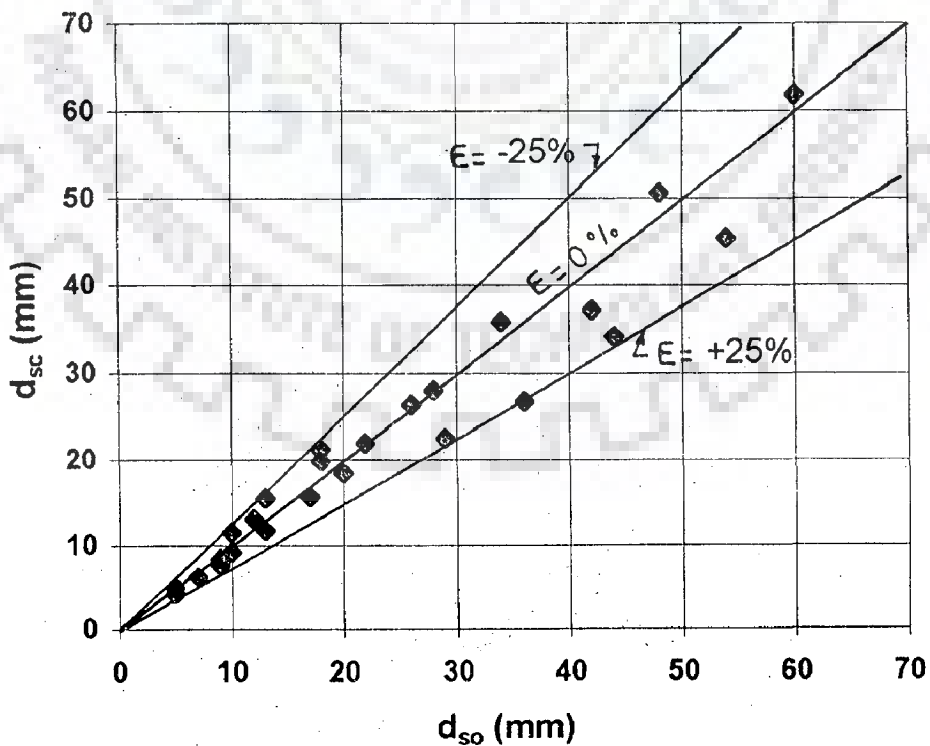


FIG. 5.3 b: AGREEMENT BETWEEN COMPUTED AND OBSERVED SCOUR DEPTH FOR PILE SPURS ($d = 2.8\text{mm}$, $b = 100\text{mm}$)

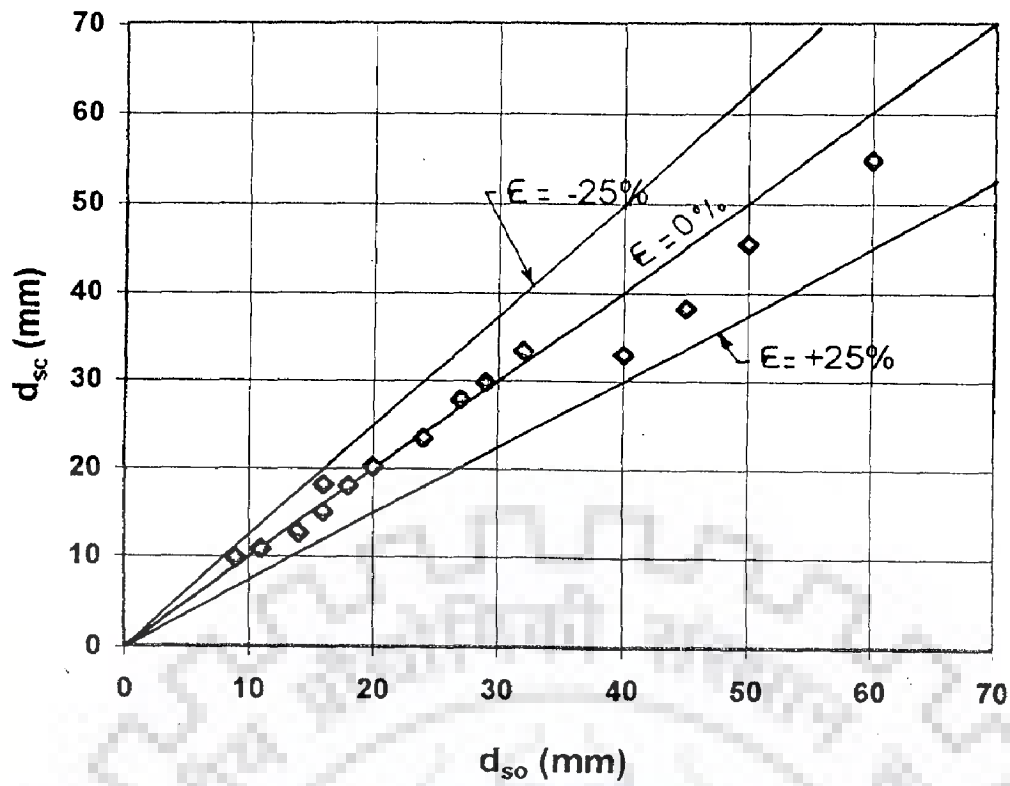


FIG. 5.3 c : AGREEMENT BETWEEN COMPUTED AND OBSERVED SCOUR DEPTH FOR PILE SPURS ($d = 0.424\text{mm}$, $b = 50\text{mm}$)

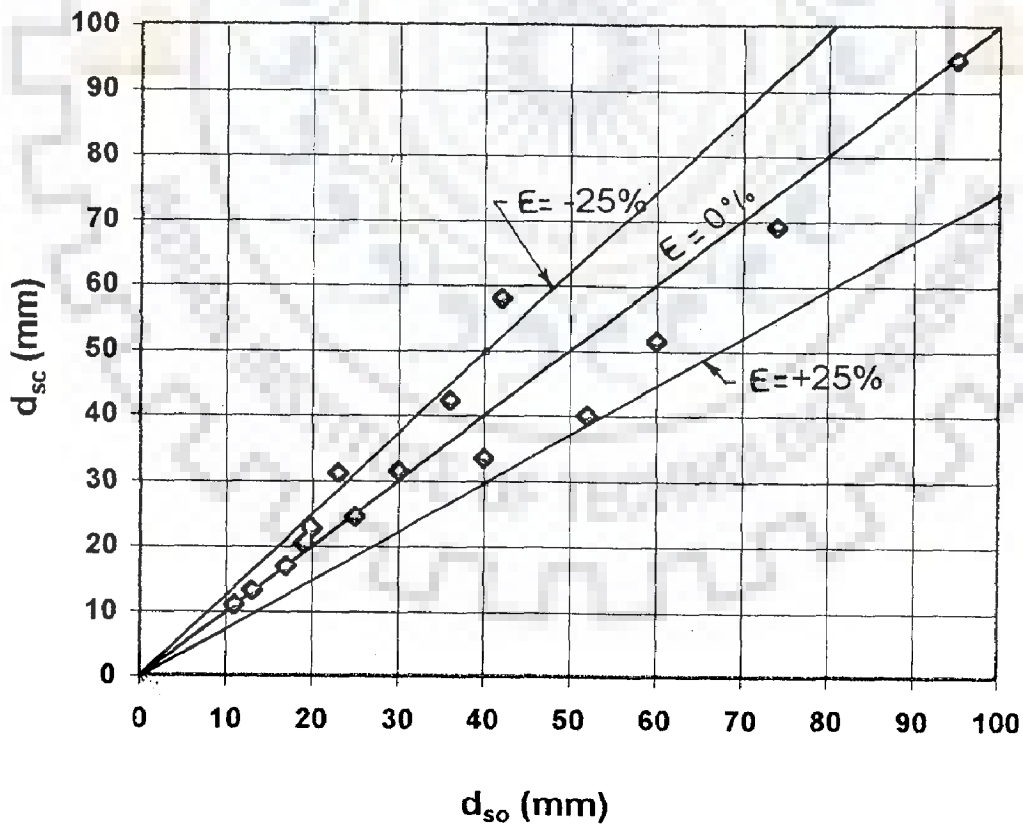


FIG. 5.3 d : AGREEMENT BETWEEN COMPUTED AND OBSERVED SCOUR DEPTH FOR PILE SPURS ($d = 0.424\text{mm}$, $b = 100\text{mm}$)

$$\frac{d_{sc}}{w} = 2.413 F_r^{1.2117} \beta^{.3649} \quad (5.14)$$

$$\frac{d_{sc}}{w} = 2.413 F_r^{1.2117} \beta^{.605} \quad (5.15)$$

$$\frac{d_{sc}}{w} = 6.197 F_r^{1.2117} \beta^{.3649} \quad (5.16)$$

$$\frac{d_{sc}}{w} = 6.197 F_r^{1.2117} \beta^{.6226} \quad (5.17)$$

Similarly, if d_{sc} is non-dimensionalized as d_{sc}/d , eqs. 5.10 to 5.13 may be transformed to eqs. (5.18)-(5.21), respectively,

$$\frac{d_{sc}}{d} = 7.33 F_r^{1.2117} \beta^{.3649} \quad (5.18)$$

$$\frac{d_{sc}}{d} = 7.33 F_r^{1.2117} \beta^{.605} \quad (5.19)$$

$$\frac{d_{sc}}{d} = 124.33 F_r^{1.2117} \beta^{.3649} \quad (5.20)$$

$$\frac{d_{sc}}{d} = 124.33 F_r^{1.2117} \beta^{.6226} \quad (5.21)$$

Another choice of using eqs. (5.10) to (5.13) in a dimensionless form may be with the help of flow depth, y . In this case, eqs. (5.10) to (5.13) may be transformed to eqs. (5.22)-(5.25), respectively.

$$\frac{d_{sc}}{y} = 0.186 F_r^{1.2117} \beta^{.3649} \quad (5.22)$$

$$\frac{d_{sc}}{y} = 0.186 F_r^{1.2117} \beta^{.605} \quad (5.23)$$

$$\frac{d_{sc}}{y} = 0.527 F_r^{1.2117} \beta^{.3649} \quad (5.24)$$

$$\frac{d_{sc}}{y} = 0.527 F_r^{1.2117} \beta^{.6226} \quad (5.25)$$

The use of parameter b leads to the following non-dimensionalised form of eqs. 5.10-5.13.

$$\frac{d_{sc}}{b} = 0.41 F_r^{1.2117} \beta^{.3649} \quad (5.26)$$

$$\frac{d_{sc}}{b} = 0.205 F_r^{1.2117} \beta^{.605} \quad (5.27)$$

$$\frac{d_{sc}}{b} = 1.054 F_r^{1.2117} \beta^{.3649} \quad (5.28)$$

$$\frac{d_{sc}}{b} = 0.527 F_r^{1.2117} \beta^{.6226} \quad (5.29)$$

Another way to non-dimensionalize the scour depth may be with the help of channel width, B . With the use of this, eqs. (5.10)-(5.13) transform to

$$\frac{d_{sc}}{B} = 0.041 F_r^{1.2117} \beta^{.3649} \quad (5.30)$$

$$\frac{d_{sc}}{B} = 0.041 F_r^{1.2117} \beta^{.605} \quad (5.31)$$

$$\frac{d_{sc}}{B} = 0.1054 F_r^{1.2117} \beta^{.3649} \quad (5.32)$$

$$\frac{d_{sc}}{B} = 0.1054 F_r^{1.2117} \beta^{.6226} \quad (5.33)$$

5.5 VALIDATION OF CALIBRATED RELATIONSHIPS

It can be seen from the preceding section that based on a limited set of experiments, it is possible to evolve many dimensionless relationships. However, all of these relationships are not acceptable. To identify a suitable relationship, it is essential to test the performance of these relationships at a different scale. By different scale, we mean the experimental conditions, which are different than those used in the process of calibration.

To test the performance of above relationships, an experimental program was undertaken in a nearby stream, known as Solani. In Chapter 3, details of the experimental program are given. Table 5.1 provides the data collected in the experiment within an interval of 0-24 hrs. As four different types of permeable spurs have been used in the field, details of these spurs with regard to their lengths b and porosity p are also included in Table 5.1. The average size of the bed particle is 0.21 mm. The values reported for the flow variables are the average values within the time interval.

Table 5.1: Data related to different permeable pile spurs (placed in Solani river) for steady state analysis (width of pile spur = 6 cm, and width of Solani river as 30.0 m)

Spur type	b(m)	p (%)	V(m/s)	D (m)	Q (m ³ /s)	d (mm)	d _{so} (m)
RA	3.0	20	0.320	0.387	3.70	0.30	0.575
RB	3.0	40	0.320	0.387	3.70	0.30	0.385
RC	3.0	60	0.320	0.387	3.70	0.30	0.200
RD	3.0	80	0.320	0.387	3.70	0.30	0.090

The conditions of the experiments correspond closely to those of 0.424 mm bed particle size and b/B ratio of 0.1. For this reason, we have considered only eqs. (5.12), (5.16), (5.20), (5.24), (5.28) and (5.32) for validation. With the assumption that steady state scour had developed in first 24 hrs, we considered this scour for validation using these equations. In the next chapter, this assumption is relaxed. Here, the discharge is considered steady and equal to the average of discharge within first 24 hours. The data used for steady state analysis are processed and shown in Table 5.2. Using the data from Table 5.2, the steady state scour is computed using eqs. (5.12), (5.16), (5.20), (5.24), (5.28) and (5.32).

Table 5.2 : Performance evaluation of different dimensionless scour relationships

Spur Type	d _{so} (m)	d _{sc} (m), eq. 5.12	d _{sc} (m), eq. 5.16	d _{sc} (m), eq. 5.20	d _{sc} (m), eq. 5.24	d _{sc} (m), eq. 5.28	d _{sc} (m), eq. 5.32
RA	0.575	0.0229	0.162	0.0162	0.088	1.375	1.375
RB	0.385	0.0178	0.126	0.0126	0.0689	1.068	1.068
RC	0.200	0.0154	0.108	0.0109	0.0594	0.921	0.921
RD	0.090	0.0138	0.0976	0.0098	0.0535	0.829	0.829

In Figures 5.4a-d, a comparison of observed scour and those predicted by these equations is also presented. It can be seen from these figures that eq. 5.16 provides relatively a better agreement with the observed values indicating its acceptability, as a representative dimensionless relationship. The purpose of using eq. (5.16) is to identify a suitable parameter for making the scour term dimensionless. Despite the fact that it is based on a diameter of 0.424 mm and is tested for a condition conforming to 0.424 mm, it helps in the correct identification of scaling parameter w . The discussion related to the development of a generalized model based on the lab data as well as development of critical velocity based models is best included in Chapter 7.

5.6 SUMMARY

In this Chapter, a set of equations for representing scour have been calibrated. The equations pertaining to minimum error have been given preference for inclusion and their validity is limited to the range of parameters used here. As the nature of data is restricted in respect of many variables, no attempt was made to develop a generalized model in this Chapter. Use of the ratio of shear velocity to flow velocity can be also considered in the analysis, as in the literature, this parameter reflects the behavior that as the velocity of flow becomes less than or equal to the critical shear velocity, the scour becomes zero. However, the error introduced by this parameter is always on a conservative side. Nevertheless, a relationship in terms of the critical velocity is developed in Chapter 7 to cover certain issues related to scour prediction. It is also cautioned to not use the suggested relationships for spurs with zero

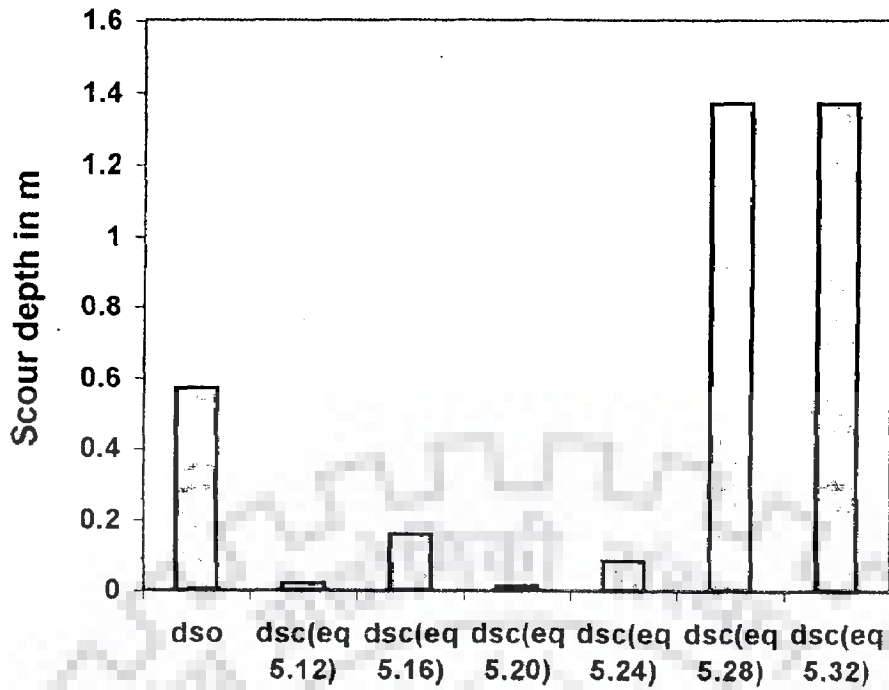


FIG.5.4 a : PERFORMANCE EVALUATION OF VARIOUS EQUATIONS TO JUDGE THE SUITABLE SCALING PARAMETERS (SPUR TYPE-RA)

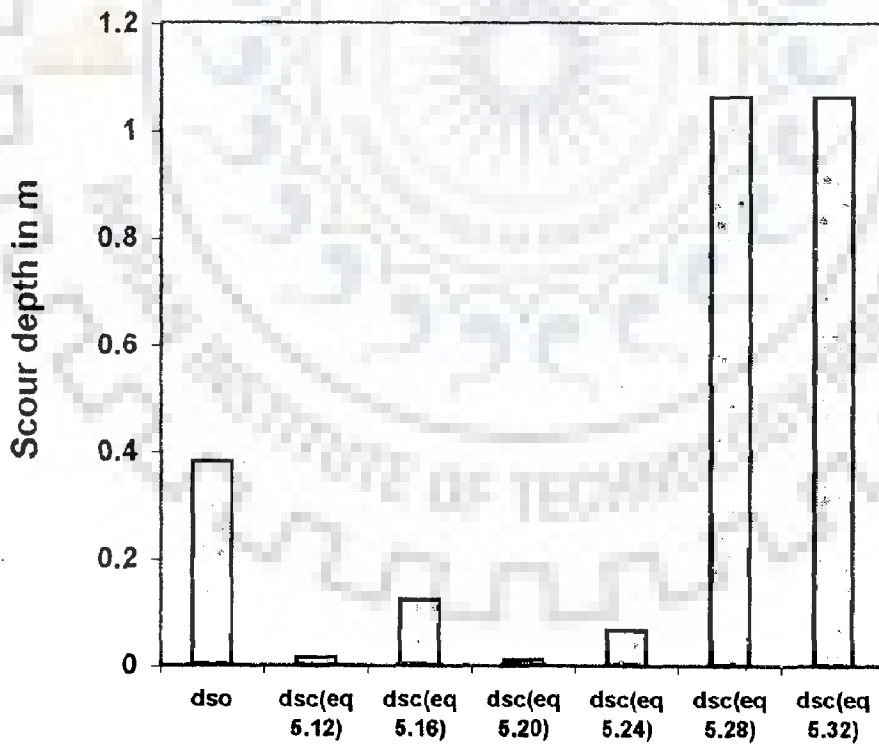


FIG.5.4 b: PERFORMANCE EVALUATION OF VARIOUS EQUATIONS TO JUDGE THE SUITABLE SCALING PARAMETERS (SPUR TYPE-RB)

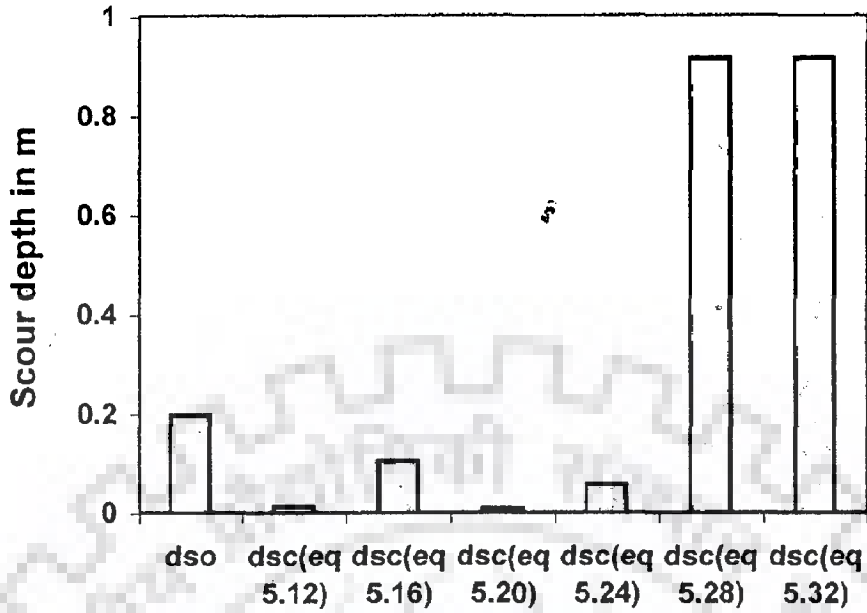


FIG.5.4 c : PERFORMANCE EVALUATION OF VARIOUS EQUATIONS TO JUDGE THE SUITABLE SCALING PARAMETERS (SPUR TYPE-RC)

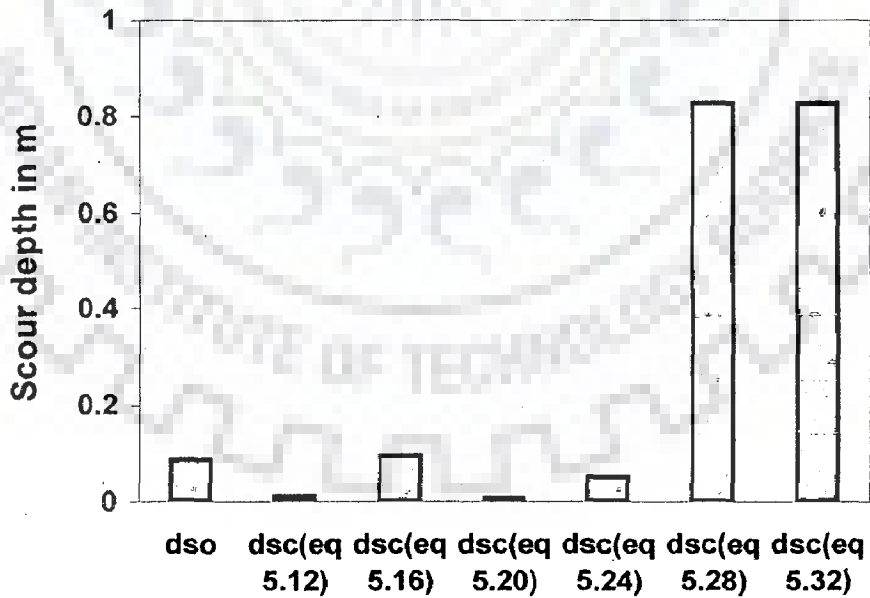


FIG.5.4 d : PERFORMANCE EVALUATION OF VARIOUS EQUATIONS TO JUDGE THE SUITABLE SCALING PARAMETERS (SPUR TYPE-RD)

permeability, as the range of these relationships included the porosity variation from 20% to 80%. In the field, the permeable spurs have been provided with a porosity around 40-50 % (personal communication, Mr. Y.N. Goyal, Ex. Engineer, IRI, Roorkee). The reduction in porosity may occur due to entrapment of silt/sand and the porosity may drop. However, this reduction in porosity has never been found to correspond to an impermeable spur situation. The present Chapter also indicates that among many ways of non-dimensionalising the scour depth, the use of pier width appears to be a relatively better performer for field applications.



MODELLING OF TRANSIENT SCOUR

VARIATION

6.1 INTRODUCTION

In natural condition, frequently encountered in alluvial streams, the flow is in rarely a steady state. This is particularly true when the river is in flood stage. Thus, computation of steady state scour based on maximum flood discharge (assumed to be steady) may lead to estimates of scour depth on a non-conservative side. For this reason, the transient modelling of scour has received the attention in literature. Basically, the approach suggested in the literature considers the unsteady discharge into different segments of assumed quasi steady state discharges. In this chapter, the field experiments, which were conducted in a nearby stream, are considered for the analysis. The chapter begins with the analysis of transient variations of scour in lab based experiments and based on the analysis of such experiments data, reliability of scour depth estimation in field condition is also investigated.

6.2 ANALYSIS OF LAB EXPERIMENTS FOR TRANSIENT SCOUR

It has been described in Chapter 3 that a total of 80 experiments on pile spurs were subjected to steady flows. In each of these experiments, the scour varies with time and after some time, the variation of scour may not be significant. In fact, there

are differences in precisely identifying this equilibrium time, corresponding to the equilibrium scour depth (also the maximum scour depth in case of clear water flow). According to Melville and Chiew (1999), the equilibrium time is attained in days. In fact, it is apparent from Chapter 5 that the experiment performed at Roorkee, in particular, have reported equilibrium time, which is of the order of few hours only. In the course of present investigation, we tried to study the variation of scour for a longer time extending beyond 24 hrs. However, such an endeavour could not be continued because of the difficulty of having continuous power supply. Thus, the experiments in this study might be underestimating the equilibrium scour depth.

For the 80 lab experiments, Fig. 6.1(a)..(n) show the variation of dimensionless scour term, which is equal to the ratio of observed scour depth at any time to equilibrium scour depth, with time. To model the variation of this dimensionless scour term with time, a variety of options were attempted. However, it was observed that the transient scour during a steady state could be best achieved by following type of expression. Considering the depth of scour at any time is d_{st} and equilibrium scours depth as d_{se} , the relationship for the transient variation of scour during steady flow can be represented as

$$\frac{d_{st}}{d_{se}} = a \cdot \exp(b' \cdot t) \quad (6.1)$$

In eqn (6.1), a and b' are model parameters. The fit of eq. (6.1) is shown in Fig. 6.1. Table 6.1 provides a summary of the calibrated model parameters for various experiments. It is emphasized that a functional form similar to eq. (6.1)] was also used by Ahmad (1953) to describe the temporal scour.

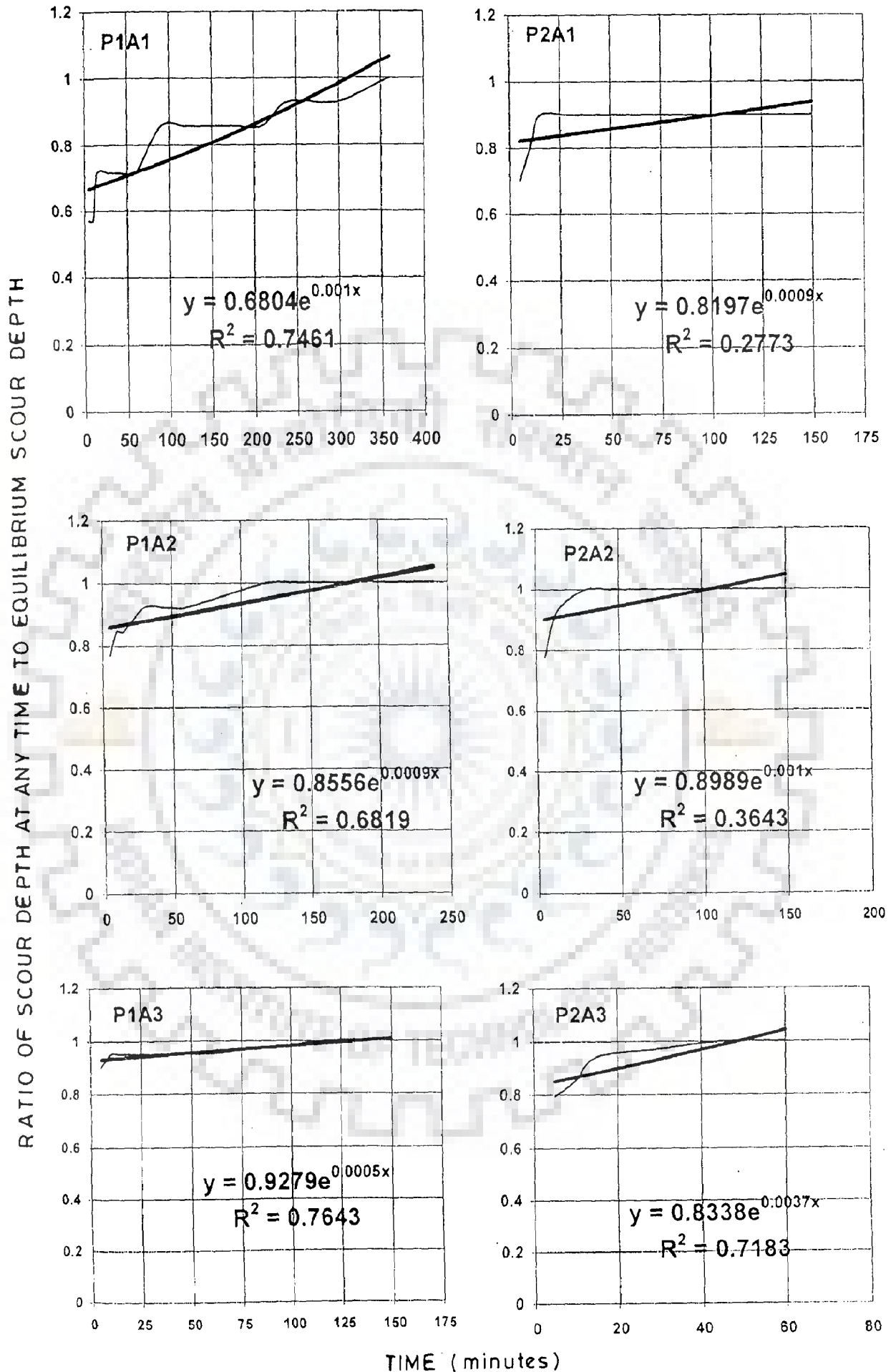


FIG. 6-1 (a) TEMPORAL VARIATION OF SCOUR DEPTH UNDER STEADY FLOW (LAB DATA)

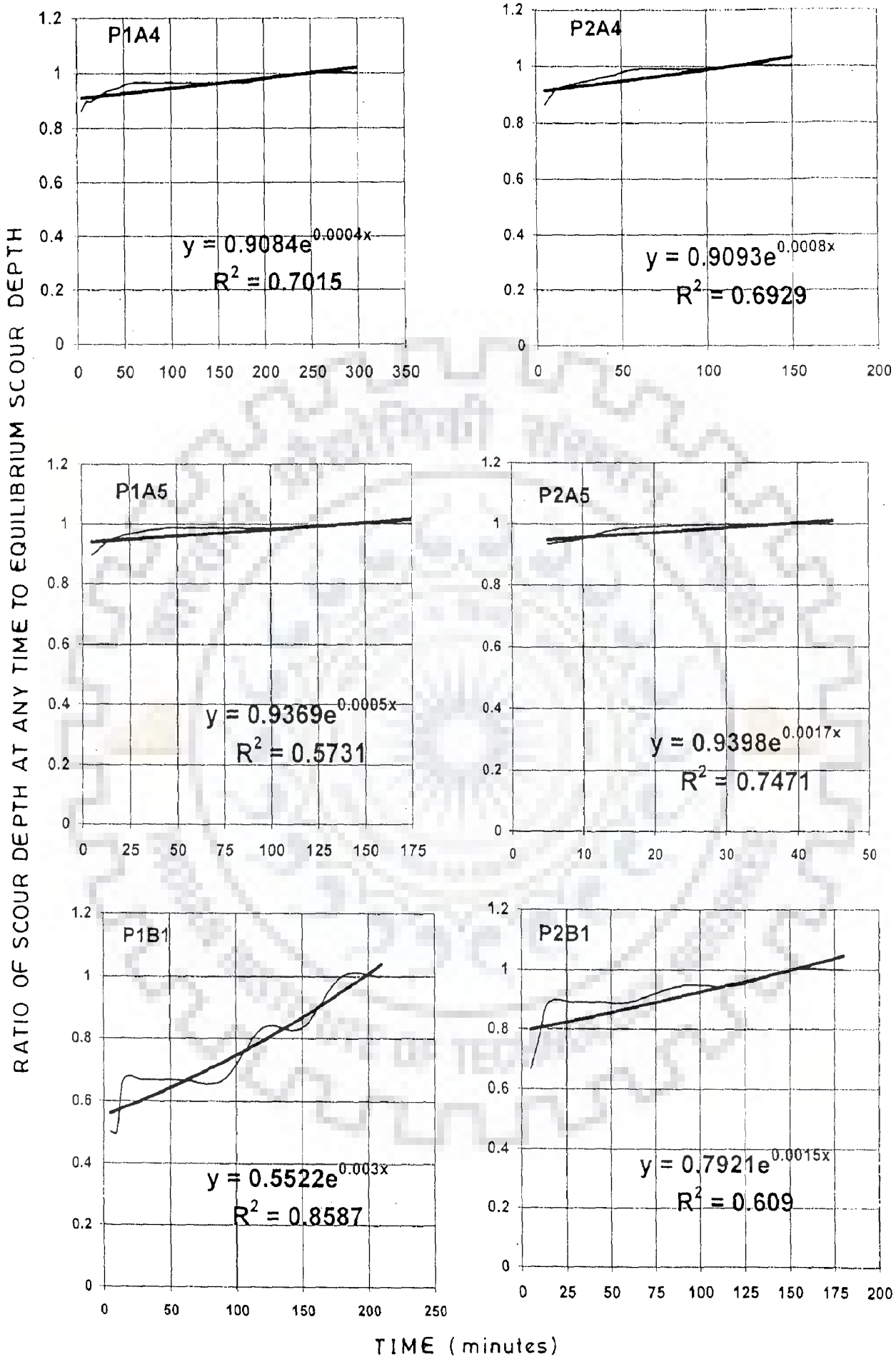


FIG. 6.1(b) TEMPORAL VARIATION OF SCOUR DEPTH UNDER STEADY FLOW (LAB DATA)

RATIO OF SCOUR DEPTH AT ANY TIME TO EQUILIBRIUM SCOUR DEPTH

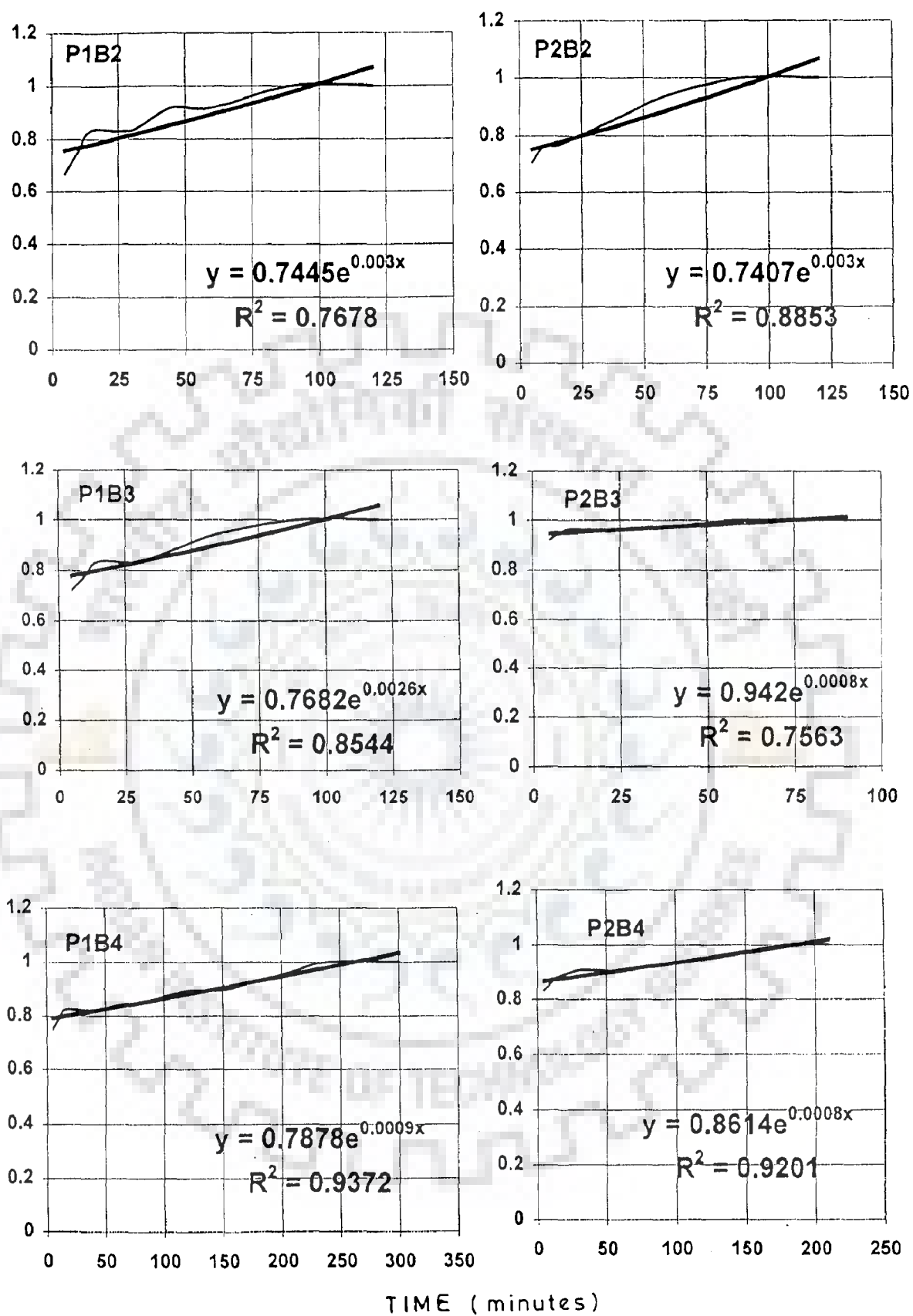


FIG. 6.1 (c) TEMPORAL VARIATION OF SCOUR DEPTH UNDER STEADY FLOW (LAB DATA)

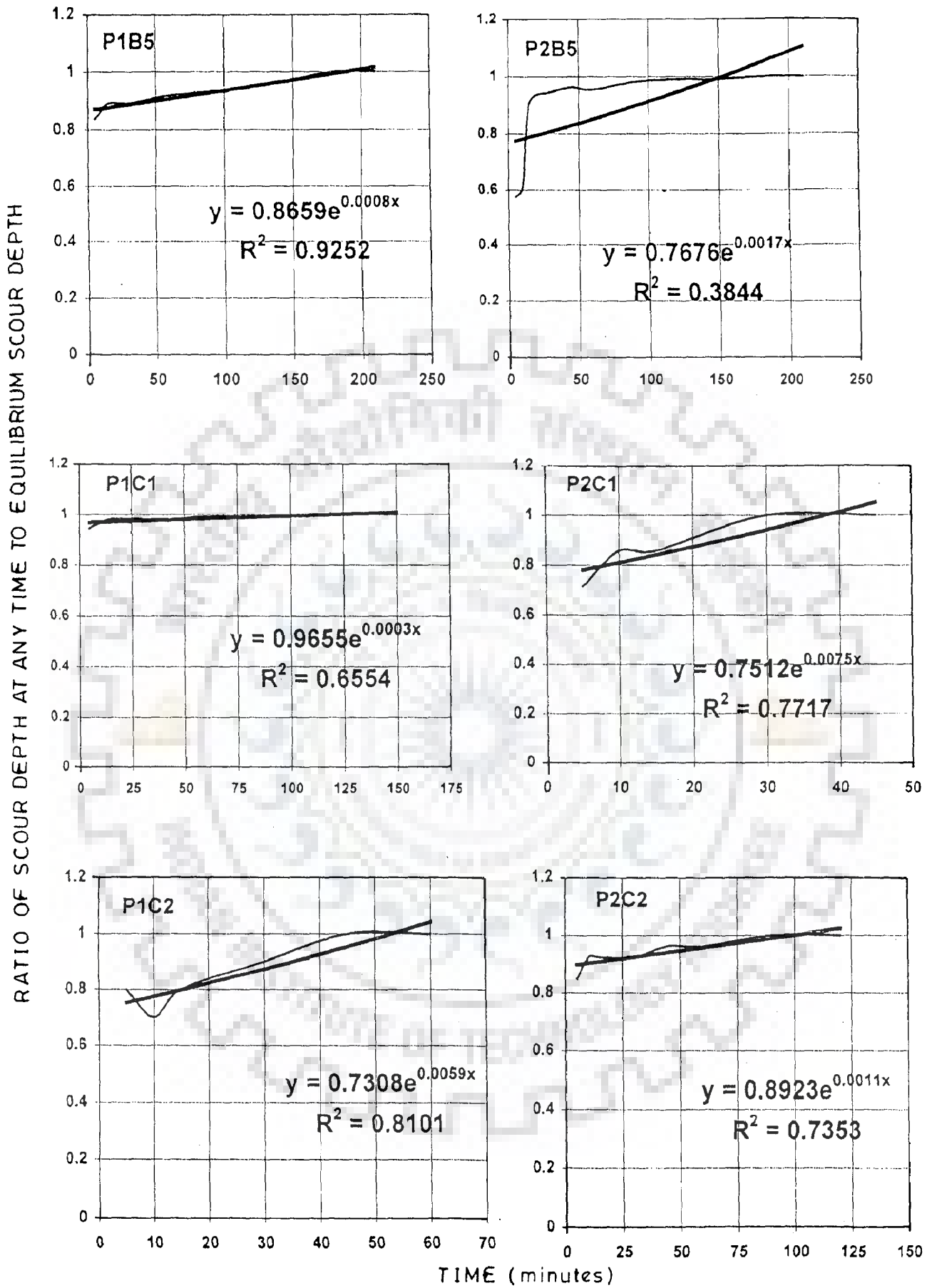
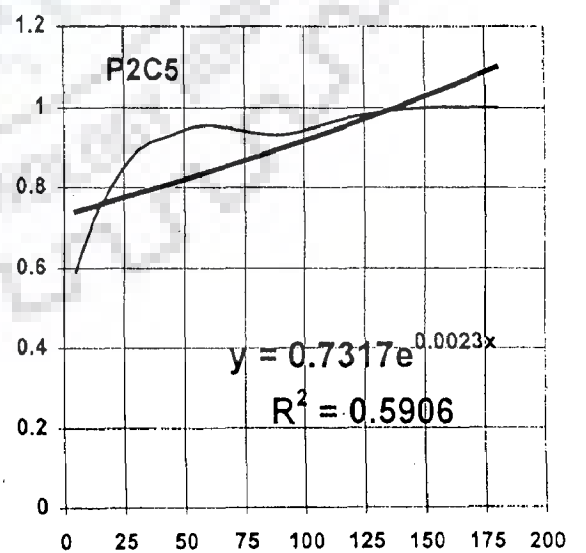
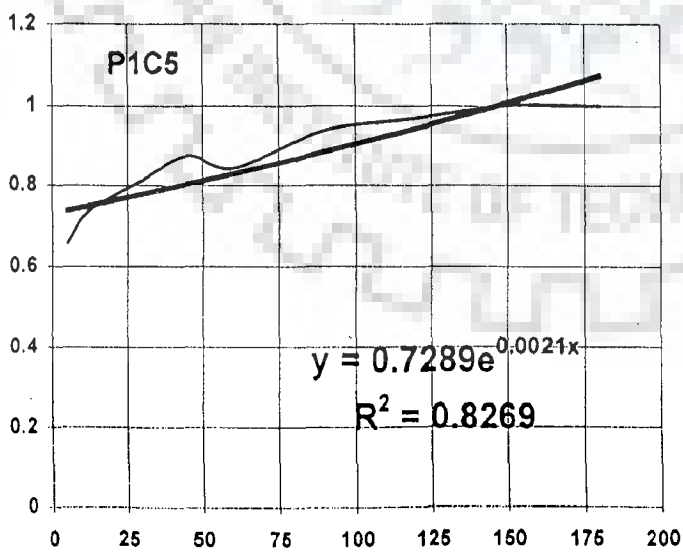
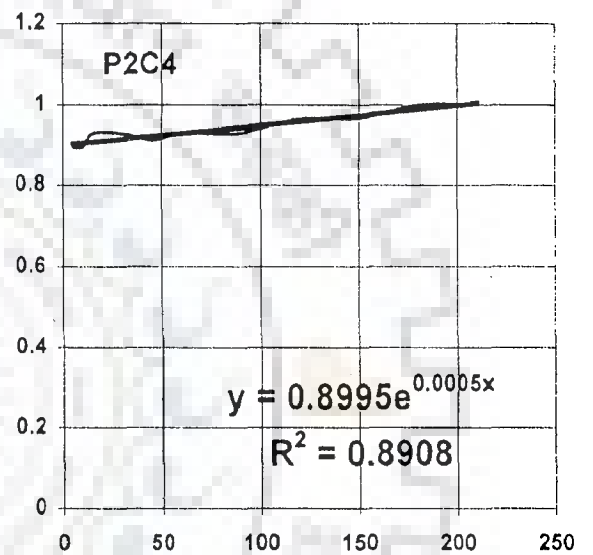
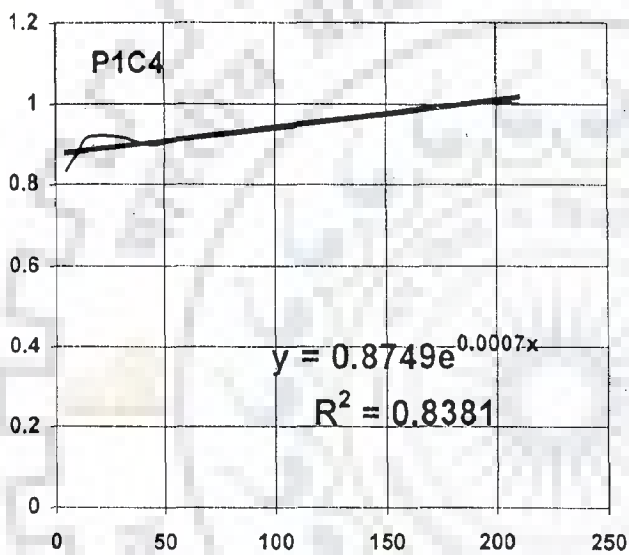
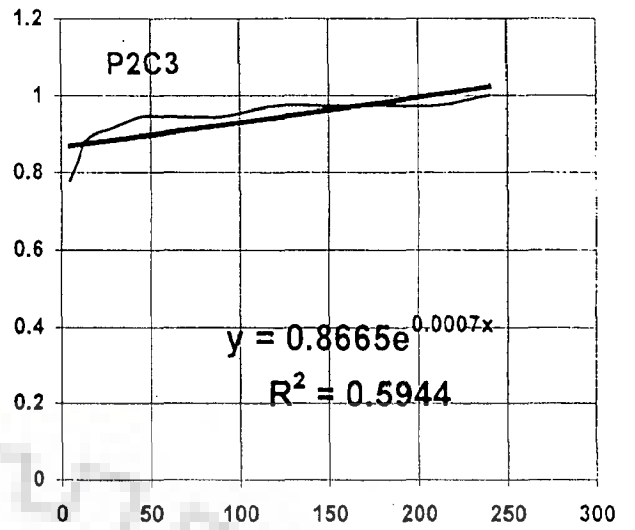
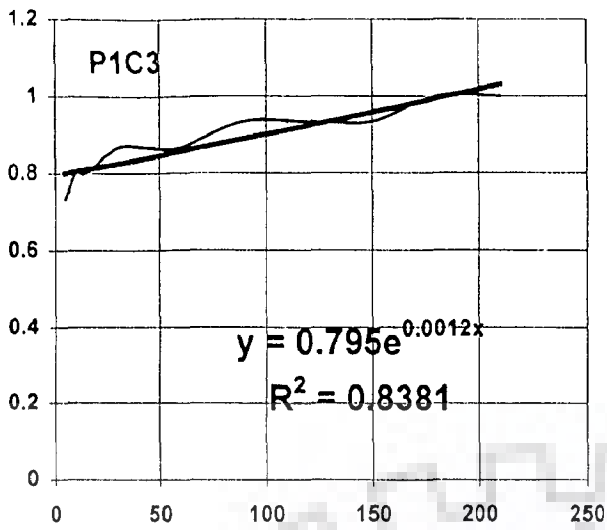


FIG. 61(d) TEMPORAL VARIATION OF SCOUR DEPTH UNDER STEADY FLOW (LAB DATA)

RATIO OF SCOUR DEPTH AT ANY TIME TO EQUILIBRIUM SCOUR DEPTH



TIME (minutes)

FIG. 6.1(e) TEMPORAL VARIATION OF SCOUR DEPTH UNDER STEADY FLOW (LAB DATA)

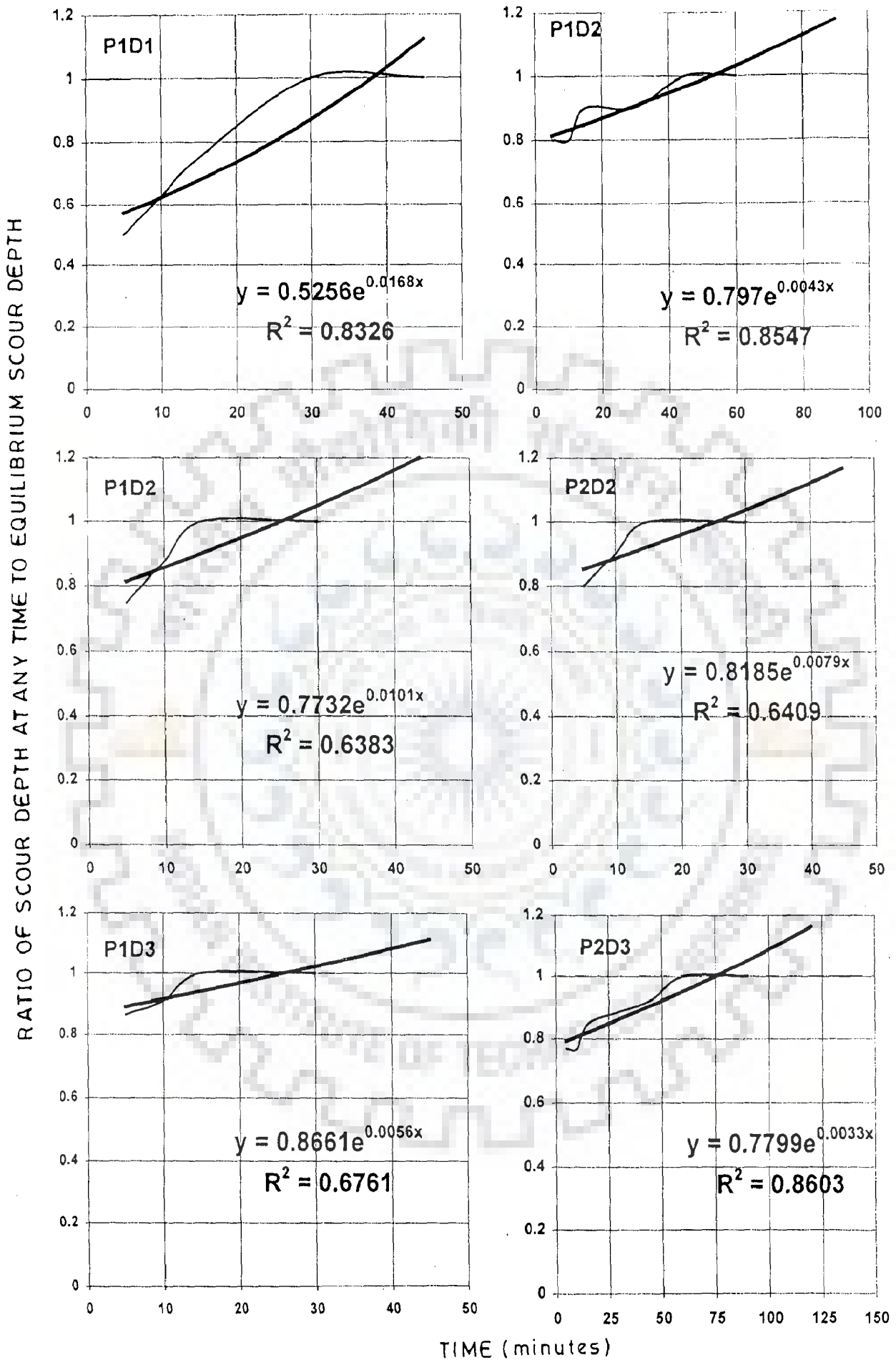
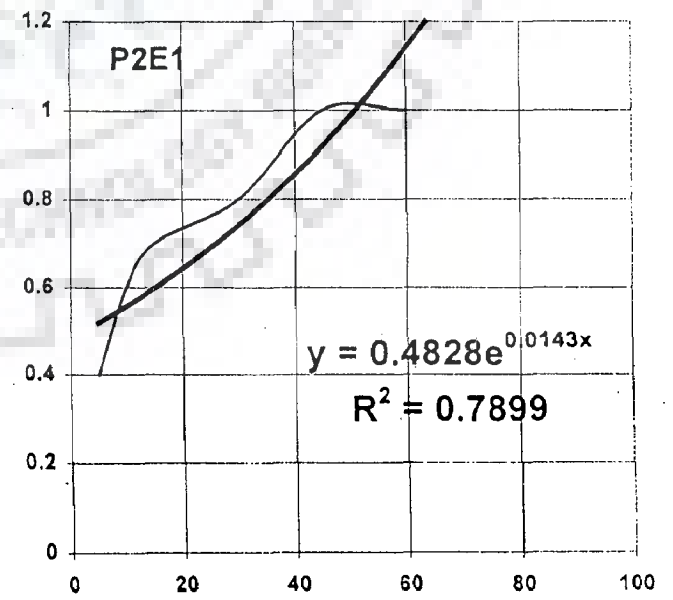
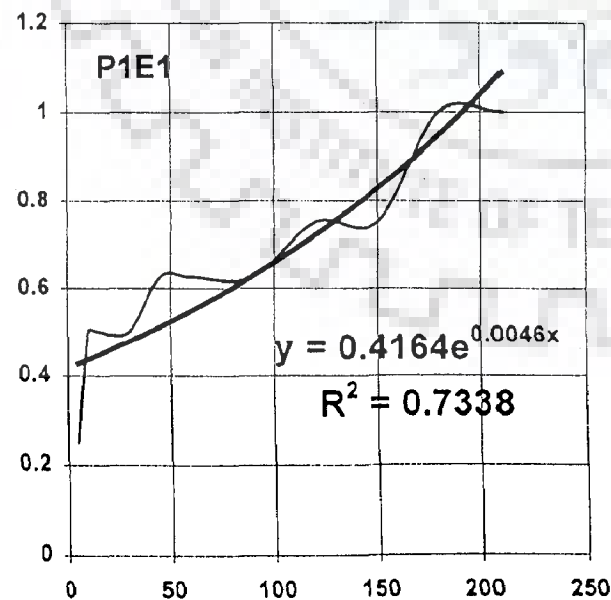
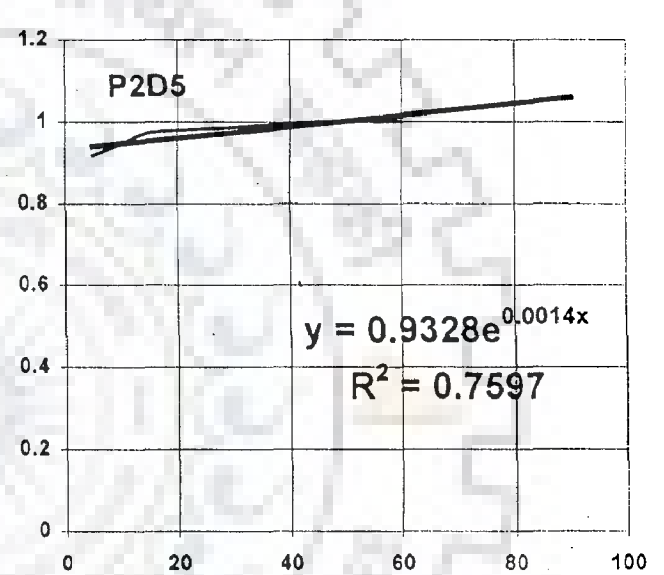
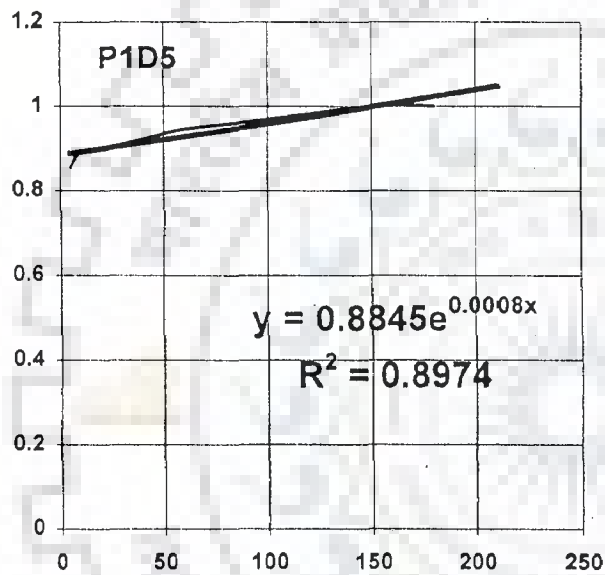
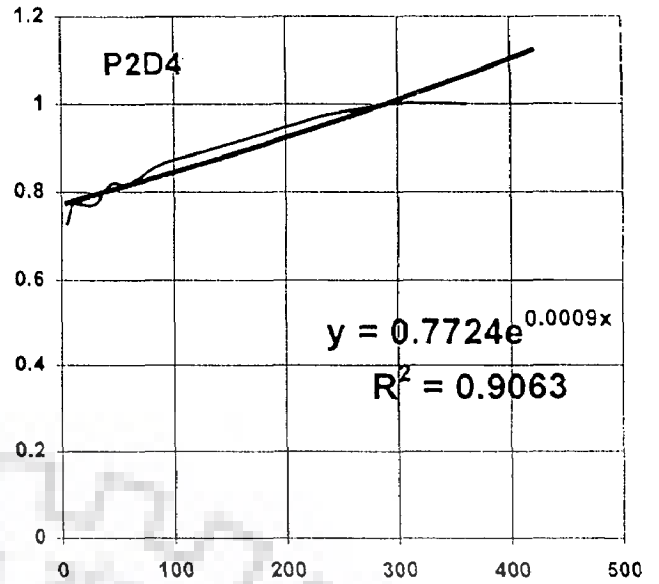
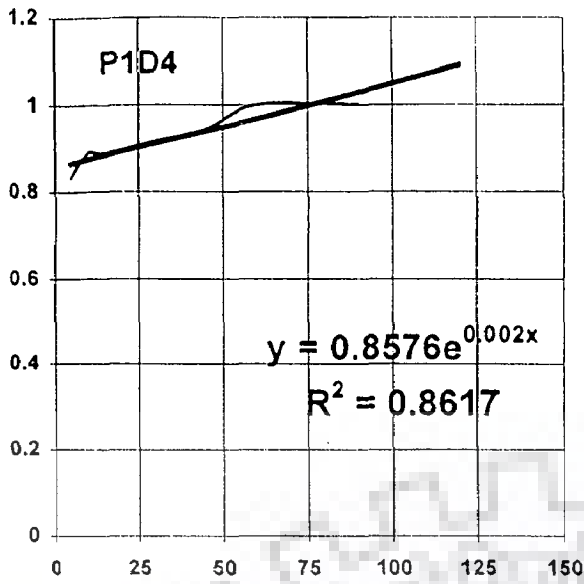


FIG. 6-1 (f) TEMPORAL VARIATION OF SCOUR DEPTH UNDER STEADY FLOW (LAB DATA)

RATIO OF SCOUR DEPTH AT ANY TIME TO EQUILIBRIUM SCOUR DEPTH



TIME (minutes)

FIG. 6-1 (g) TEMPORAL VARIATION OF SCOUR DEPTH UNDER STEADY FLOW (LAB DATA)

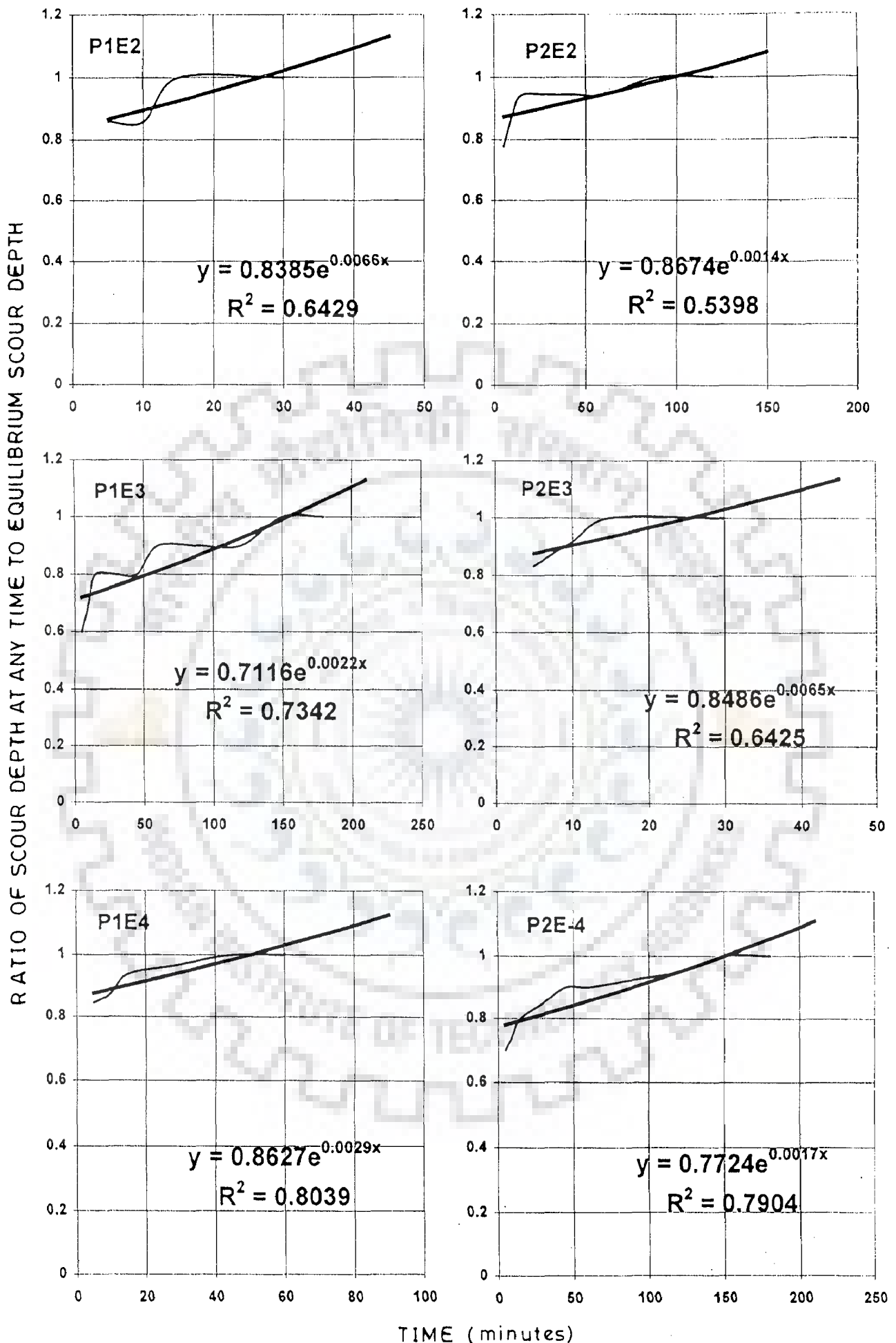


FIG. 6.1(h) TEMPORAL VARIATION OF SCOUR DEPTH UNDER STEADY FLOW (LAB DATA)

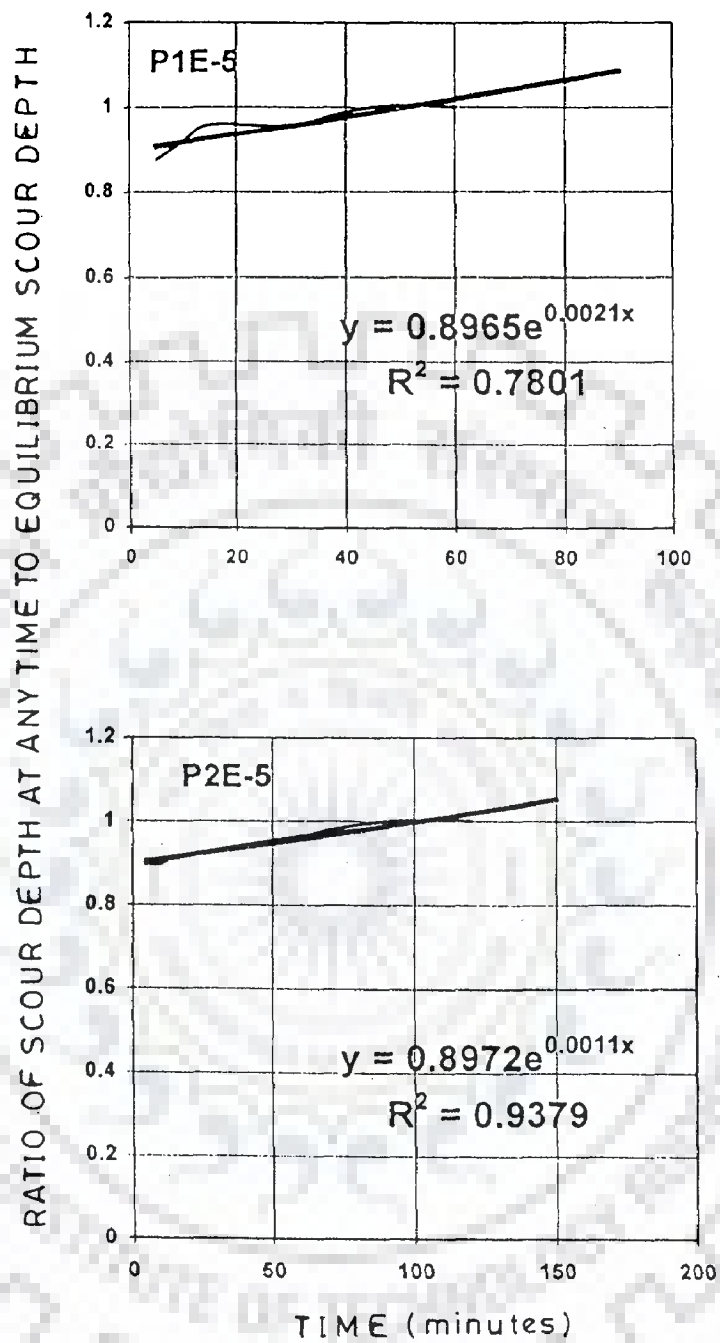


FIG. 6.1 (i) TEMPORAL VARIATION OF SCOUR DEPTH UNDER STEADY FLOW (LAB DATA)

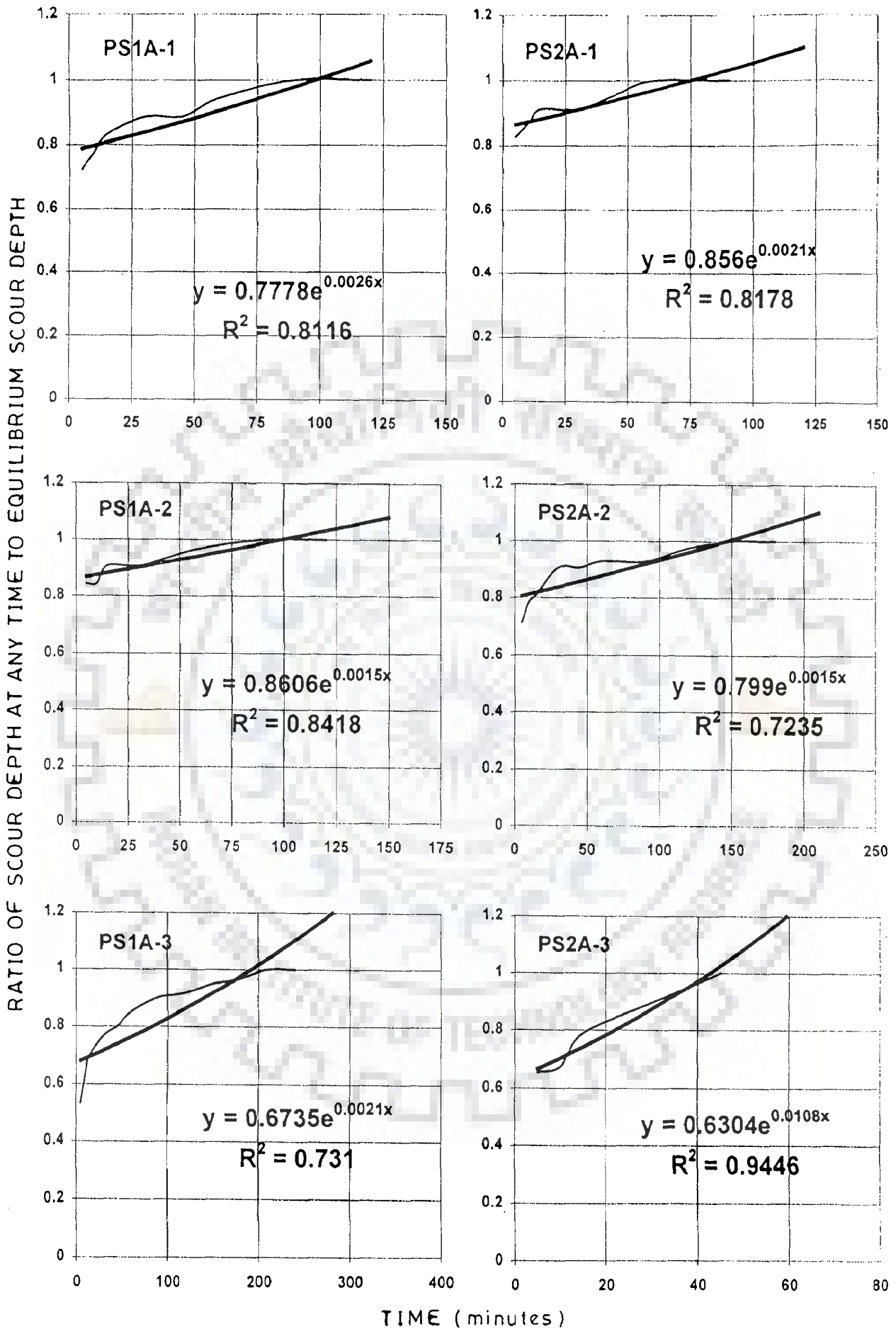


FIG. 6-1 (j) TEMPORAL VARIATION OF SCOUR DEPTH UNDER STEADY FLOW (LAB DATA)

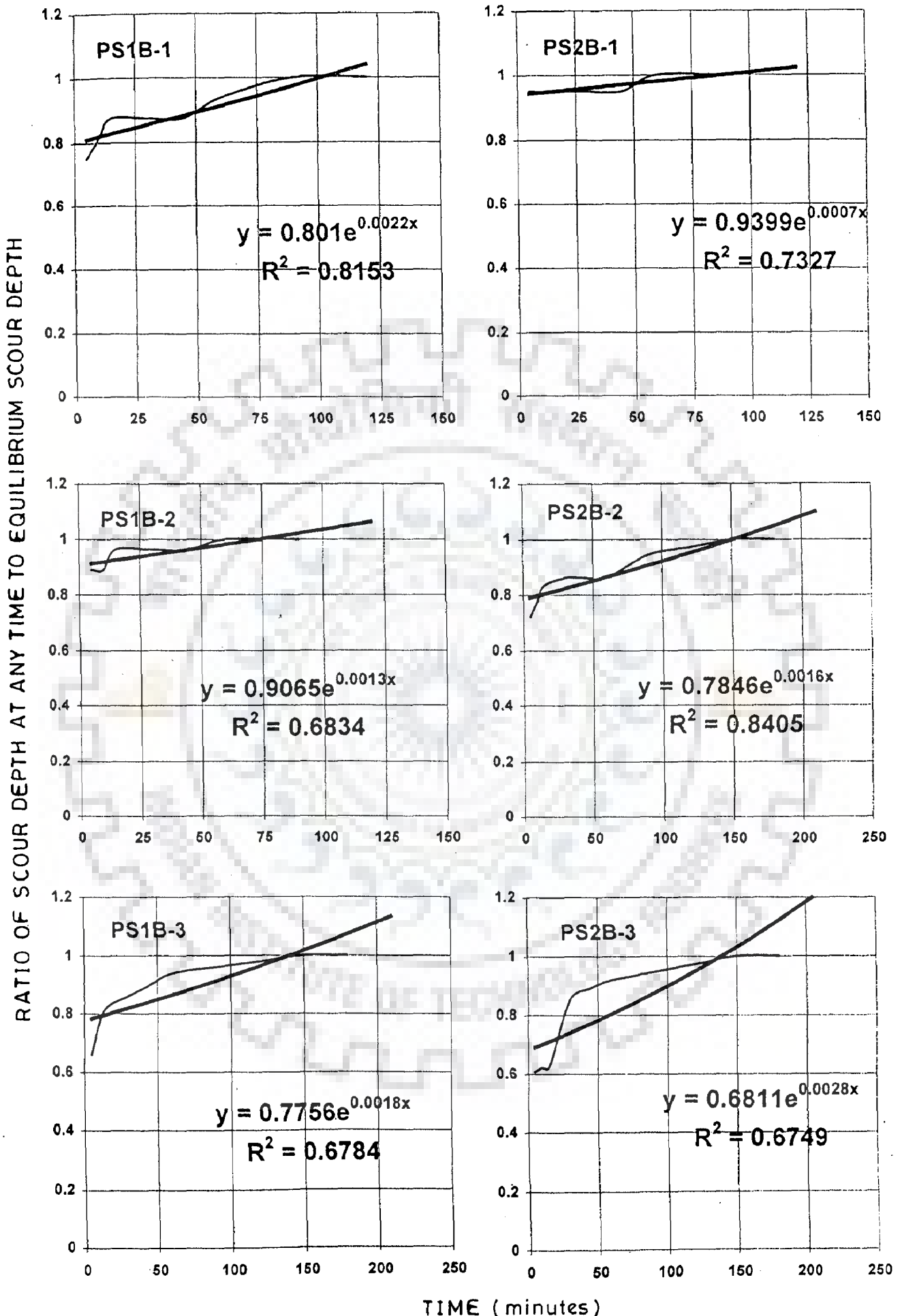


FIG. 6.1(k) TEMPORAL VARIATION OF SCOUR DEPTH UNDER STEADY FLOW (LAB DATA)

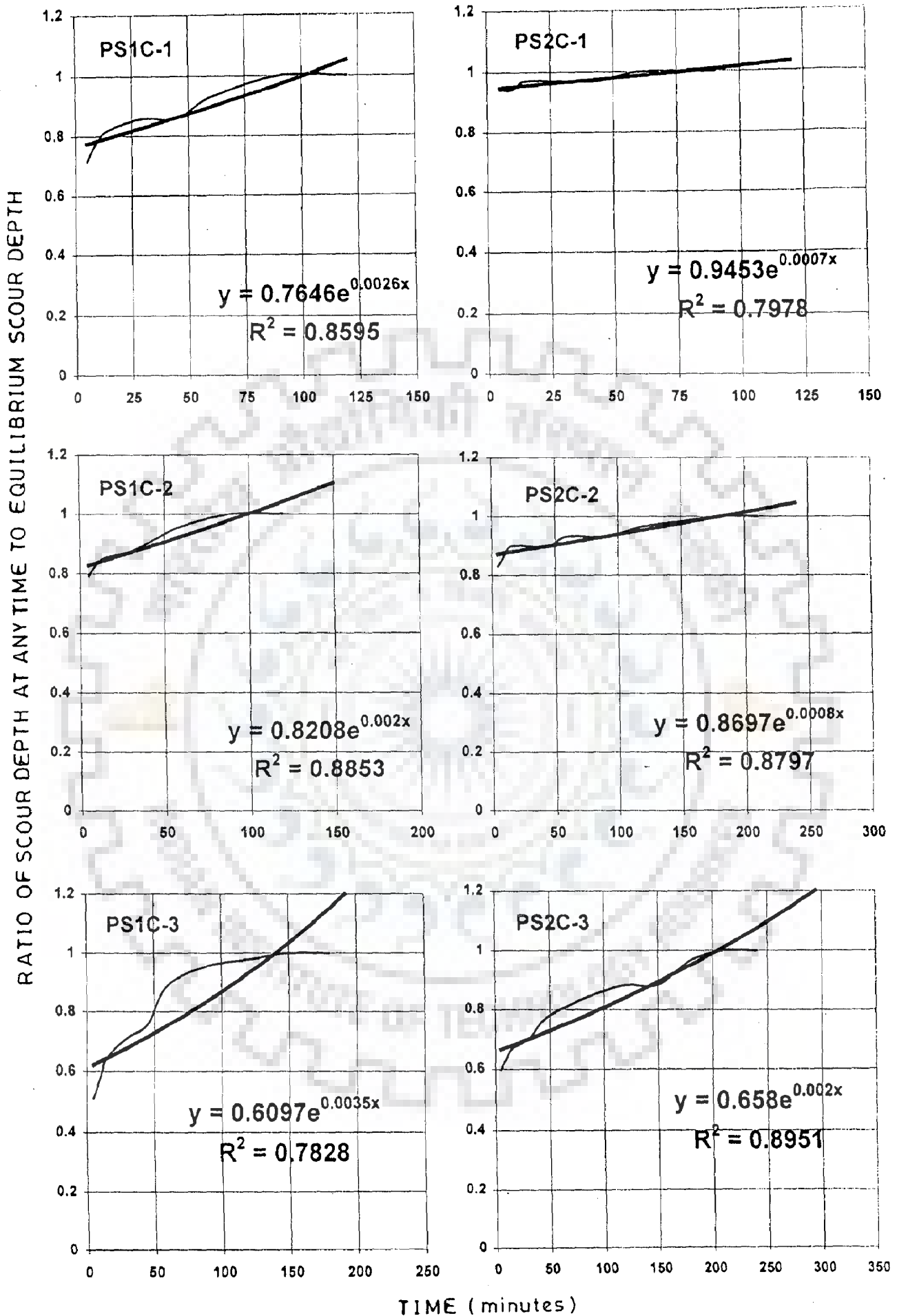


FIG.6-1 (I) TEMPORAL VARIATION OF SCOUR DEPTH UNDER STEADY FLOW (LAB DATA)

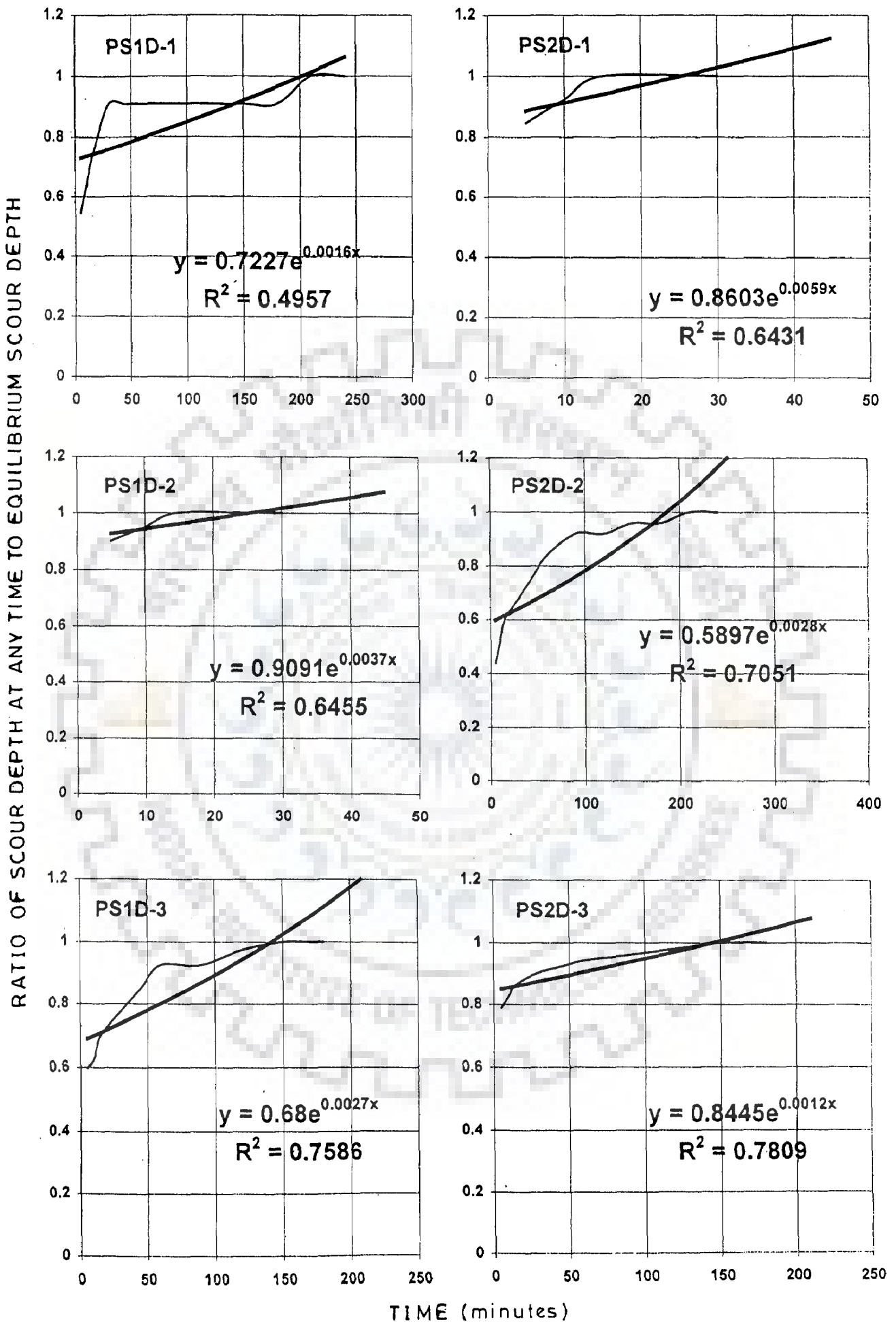


FIG. 6.1 (m) TEMPORAL VARIATION OF SCOUR DEPTH UNDER STEADY FLOW (LAB DATA)

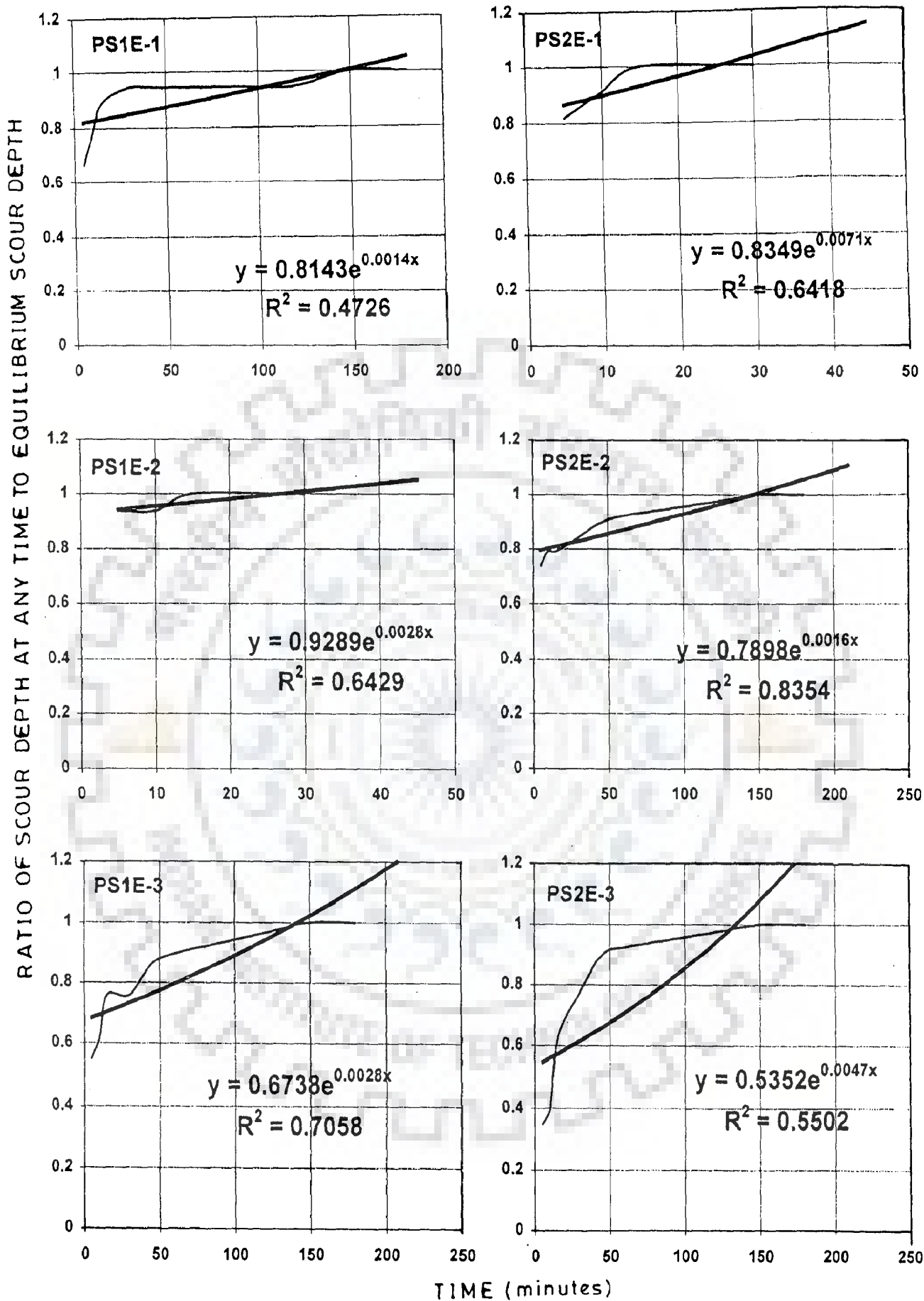


FIG. 6.1 (n) TEMPORAL VARIATION OF SCOUR DEPTH UNDER STEADY FLOW (LAB DATA)

Table 6.1: Calibrated model parameters

run no.	a	b'	R^2	run no.	a	b'	R^2
PS1A-1	0.7778	0.0026	0.8116	P1B-1	0.5522	0.003	0.8587
PS2A-1	0.856	0.0021	0.8178	P2B-1	0.7921	0.0015	0.609
PS1A-2	0.8606	0.0015	0.8418	P1B-2	0.7445	0.003	0.7678
PS2A-2	0.799	0.0015	0.7235	P2B-2	0.7407	0.003	0.8853
PS1A-3	0.6735	0.0021	0.731	P1B-3	0.7682	0.0026	0.8544
PS2A-3	0.6304	0.0108	0.9446	P2B-3	0.942	0.0008	0.7563
PS1B-1	0.801	0.0022	0.8153	P1B-4	0.7878	0.0009	0.9372
PS2B-1	0.9399	0.0007	0.7327	P2B-4	0.8614	0.0008	0.9201
PS1B-2	0.9065	0.0013	0.6834	P1B-5	0.8659	0.0008	0.9252
PS2B-2	0.7846	0.0016	0.8405	P2B-5	0.8686	0.0017	0.3844
PS1B-3	0.7756	0.0018	0.6784	P1C-1	0.9655	0.0003	0.6554
PS2B-3	0.6811	0.0028	0.6749	P2C-1	0.7512	0.0075	0.7717
PS1C-1	0.7646	0.0026	0.8595	P1C-2	0.7308	0.0059	0.8101
PS2C-1	0.9453	0.0007	0.7978	P2C-2	0.8923	0.0011	0.7353
PS1C-2	0.8208	0.002	0.8853	P1C-3	0.795	0.0012	0.8381
PS2C-2	0.8697	0.0008	0.8797	P2C-3	0.8665	0.0007	0.5944
PS1C-3	0.6097	0.0035	0.7828	P1C-4	0.8749	0.0007	0.8381
PS2C-3	0.658	0.002	0.8951	P2C-4	0.8995	0.0005	0.8908
PS1D-1	0.7227	0.0016	0.4957	P1C-5	0.7289	0.0021	0.8269
PS2D-1	0.8603	0.0059	0.6431	P2C-5	0.7317	0.0023	0.5906
PS1D-2	0.9091	0.0037	0.6455	P1D-1	0.5256	0.0168	0.8326
PS2D-2	0.5897	0.0028	0.7051	P2D-1	0.797	0.0043	0.8547
PS1D-3	0.68	0.0027	0.7586	P1D-2	0.7732	0.0101	0.6383
PS2D-3	0.8445	0.0012	0.7809	P2D-2	0.8185	0.0079	0.6409
PS1E-1	0.8143	0.0014	0.4726	P1D-3	0.8661	0.0056	0.6761
PS2E-1	0.8349	0.0071	0.6418	P2D-3	0.7799	0.0033	0.8603
PS1E-2	0.9289	0.0028	0.6429	P1D-4	0.8576	0.002	0.8617
PS2E-2	0.7898	0.0016	0.8354	P2D-4	0.7724	0.0009	0.9063
PS1E-3	0.6738	0.0028	0.7058	P1D-5	0.8845	0.0008	0.8974
PS2E-3	0.5352	0.0047	0.5502	P2D-5	0.9328	0.0014	0.7597
P1A-1	0.68	0.001	0.7461	P1E-1	0.4164	0.0048	0.7338
P2A-1	0.8197	0.0009	0.2773	P2E-1	0.4828	0.0143	0.7899
P1A-2	0.8556	0.0009	0.6819	P1E-2	0.8385	0.0066	0.6429
P2A-2	0.8989	0.001	0.3643	P2E-2	0.8674	0.0014	0.5398
P1A-3	0.9279	0.0005	0.7643	P1E-3	0.7116	0.0022	0.7342
P2A-3	0.8338	0.0037	0.7183	P2E-3	0.8486	0.0065	0.6425
P1A-4	0.9084	0.0004	0.7015	P1E-4	0.8627	0.0029	0.8039
P2A-4	0.9093	0.0008	0.6929	P2E-4	0.7724	0.0017	0.7904
P1A-5	0.9369	0.0005	0.5731	P1E-5	0.8965	0.0021	0.7801
P2A-5	0.9398	0.0017	0.7471	P2E-5	0.8972	0.0011	0.9379

6.3 TEMPORAL VARIATION DURING AN UNSTEADY STATE FLOW

Fig. 6.2 shows a typical variation of unsteady state discharge at any site. This unsteady state discharge can be also equivalently represented as histogram of quasi-steady state discharges, also shown in Fig. 6.2. In the literature, such an identification of unsteady state discharge has been found successful on earlier occasions, particularly dealing with the scour along bridge piers.

Corresponding to discharges $Q_1, Q_2, Q_3, \dots, Q_{n-1}, Q_n$, which last for time $t_{d1}, t_{d2}, t_{d3}, \dots, t_{dn-1}, t_{dn}$, the following expression for the temporal scour can be written using principle of superposition

$$\begin{aligned}
 d_{st} = & k_1 F_{r1}^n \beta^r \cdot \exp\left(\frac{b_1 t}{t_{e1}}\right) - k_1 F_{r1}^n \beta^r \cdot \exp\left[\frac{b_1(t-t_{d1})}{t_{e1}}\right] \\
 & + k_2 F_{r2}^n \beta^r \exp\left[\frac{b_2(t-t_{d1})}{t_{e2}}\right] - k_2 F_{r2}^n \beta^r \exp\left[\frac{b_2(t-t_{d1}-t_{d2})}{t_{e2}}\right] + \dots \\
 & + k_n F_{rn}^n \beta^r \exp\left[\frac{b_n(t-t_{d1}-\dots-t_{dn-1})}{t_{en}}\right]
 \end{aligned}
 \tag{6.2}$$

In eq. (6.2), k_1, k_2, \dots, k_n are model coefficients, which are simply the products of the model parameter a of eq. (6.1) with the multiplying coefficient of eq. (5.8) to (5.11). Similarly, F_{r1}, \dots, F_{rn} are the Froude numbers corresponding to discharges Q_1, Q_2, \dots, Q_n . Also, $t_{e1}, t_{e2}, \dots, t_{en}$ represent the equilibrium time corresponding to discharges Q_1, Q_2, \dots, Q_n . and b_1, b_2, \dots, b_n represent model parameters respectively.

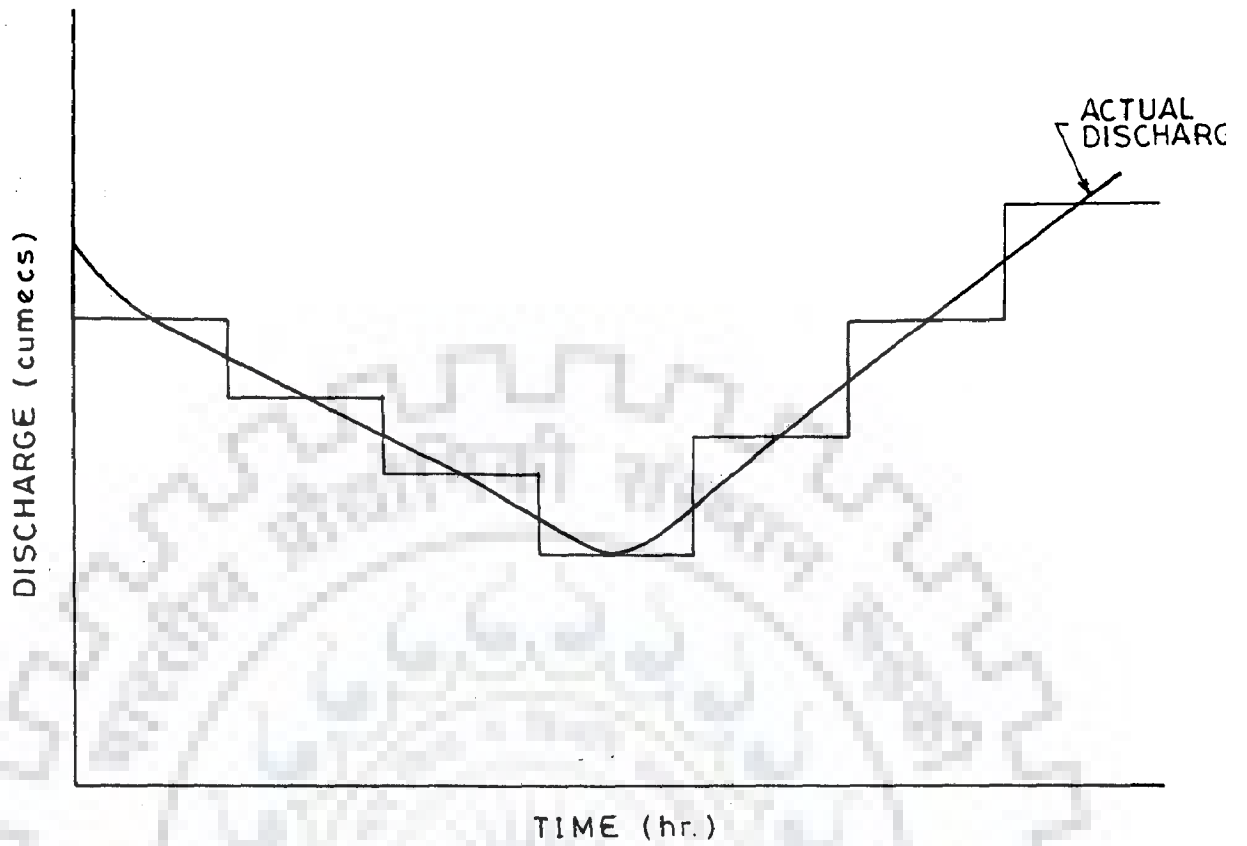


FIG. 6.2 QUASI STEADY STATE DISCRETISATION OF A HYPOTHETICAL DISCHARGE

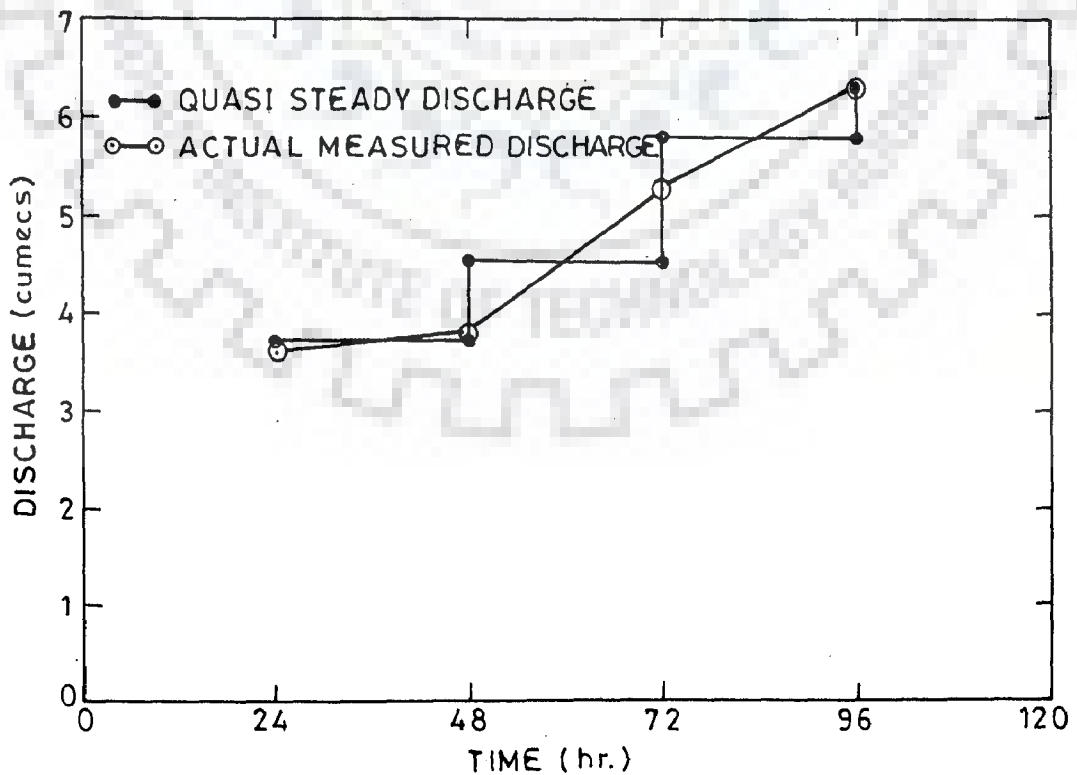


FIG. 6.3 VARIATION OF DISCHARGE IN SOLANI RIVER DURING FIELD EXPERIMENTS

6.4 APPLICATION TO FIELD DATA

To test the applications of eq (6.2), measurement of discharge and scour were made in the nearby river Solani, as described in Chapter 3. The experiments were performed with four different types of models and duration of the experiments was 96 hrs. The observations were recorded at an interval of 24 hrs. Fig. 6.3 shows the variation of discharge with time during period of experiments. Similarly, Fig. 6.4(a-d) shows the variation of scour with time. In case of Solani river, the sediment size is found to vary around 0.21 mm. This implies that eq. (5.12) and (5.13), which are valid for particle sizes of 0.424mm will be a better preference in place of eq. (5.10) and (5.11). Truly speaking, the experiments with $d_{50} = 0.21$ mm would have been a better relationship to be used corresponding to various flow discharges. Table (6.1) can be used to interpolate values of a and b' . However, one still requires an expression for equilibrium scour. Considering the wide variability in the estimation of equilibrium scour, it has been preferred to use table (6.1) for making judicious choices of equilibrium scour. As the scour depends on Froude number and parameter β , a two way interpolation is used to interpolate values of a , b' , and equilibrium scour time using the data base available from the lab experiments. Corresponding to unsteady state discharge of figure (6.3), the equivalent quasi steady state discharge distribution is hypothesized and is also shown in Fig. (6.3). Using these values of Q along with k , b , F_r , β and t_e , the scour can be computed at different times.

Melville and Chiew (1999) have suggested that the equilibrium scour may be attainable in order of days. Basically, the scour increases very fast in initial stages of the run and subsequently, it slows down as it approaches the equilibrium. Thus, it is

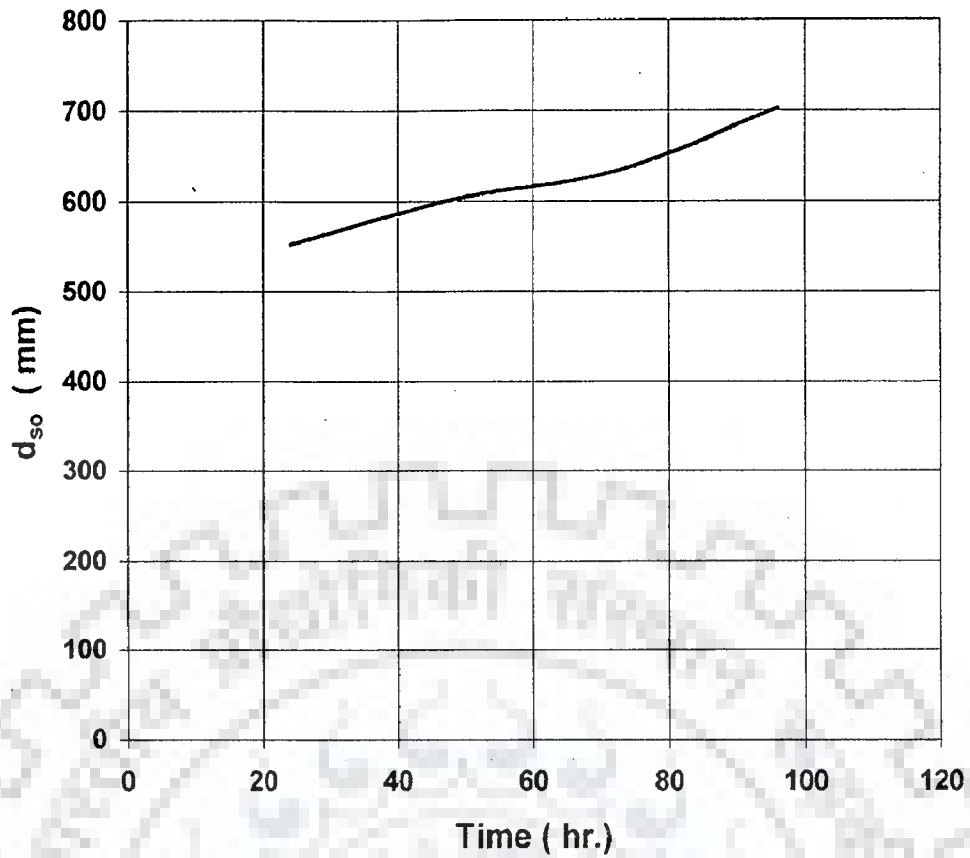


FIG. NO. 6.4 a : VARIATION OF SCOUR IN SOLANI RIVER FOR EXPERIMENT NOS. RA-1 TO RA-4 WITH PILE SPUR OF POROSITY 20%

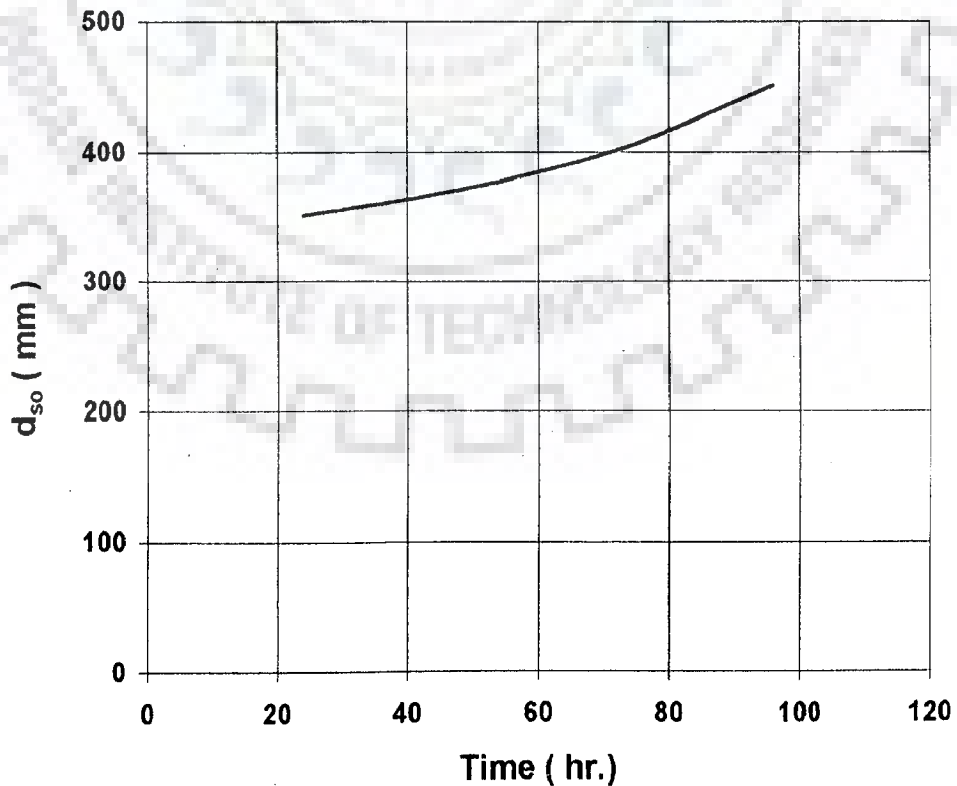


FIG.NO. 6.4 b : VARIATION OF SCOUR IN SOLANI RIVER FOR EXPERIMENT NOS. RB-1 TO RB-4 WITH PILE SPUR OF POROSITY 40%

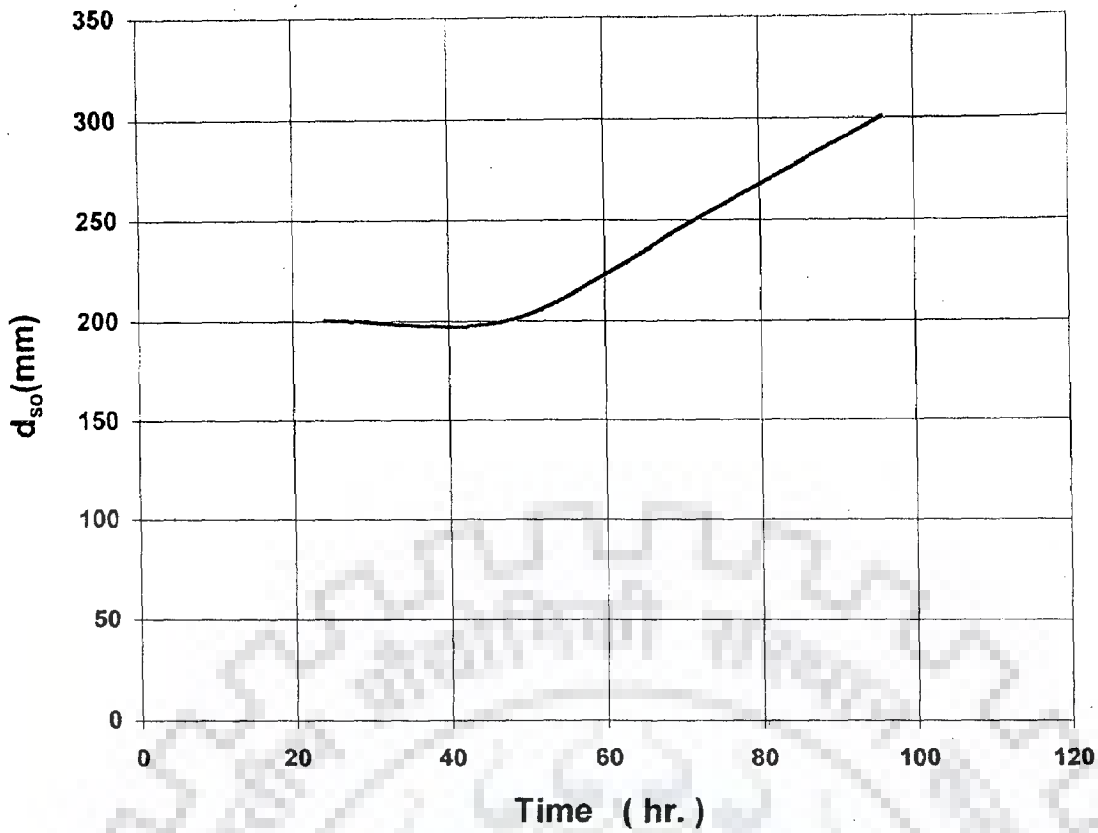


FIG. NO. 6.4 c : VARIATION OF SCOUR IN SOLANI RIVER FOR EXPERIMENT NOS. RC-1 TO RC-4 WITH PILE SPUR OF POROSITY 60%

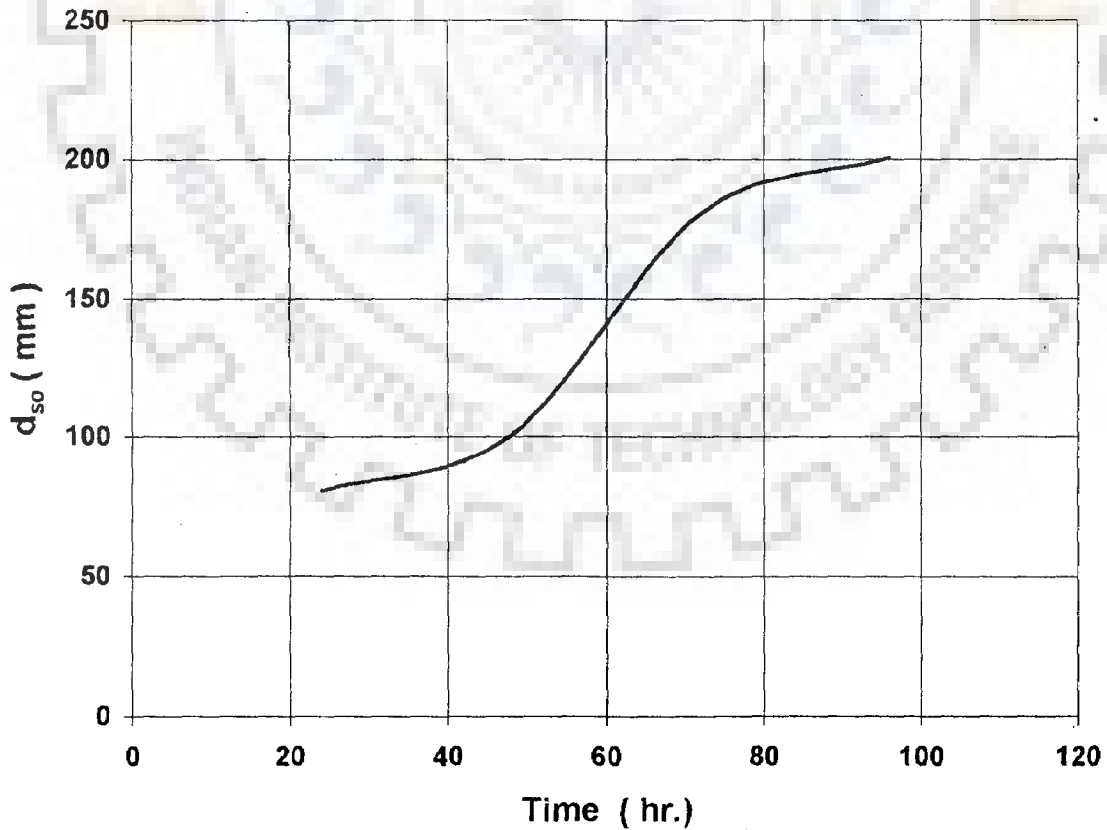


FIG. NO. 6.4 d : VARIATION OF SCOUR IN SOLANI RIVER FOR EXPERIMENT NOS. RD-1 TO RD-4 WITH PILE SPUR OF POROSITY 80%

expected that the coefficients a and b' , which have been obtained based on the analysis of lab data of few hours duration, are not expected to be valid as such for application to the present field condition. Any imperfections in a and b' values will lead to a scour depth exceeding equilibrium scour depth and this must be avoided in transient scour modelling. Thus, eq. (6.2) can be modified as follows:

$$\begin{aligned}
 d_{s,t} = & \max \left[d_{se1}, k_1 F_{r1}^n \beta^r \cdot \exp \left(\frac{b'_1 t}{t_{e1}} \right) \right] - \max \left[d_{se1}, k_1 F_{r1}^n \beta^r \cdot \exp \left(\frac{b'_1 (t - t_{d1})}{t_{e1}} \right) \right] \\
 & + \max \left[d_{se2}, k_2 F_{r2}^n \beta^r \exp \left(\frac{b'_2 (t - t_{d1})}{t_{e2}} \right) \right] \\
 & - \max \left[d_{se2}, k_2 F_{r2}^n \beta^r \exp \left(\frac{b'_2 (t - t_{d1} - t_{d2})}{t_{e2}} \right) \right] \\
 & + \max \left[d_{sen}, k_n F_m^n \beta^r \exp \left(\frac{b'_n (t - t_{d1} - \dots - t_{dn-1})}{t_{en}} \right) \right] \quad (6.3)
 \end{aligned}$$

In eq. (6.3), d_{se1}, \dots, d_{sen} represent the equilibrium scour depths due to discharges Q_1, \dots, Q_n . In eq. (6.3), it must be ensured that once a bed has been scoured, the scour will not decrease in a clear bed condition with a decrease in the discharge.

Using eq.(6.3) and the relevant parameters and variables, the temporal scour has been computed and a plot of the same with the observed scour is shown in Fig. 6.5 (a-d). As the data are available only at 24 hr interval, only the values at days 1, 2 and 3 are shown in Fig. 6.5. Figure 6.5a represents the agreement for spur type RA, in which the permeability is 20%. The agreement is not very good and the predicted scours are at least 30 to 40 cms less than the observed scour. Figure 6.5b represents the agreement for the spur type RB, in which the permeability is 40%. Here, also the predicted scour is less than the observed scour but the difference in two values is less

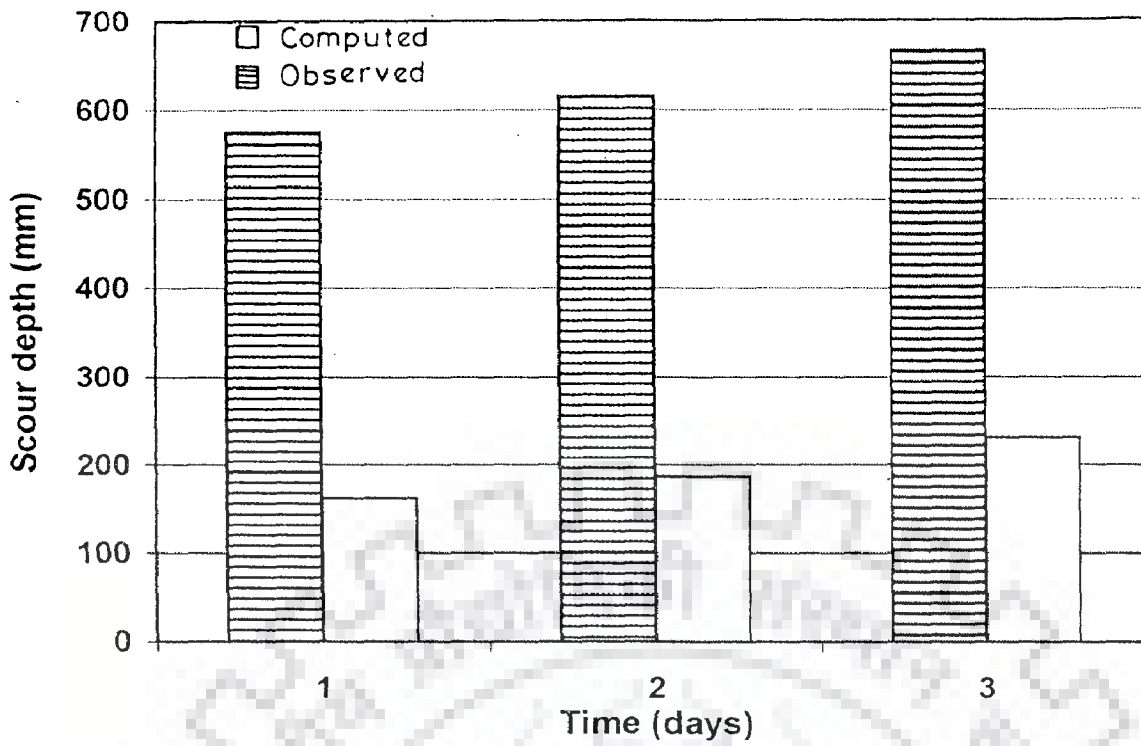


FIG. 6.5a: AGREEMENT BETWEEN OBSERVED AND COMPUTED SCOUR FOR RA TYPE PERMEABLE SPURS

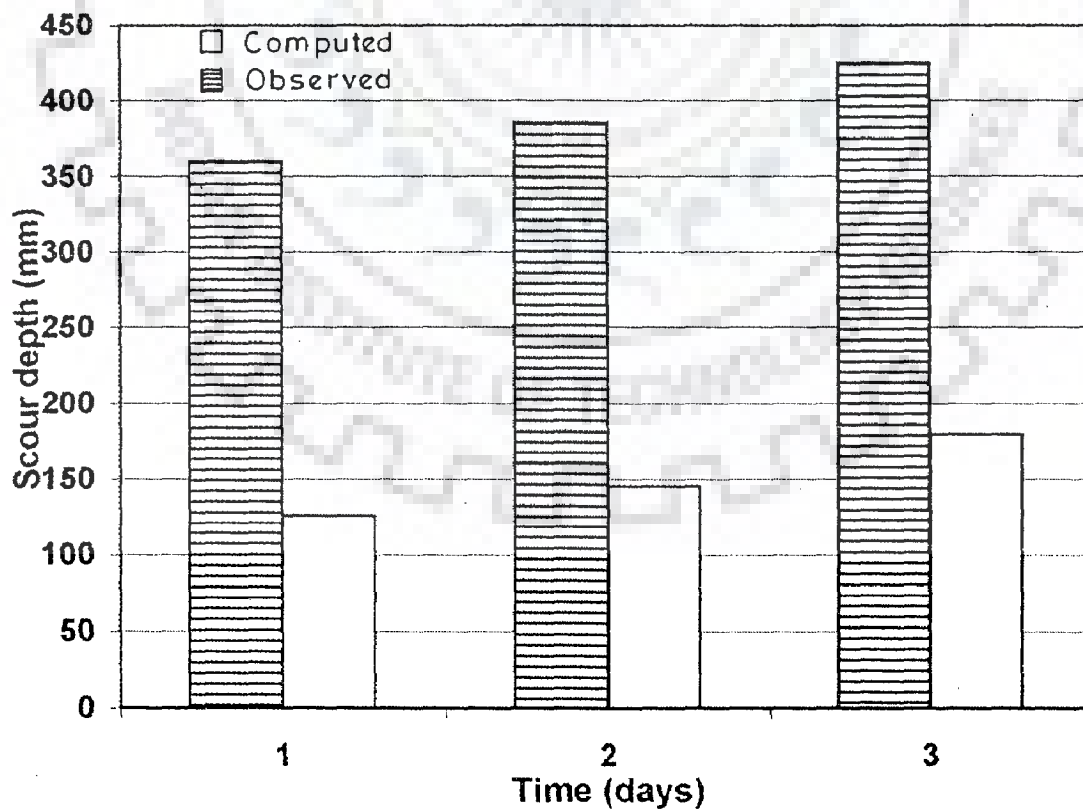


FIG. 6.5b: AGREEMENT BETWEEN OBSERVED AND COMPUTED SCOUR FOR RB TYPE PERMEABLE SPURS

than that of RA type of spurs. In fact, this behavior is also supported from fig. 6.5c, which is for the spur type RC with a permeability of 60%. With the further increase in permeability to 80% in RD type of spurs, the agreement further improves, as can be seen in fig. 6.5d. From a perusal of figs. 6.5a-d, it appears that while constructing the pile spurs with a minimum permeability, there is a pronounced disturbance of the soil bed, leading to its loosening and dislodging of bed particles.

6.5 SIGNIFICANCE OF TEMPORAL SCOUR STUDY

Much has been said already about this aspect in literature. The temporal variation of scour during unsteady flow is of great significance in studies with solid spurs and with piers, where construction costs are enormous. Thus, any deviation from the observed scours may matter much to the project cost. Fortunately in case of pile spurs, the temporal variation of scour during unsteady flow has no significant influence on the cost of the project. Even a departure of 50 cm to 1 m may not really increase the cost of pile spurs. From stability considerations, a minimum grip length is essential and the magnitude of scour being low, may not adversely affect the stability of permeable spurs. Considering the difficulties encountered in the field, in terms of uniform distribution of velocity within the entire stream width, assumption of uniform depth at the section of the pier, and non availability of laboratory experimental results conforming precisely to the bed particle size of river, the extent of match between observed and computed temporal scour profile should be considered encouraging.

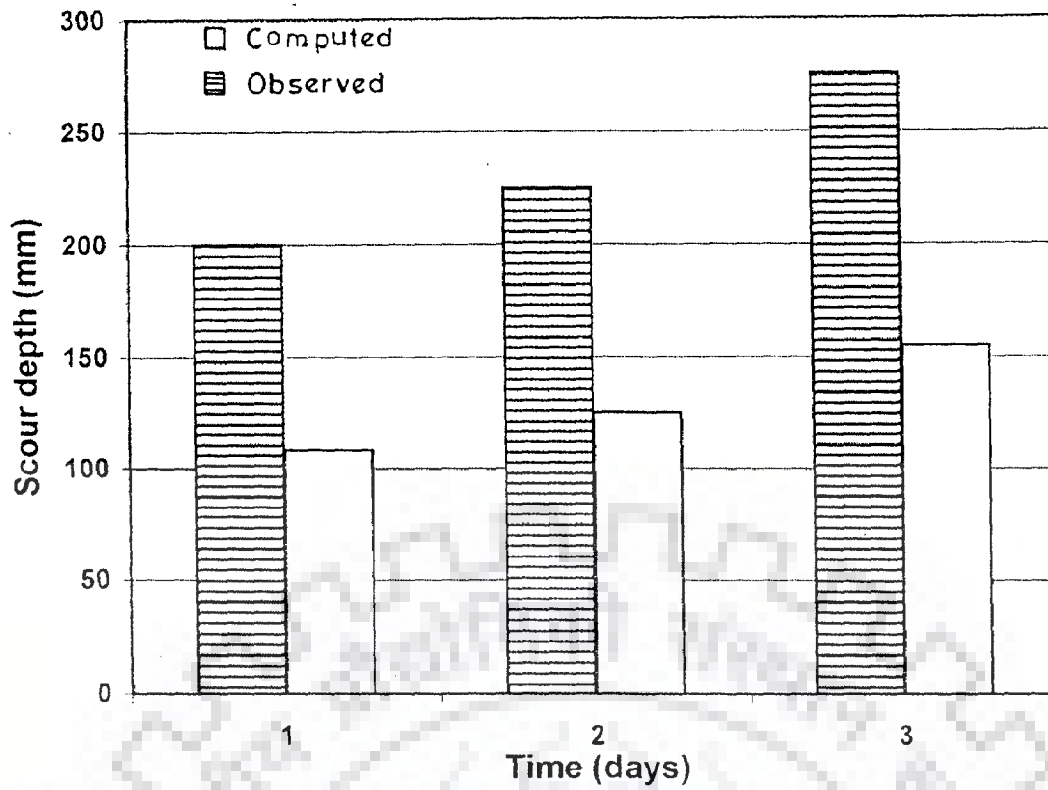


FIG. 6.5c: AGREEMENT BETWEEN OBSERVED AND COMPUTED SCOUR FOR RC TYPE PERMEABLE SPURS

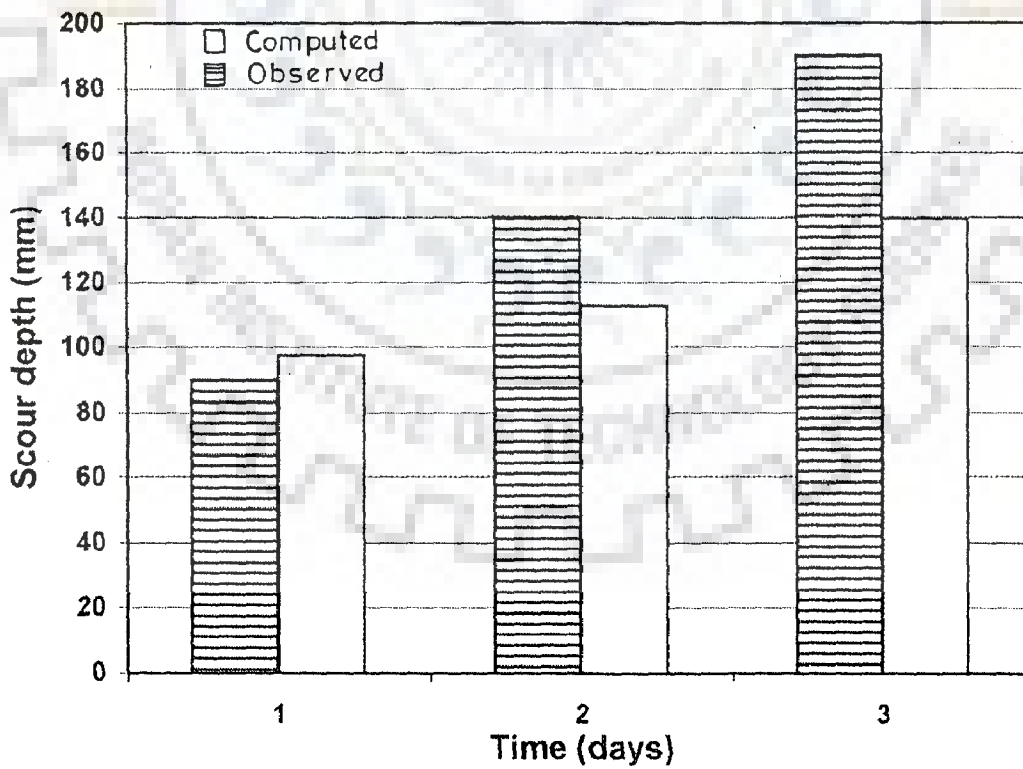


FIG. 6.5d: AGREEMENT BETWEEN OBSERVED AND COMPUTED SCOUR FOR RD TYPE PERMEABLE SPURS

GENERAL DISCUSSION

In the preceding chapters, different aspects of scour around permeable spurs have been considered and discussed individually in different chapters. A consideration of these individual discussions and conclusions reached in the previous chapters may require a further discussion. Such discussion is vital to the overall assessment of the present study and is helpful to understand the areas where further research is required.

Every year, Indian government spends a large amount of money on flood protection work. Major problem is that in many places the river course is under a continuous change. Thus, use of permanent protection works involving solid spurs is not only uneconomical but also ineffective in the long run. For these reasons, use of permeable spurs has gained a lot of importance in recent years. As introduced earlier, many such spurs have come into existence. However, there is no basis for the design of such spurs and it was this major issue which has laid to the present study.

In fact, the phenomena of scour around bridge piers, abutments and solid spurs have been studied to a large extent. However, the same has been lacking with regard to varying configurations of different types of permeable spurs, as experimented with in chapter 3. In fact, many of these permeable spurs can not be easily fabricated in field. In this respect, also the fabrication of pile spurs is very simple, convenient and less time consuming. In some of the places, two rows of permeable spurs is filled with locally available shrubs. Such type of modification in pile spurs can be seen from plates 1 and 2 of Chapter one. These spurs have been found to be achieving a

comparable protecting length as obtained in case of solid spurs. As investigation of such type of spurs is not feasible in lab experiments, it was preferred to use pile spurs with varying spacing in order to simulate the varying level of porosity.

The ranges of porosity considered in experiments are wide enough to reflect the values encountered in field situations. One of the major concerns in the case of pile spurs is their stability. Unless the extent of scour around such spurs is known, the length of such spurs embedded in foundation can not be precisely quantified. Also, the extent of scour may be dependent on porosity of such spurs, in addition to their projected length within the stream. Based on the analysis of lab experiments, it has been shown for the first time in the study how the scour is sensitive to porosity and projected length of pile spurs. Thus, eqs. (5.10) to (5.13) are expected to help the planning, lay out and placement of pile spurs in field.

Equations (5.10)-(5.13) are dimensional in nature. Various ways to achieve dimensionless form of these equations were considered. From the review of literature, it is observed that the scour depth has been made dimensionless using a variety of parameters and for this reason, the influence of the same was demonstrated in this study. With the use of w , the width of the pier, the scour relationship performed better in field. It is not known whether this approach may work well for other field data as well as other functional relationships. Thus, this aspect merits attention in future investigations.

In the literature on scour around hydraulic structures, the concept of clear water and live bed scour have received enough attention in the literature. It is now well established that for similar set of conditions, the live bed scour is less in magnitude to that of clear water scour. Thus, the clear water condition was preferred in lab experiments. However in field condition, particularly during flood, the clear

water condition may not precisely exist. Thus, the validation of the lab based model against the field data should be also considered in this perspective.

In the present study, the planning of the experiments was restricted to only two types of bed material and two projected lengths, although the variation of porosity and Froude numbers were kept in a wider range, commonly encountered in field conditions amenable to pile spurs. For different conditions than those in the lab experiments, it may be necessary to generalize this model and future work is needed in this direction.

One of the interesting things studied in the present investigation relates to the study of Melville's approach. Clearly the Melville's view that the equilibrium scour depth may not be attainable only in few hours is justified while applying the present lab based model to field data. We also considered the possibility of extending Melville's approach for the computation of scour around pile spurs. Considering the fact that all the effectiveness factors will also hold good in case of pile spurs, an attempt was made to derive the effectiveness factor accounting for the variation of porosity. In Fig. 4.6, such effectiveness factors are not found to be function of only the porosity. In Chapter 4, the analysis of the scour around solid spurs based on the approach of Melville (1997) was considered to assess the relative merit in using this relationship. The use of this relationship was also considered for pile spurs. As the approach did not indicate the feasibility of obtaining effectiveness factor as a function of porosity only, no attempts were made to amend Melville's approach for pile spurs. Thus, a future work in this direction can also be planned to extend Melville's approach for pile spurs.

A certain discussion related to Chapter six is also relevant here. In the present field experiments, the bed was not visible from top. Therefore, the experimental data

were collected by displacing the ranging rod around nose of pile spurs. So the errors of the order of few centimeters are likely to be there in measurements. Also, the distribution of flow at the spur section was not uniform and the site condition was such that there was a tendency of concentration of flow around the bank of spur. The spur type RD was more exposed to the concentrated flow as it was closer to the bridge. The spur type RA with 20% permeability was located in the last of the test reach and it was likely to be exposed to a relatively uniform flow field. In addition, the water was muddy in appearance and it is likely that the condition was closer to a live bed situation. Certain loosening of the soil below the spur was also inevitable. Thus, the results of Fig. 6.5 should be considered only in the light of the above facts.

For linear systems, the principal of superposition is valid. However, as can be seen from eq. (5.10) to (5.13) that the system behavior is not truly linear. An attempt was also made to linearise eqs (5.10) to (5.13). However, it was observed that such a linearisation could lead to an increase in the error metric associated with calibrated relationships. Furthermore use of such linearised relationship could not lead to results very different from Fig. 6.5.

In the end, it is also important to address the issue of data collection and planning of future experiments. To address this, let us consider that only the experimental data pertaining to bed particle size of 0.424 mm and $b = 5$ cm is available. Based on the analysis of this data, many relationships can be developed. However, as a departure from what has been done in Chapter 5 and also to highlight the use of critical shear velocity based scour relationships, the following relationship can be calibrated based on the experiments having bed sediment size of 0.424 mm and $b = 5$ cm.

$$\frac{d_{sc}}{w} = 0.04 \left(\frac{V}{V_c} - 1 \right)^{1.20} \beta^{0.4} \quad (7.1)$$

The error metric associated with the calibration of eq. (7.1) is 8.79%. The agreement diagram using (7.1) is shown in Fig. 7.1. If eq. (7.1) is used to predict the scour in the field, the agreement diagram of Fig. 7.2 will result.

Figures 7.2 a-d indicate that eq. (7.1) does very well in case of RA and RB type spurs. But, a perusal of Fig. 7.2c and 7.2d also indicates that the agreement between observed and predicted scour has been poor in comparison to those depicted by Fig. 6.5c and 6.5d. The purpose of this presentation is to highlight the fact that the functional form of the scour relationships can also influence their predictive performance. Thus, prior to selecting or recommending any relationship for scour prediction, it is necessary to test a large number of data represented by different conditions. For example, if eq. 7.1 is tested against the remaining lab data, Fig. 7.3 results indicating its poor performance, particularly with the beds having a size of 2.8 mm with average error being 55.59%. For the bed having a sediment size of 0.424 and $b=10$ cm eq. (7.1) yields average error of 40.37%. If the errors of the order of few ten centimeters are permissible, an user will have no doubt that eq. 5.10 as well as eq. 7.1 serve the objective of predicting scour in the river Solani within the framework of the present study. It is noted, however, that eq. (7.1) may be preferred by hydraulic engineers as it ensures the condition of no movement of particle if flow velocity is less than or equal to critical shear velocity.

Studies at Roorkee have used the horse-shoe vortex characteristics in the modelling of scour phenomenon. These characteristics are dependent on pier shape, size, and flow conditions (Garde and Ranga Raju, 1985). In the present work, this approach has not been considered and may merit attention in the future.

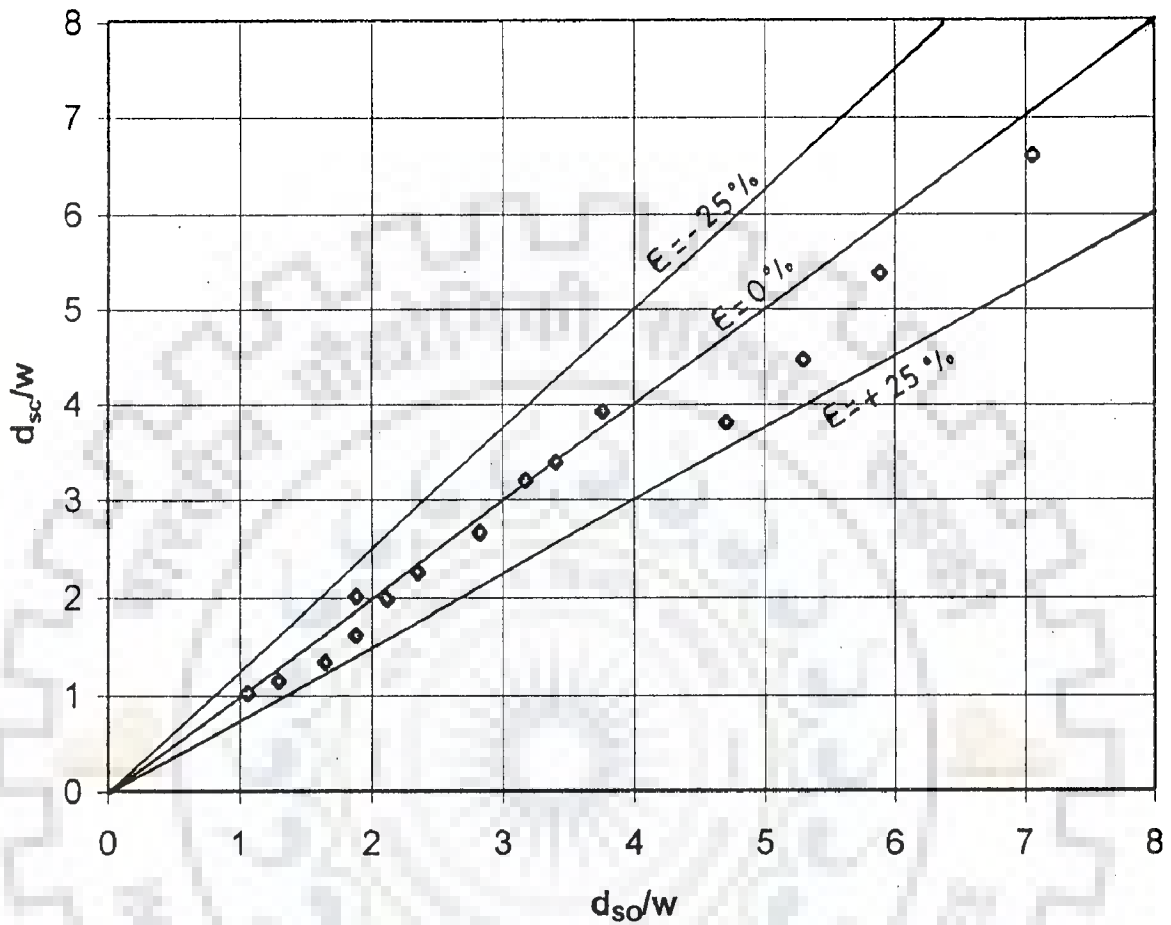


FIG. 7.1: AGREEMENT BETWEEN COMPUTED AND OBSERVED SCOUR/ WIDTH OF PILE SPUR ($d=0.424$ mm, $b=50$ mm)

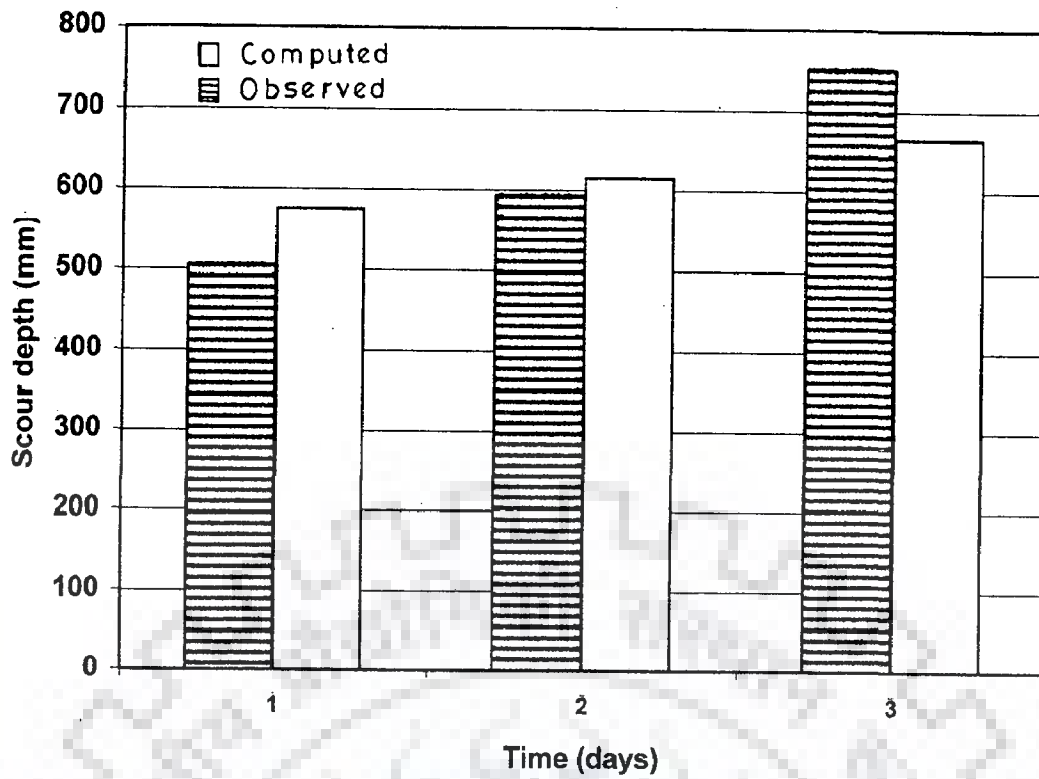


FIG. 7.2a: AGREEMENT BETWEEN OBSERVED AND COMPUTED SCOUR FOR RA TYPE PERMEABLE SPURS

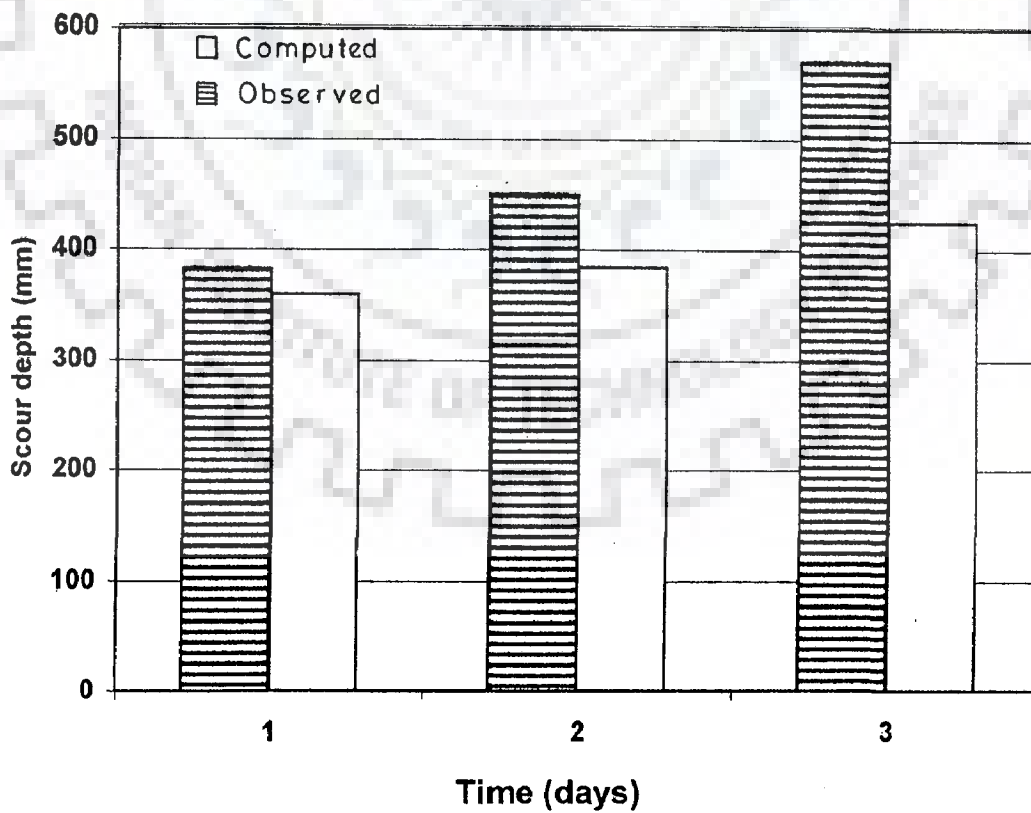


FIG. 7.2b: AGREEMENT BETWEEN OBSERVED AND COMPUTED SCOUR FOR RB TYPE PERMEABLE SPURS

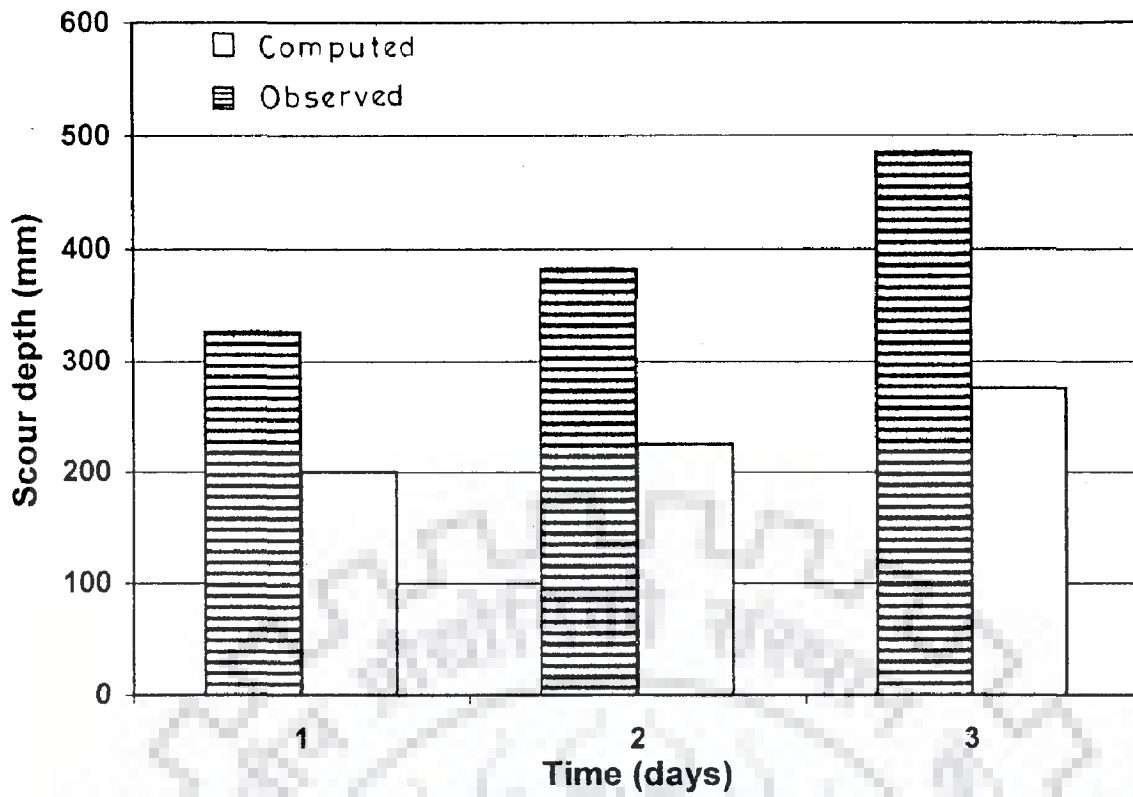


FIG. 7.2c: AGREEMENT BETWEEN OBSERVED AND COMPUTED SCOUR FOR RC TYPE PERMEABLE SPURS

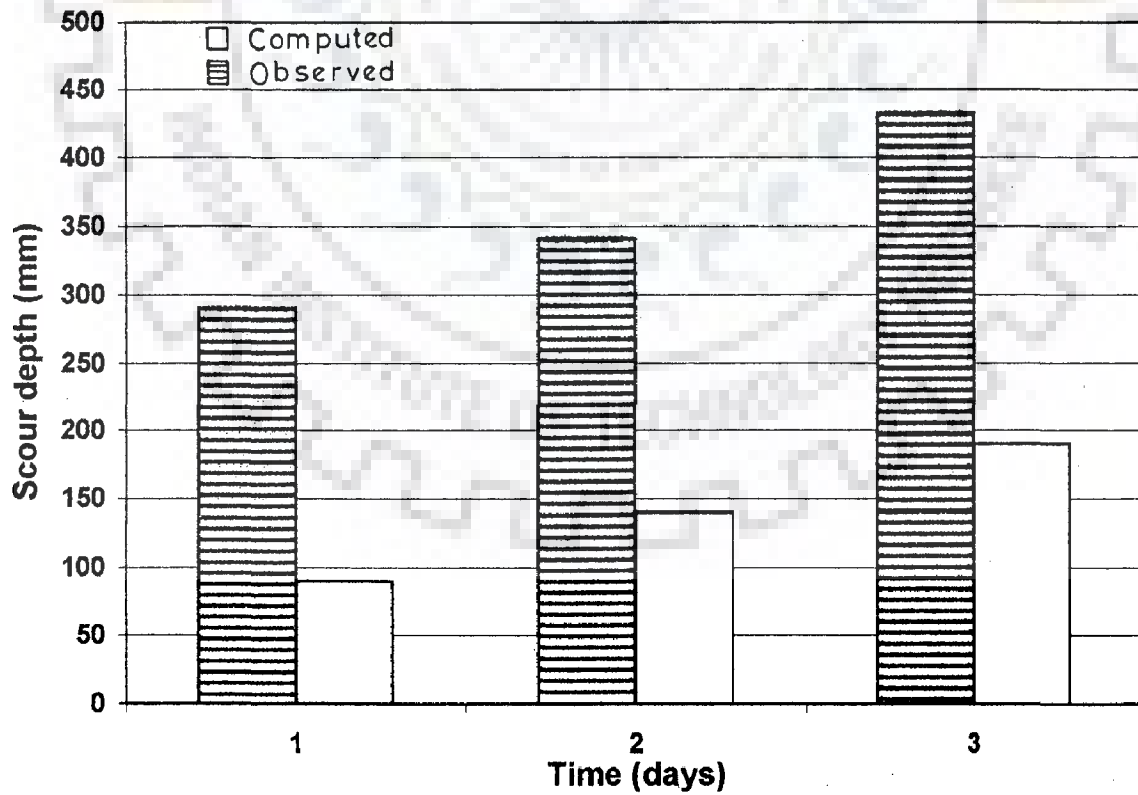


FIG. 7.2d: AGREEMENT BETWEEN OBSERVED AND COMPUTED SCOUR FOR RD TYPE PERMEABLE SPURS

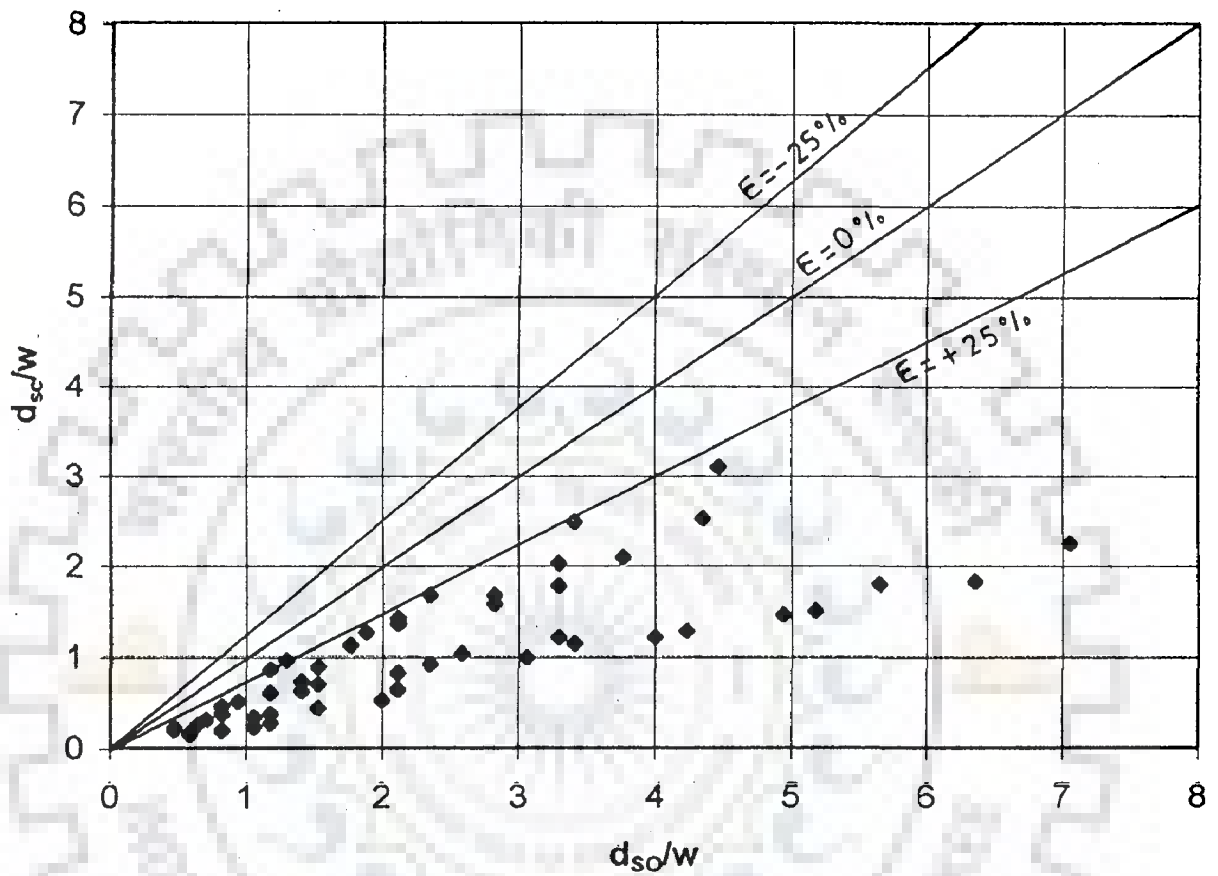


FIG. 7.3: AGREEMENT BETWEEN COMPUTED(EQ.7.1) AND OBSERVED SCOUR/ WIDTH FOR EXPERIMENTS HAVING BED PARTICLE SIZE OF 2.8 mm

Many a times, one is concerned with the bed conditions. For example, the river bed may be uniform, non-uniform, and stratified. In such situations, approaches exist to select the representative bed sizes. So far, the conditions in the Solani river are concerned, the bed consisted of particles of nearly uniform size. As a further extension of the work, it may be necessary to consider the scour around permeable spurs in different bed conditions. It will, thus, be more appropriate to develop a generalized model of scour around permeable pile spurs with the help of such a comprehensive experiments. As far as present experiments are considered, the following relationship may also describe the response of all the lab based experiments

$$\frac{d_{sc}}{w} = \left[6.20 - 13.5 \left(\frac{d}{w} - 0.05 \right) \right] F_r^{1.2117} \beta^{\left(0.3649 + 2.577 \left(\frac{b}{B} - 0.1 \right) \right)} \quad (7.2)$$

The agreement diagram in respect of all the lab based experiments on pile spurs is given in Fig. 7.4. The average error associated using eq. (7.2) is 9.566%. The performance evaluation of eq. 7.2 is shown in Fig. 7.5 for the data of river Solani, as considered in Chapter 5. Despite the fact that eq. (7.2) may describe the scour around all the lab based data collected in the present study, it does not improve its predictive capabilities in preference to eq. (5. 12), as far as the data on Solani river is concerned. The trend of predicted scour are essentially similar to what has been described in chapter 5.

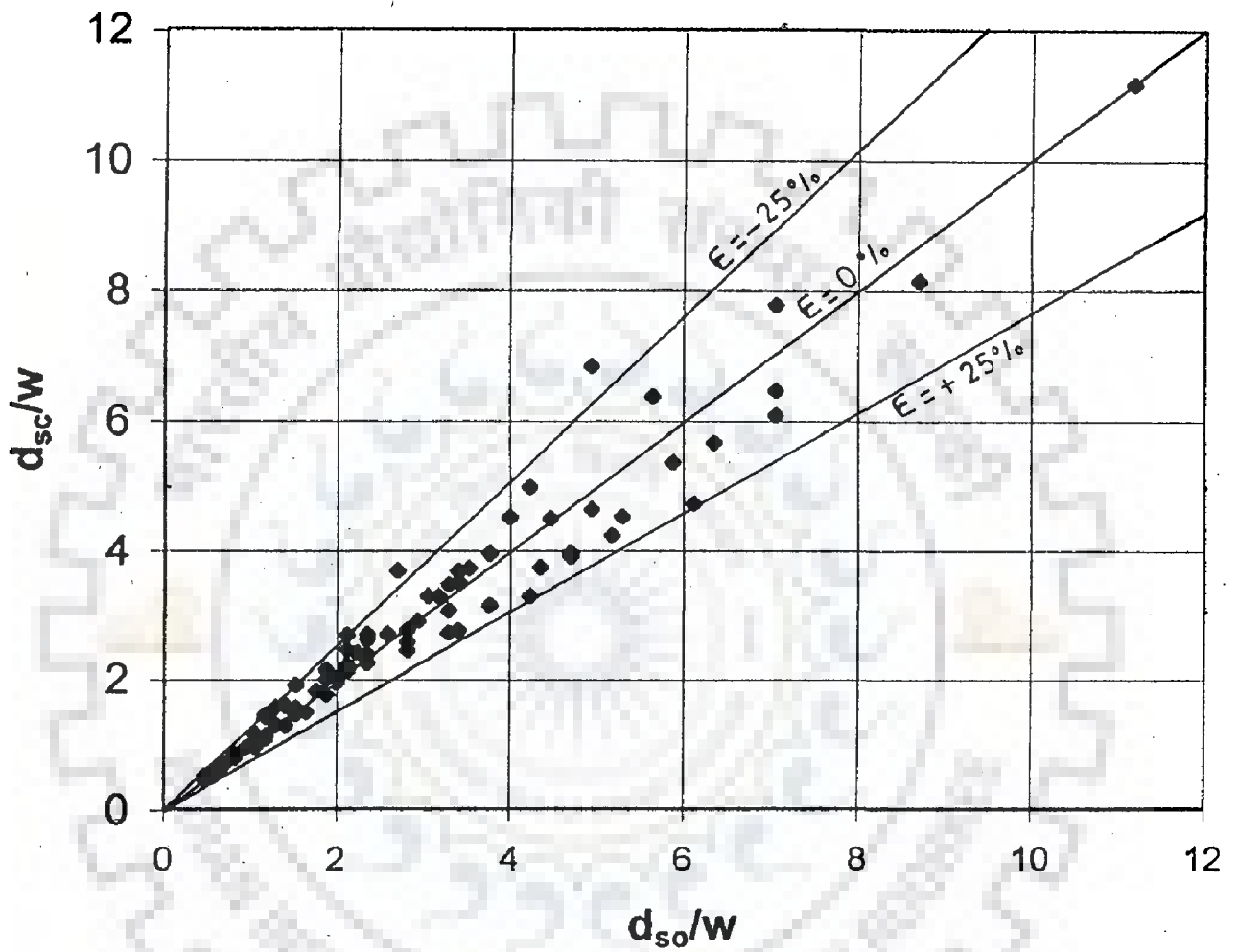


FIG.7.4: PERFORMANCE EVALUATION OF EQUATION 7.2 FOR EXPERIMENTAL DATA OF PHASE II

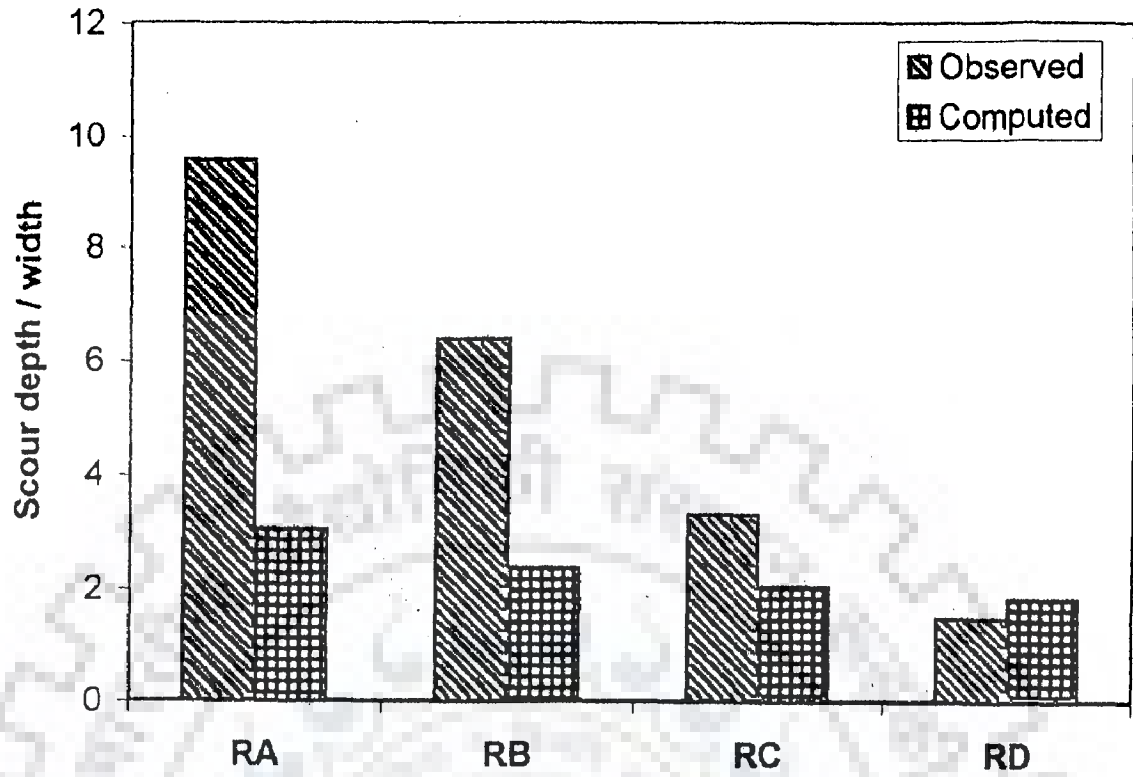


FIG.7.5: STEADY STATE SCOUR PREDICTION USING EQUATION 7.2 FOR SOLANI RIVER EXPERIMENTS

CONCLUSIONS AND SCOPE FOR FUTURE WORK

8.1 CONCLUSIONS

Based on the present study, the following conclusions can be arrived:

1. Based on experiments with different permeable spurs including slotted (horizontal as well as vertical) and pile spurs, it has been observed that less scour occurs at the nose of permeable pile spurs. For these experiments, range of Froude number is between 0.1 to 0.5.
2. Scour at the nose of permeable pile spurs is found related to Froude number and dimensionless term, defined as the ratio of available flow cross-section in unconstricted and constricted zones. Here, the constricted zone refers to the one occupied by the permeable spurs. In addition, the role of bed particle size has been also observed on the scour. In case of fine grain sand bed, the scour was observed to be more than that of coarse grain sand bed.
3. Considering the utility of Melville's approach in describing the scour around abutments and bridge piers, an attempt was made to develop an effectiveness factor as function of porosity. However, it was observed that the effectiveness factor depends not only on porosity but also on Froude number.
4. Analysis of several experiments conducted particularly at Roorkee, reveals that

the scour predicted by Melville's approach is more than the scour reported in different experiments. This finding is in conformity with Melville's observation that equilibrium scour may take a sufficiently long time (in days) to develop.

5. Several ways to make the scour depth dimensionless were attempted. The performance evaluation of these relationships against the field data indicates that the use of pier width to make scour depth dimensionless represents the scale effects in a better manner.
6. Using the calibrated model of steady state flow, an attempt was made to develop an approach for the modeling of scour in an unsteady state flow situation. However, the scour predicted were found to be lower than those observed in field. It is possible that while constructing the model, the portion of the bed surrounding the spur might have been disturbed and loosened up. Another possibility is that as the present steady state experiments were run only for few hours, the equilibrium scour attained in these experiments might have been on a lower side.
7. A model based on the ratio of flow velocity to critical shear stress velocity was also calibrated using a limited number of experiments. The predicted scour depths using this model performed better in case of pile spurs with lower porosity. On the contrary, the Froude number based model performed better with the pile spurs of larger porosity. Within a permissible tolerance of the few tens of centimeters, the use of these models is advocated. At the same time, it is also recommended to test these models against additional data to assess their merit.
8. Considering that the depth of scour around permeable spur is comparatively very

low in preference to other models, the uncertainty related to scour depth prediction may not adversely effect the cost of such type of permeable spur.

8.2 SCOPE FOR FUTURE WORK

- (i) As the study was focussed only on uniform sand, its extension to non uniform sand bed as well as stratified bed can be considered for future work.
- (ii) As the experiments have been performed on single row with only two values of bed particle size and spur length, future experiments can be performed with additional values of these variables.
- (iii) In the present study, only one size of pile diameter was used. Thus, experiments can be performed with other pier diameters to include the effect of pier diameter in the scour relationship.
- (iv) In view of Melville's suggestion, efforts should be made to perform these experiments for a longer time. This will help in better estimation of equilibrium time and equilibrium scour depth.
- (v) Retrospection of effectiveness factors with regard to pile spurs is also needed considering the fact that the effectiveness factor for the permeability is found dependent on permeability as well as Froude number.
- (vi) Construction of field model may be done in such a way so that bed remains stabilized before being exposed to flow.

REFERENCES

1. Ab. Ghani, A. and Nalluri, C. (1996). " Deveopment of pier-scour equations using field data." Proc., Tenth Congress- Asian and Pacific Division of IAHR, Longkawi Island, Malaysia, Vol. 1, 295-302.
2. Ahmad, M. (1951). " Spacing and projection of spurs for bank projection. (Part-1)" Civil Engineering and Public Works Review, London, Vol. 46, No. 537, 172-174.
3. Ahmad, M. (1951). " Spacing and projection of spurs for bank projection. (Part-11)" Civil Engineering and Public Works Review, London, Vol. 46, No. 538, 256-258.
4. Ahmad, M. (1953). " Experiments on design and behaviour of spur-dikes." Proc., IAHR conference Minnesota, 145-159.
5. Alam, S.M.Z., Faruque, H.S. (1986). "Bank protection methods used in Bangladesh." Proc., Regional Workshop on Erosion and Sediment Transport, Dhaka, Bangladesh, Dec., 20-23.
6. Altunin, S.T. (1962). " Regulirowanie rusel. (in Russian). River training." Moscow, SLJP.
7. Altunin, S. T. and Buzunow, I.A. (1953). " Zascitnyje sooruzhenyia na rekakh. (in Russian). Protective works on rivers." Moscow, Selkhozgiz Publ. House.
8. Beckstead, G. (1975). " Design consideration for stream groynes." Alberta, Department of the Environment, Environmental Engineering, Support Services, Canada.
9. Barbe, D.E. , Cruise , J.F., Singh, V.P., (1992), "Probabilistic approach to local bridge pier scour." Transportation Research Record No. 1350, 28-33.
10. Bathurst, J. C. (1978). " Flow resistance of large scale roughness." Journal of Hydraulic Division, ASCE, Vol. 104, No. HY 12, 1587-1603.
11. Bognar, S. and Rakoczi, L. (1988). "Further improvements in quasi-2D morphological modelling." Proc., International Conference on Fluvial Hydraulics' 88, 30 May - 3 June, Budapest, Hungary, 321-326.
12. Bureau of Indian Standard Code IS : 8404 - (1976).
13. Bureau of Indian Standard Code IS : 1808 - (1976).

14. Buy N.T.(1981)."Issledovanie mestnogo razmyva v zone ogolovkov rusloregulirujushchikh sooruzhenij tipa glukhoj shpory. (in Russian). Investigation of local scour around heads of groyne-like structures." Ph.D Thesis, Hydro-reclamation Institute, Moscow.
15. Chiew, Y. M. (1984). "Local scour at bridge piers." Rep. No. 355, Dept. of Civil Engrg., University of Auckland, Auckland, New Zealand. .
16. Doddiah, D., Albertson, M., and Thomas, R. (1953)."Scour from jets." Proc., Minnesota International Hydraulic Convention, Minneapolis, Minn., Sept., 161-169.
17. Ettema, R. (1980). "Scour at bridge piers." Rep. No. 216, School of Engrg., University of Auckland, Auckland, New Zealand.
18. Garde, R.J. (1953). "Some exploratory studies on scour around spur-dikes." Research Journal, University of Roorkee, Roorkee (India) Vol. II. 45-54.
19. Garde, R.J. and Subramanya, K. (1960). "Exploratory study of scour around spur-dikes." Research journal, University of Roorkee, Roorkee (India) Vol. III., 59-73.
20. Garde, R.J., Subramanya, K., and Nambudripad, K.D. (1961). "Study of scour around spur-dikes." Journal of Hydraulic Division, ASCE.,Vol. 87, No.HY-6, 23-37.
21. Garde, R.J. and Chandra, G. (1969). "Criteria for determination of length of spur for bank protection." *Symposium on "Simulation Techniques and Prototype Behaviour in Water Resources"*, C.B.I.P., 42nd annual session, 97-105.
22. Garde, R. J., and Ranga Raju (1985). *Mechanics of sediment transportation and alluvial stream problems*, 2nd edition, Wiley Eastern limited, New Delhi.
23. Gill, M. A. (1972). "Erosion of sand beds around spur-dikes." Journal of Hydraulic Division, ASCE, Vol. 98, No. HY-9, 1587-1602.
24. Gole, C.V., Chitale, S. V., and Kulkarni, V. K. (1975). "Slotted spur." Proc., 44th annual research session , Central Board of Irrigation and Power, Chandigarh, Hydraulics Vol. I., Jan., 1-6.
25. Inglis, C. C. (1949). "Behaviour and control of river and canal with aids of models." Research Publication No. 13, Part II, C.W.I & N.R.S. Poona, India.

26. Jain, S.C. (1981), "Maximum clear water scour around circular piers." *Journal of Hydraulic Division, ASCE*, Vol. 107, No. 5, 611-626.
27. Khosla, A.N. (1936). "Design of weirs on permeable foundations." Publication No. 12, C.B.I.P. India.
28. Kilner, F. A. (1952). "Local scour in river models due to spurs." M. E. Thesis, Civil. Engg. Deptt., University of London, England.
29. Komura, S. (1971). "River-bed variation at long constrictions." 14th Congress of IAHR, Vol. 3, Subjects C, 29 Aug. - 3 Sept., 109-116.
30. Lacey, G. (1920). "Stable channels in alluvium." *Proc., Institution of Civil Engineers*, Vol. 229, Part 1, 259-292.
31. Laursen, E. M., (1963). "An analysis of bridge relief scour." *Proc., Journal of Hydraulic Division, ASCE*, Vol. 89, No. HY3, 93-117.
32. Laursen, E.M. and. Toch, A. (1953). "A generalized model study of scour around bridge piers and abutment." *Proc., Minnesota International Hydraulic Convention, Minneapolis, Minnesota., Sept., 123-131.*
33. Laursen, E. M., and Toch, A. (1956). "Scour around bridge piers and abutment." *Iowa Highway Research Board, Bull. No. 4.*
34. Liu, H. K. G. and Skinner, M.M. (1960). "Laboratory observations of scour at bridge abutments." *Highway Res. Board, Bull. No. 242.*
35. Manual on "River Behaviour, Control and Training", C.B.I.P. Publication No.204 Vol. I, (1989).
36. Melville, B.W. (1997). "Pier and abutment scour – an integrated approach." *Journal of Hydraulic Engineering, ASCE*, Vol. 123, No. 2, 125-136.
37. Melville, B. W., and Chiew Y. M. (1999). "Time scale for local scour at bridge Pier." *Journal of Hydraulic Engineering, ASCE*, Vol. 125, No.1, 59-65.
38. Michiue, M., Suzuki, K., and Hinokidani, O. (1984). "Formation of low-water bed by spur-dikes in alluvial channel." *Proc., 4th APD, IAHR*, 685-698.
39. Mukhamedov, A.M., Abduraupov, R.R., Irmukhamedov, K.A., Kayumov, O.A., and Urkinbaev, R. (1971). "Study of local scour and Kinematic structure of flow around solid and through spur-dike." *Proc., 14th Congress of IAHR, Paris, Vol.3, Report No. C-47, 1-8.*

40. Nambudripad, K. D. (1961). "Effect of sediment characteristics on scour around spur-dikes in alluvial channels." M. E Thesis, U.O.R., Roorkee, India.
41. Neill, C.R. and Chaplin, T.K. (1962). Discussion on the paper "Study of scour around spur-dikes" by Garde, R.J., Subramanya, K. and Nambudripa, K. D. (1961). Journal of the Hydraulic Division, ASCE, Vol. 88. No. HY2, 191-192.
42. Neill, C.R. (1973). "Guide to bridge hydraulics." Toronto and Buffalo, RTAC, University of Toronto press.
43. Neill, C.R. (1980). "Metric revision supplement to the guide to bridge hydraulics." Ottawa, RTAC.
44. Orlov, J.Y. (1951). "Skvoznoje zailiteli dla zascity beregov to razmyva. (in Russian). Silting permeable structure for bank protection against erosion", Gidrotekhnicheskoe stroitelstvo: 12.
45. Paintal, A.S., and Garde, R.J.(1965). "Effects of inclination and shape of obstruction on local scour." Research journal, University of Roorkee, Roorkee (India), Vol. 8, 51-63.
46. Przedwojski, B., Blazejewski, R., and Pilarezyk, K.W.,(1995),"River Training Techniques", A.A. Balkema, Rotterdam, Brookfield, Netherlands.
47. Ramu, K. L. V. (1964). "Effect of sediment size on scour." M. E. Thesis, Civil Engg. Deptt., U.O.R., Roorkee, India.
48. Richardson, E. V., Harrison, L. J., Richardson, J.R., and Davis, S. R.(1993). "Evaluating scour at bridges." Hydr. Engrg., Circular No. 18, Federal Highway Administration., U.S. Dept. of Transp., Washington, D.C.
49. Rouse, H. (1940). "Criteria for similarity in the transportation of sediment." Proc., First Hydraulic Conference, State University of Iowa, Iowa City, Iowa, Bull. 20., Mar., 33-49.
50. Sastry, C.L. (1962). "Effect of spur-dike inclination on scour characteristics." M.E. Thesis, University of Roorkee, Roorkee, India.
51. Sharma, L. R. (1991). "Experimental study of redeveloping boundary layer flow past fences." Ph.D. Thesis, Department of Civil Engineering, University of Roorkee, Roorkee, India.

52. Shen, H. W., Schneider, V. R. and Karaki, S. S. (1966). "Mechanics of local scour." U.S. Department of Commerce, National Bureau of Standards, Institute of Applied Technology, Washington, D.C.
53. Singh, A. K. (1993). "Comparative study of solid and permeable spurs." M.E. Dissertation, Water Resources Development Training Centre. University of Roorkee, Roorkee, India.
54. Subramanya, K., and Gangadharaiyah, T. (1989). "Flow around slotted spurs." *Third International Workshop on Alluvial River Problems*, University of Roorkee, Roorkee, India, 225-263.
55. Tyagi, A. K. (1967). "Effect of specific gravity of sediment on scour." M.E Thesis, Civil Engg. Deptt., University of Roorkee, Roorkee, India.
56. Tyagi, A. K. (1973). "Modeling of local scour around spur-dikes in stream." *IAHR, Symposium on River Mechanism*, Bangkok, Thailand, A 15, 1-11.
57. United Nations Economic Commission for Asia and the Far East (1953). "River training and bank protection." Bangkok.



Appendix

Table A -1: Details of classification of model experimental runs of 1st phase in clear water conditions in flume of width = 500mm, $d_{50} = 0.424\text{mm}$ with two model lengths (min. and max. permissible), $S = 1$ in 5000, all models in all experiments are placed at 90° to vertical rigid bank

Series	Type
A	Solid spur models, i.e. with zero permeability.
B	Models with round holes
CA	Models with rectangular holes. Two holes are in each row. Two rows in 8cm depth & three rows in 10cm depth. Slits are closed in all sides. 1st row starts from the test bed
CB	Three rectangular slits/holes in each row. The slits on the extreme edge from the spur bank are open in the mid stream.
DA	Models with two vertical slots. Slots start from the test bed surface. Slots are open on top.
DB	Models with three vertical slots. Slots start from the test bed surface. Slots are open on top.
EA	Models with horizontal slots. Three rectangular, horizontally placed slots in 10cm depth & two slots in 8cm depth. Slots are closed on mid stream side. 1st slot starts from bed level.
EB	Models with horizontal slots. Three rectangular, horizontally placed slots in 10cm depth & two slots in 8cm depth. Slots are open on mid stream side. 1st slot starts from bed level.
FA	Bamboo or wooden Pile Spur in form of pencils. For 10.7cm only two & for 16.9cm/15.8cm four pencils are used. Pencils dia.= 0.85cm. Spacing bet. every two pencils is 4.5cm from edge to edge.
FB	Bamboo or wooden Pile Spurs. Two II rows of pencil piles & vertically slotted spurs. Each have four solid vertical portions in each II row. Length is 10cm in perspex, vertically slotted spurs & is 17cm & 19.5cm for pencil spurs. Distance bet. rows is 5cm for all models. Pencils dia.= 0.85cm.

Table A - A : Solid spur models.

run no.	b mm	Q	y	d ₅₀	t _e	Fr	% p
		m ³ /sec	mm	mm	hr:min		
A - 1	50	0.0063	80	45	11:15	0.176	0
A - 2	100	0.0063	80	60.5	11:45	0.176	0
A - 3	100	0.0099	100	103	10:00	0.2	0
A - 4	50	0.0099	100	54	10:35	0.2	0

Table A - B : Models with round holes.

Holes are of 6mm dia in models with 30.7% p.

Holes are of 1cm dia. and 4mm dia. in alternate rows & columns for 58 %p.

run no.	b mm	Q	y	d ₅₀	t _e	Fr	% p
		m ³ /sec	mm	mm	hr:min		
B - 1	50	0.0063	80	25	10:30	0.176	30.7
B - 2	100	0.0063	80	38	11:45	0.176	30.7
B - 3	100	0.0099	100	82	10:00	0.2	30.7
B - 4	50	0.0099	100	40	7:40	0.2	30.7
B - 5	50	0.0099	100	26	6:30	0.2	58
B - 6	100	0.0099	100	52	8:30	0.2	58
B - 7	50	0.0063	80	29	12:00	0.176	58
B - 8	100	0.0063	80	28	10:45	0.176	58

Table A - CA : Models with rectangular holes.

run no.	b mm	Q	y	d ₅₀	t _e	Fr	% p
		m ³ /sec	mm	mm	hr:min		
CA - 1	51	0.0099	100	39	10:00	0.2	57.1
CA - 2	100	0.0099	100	52	5:00	0.2	58.02
CA - 3	51	0.0063	80	10	7:30	0.176	54.7
CA - 4	100	0.0063	80	38	10:10	0.176	55

Table A - CB : Rectangular slits/holes.

run no.	b mm	Q	y	d _{so}	t _e	Fr	% p
		m ³ /sec	mm	mm	hr:min		
CB-1	50	0.0063	80	17	11:10	0.176	54.05
CB-2	50	0.0099	100	42	7:30	0.2	57.48
CB-3	100	0.0099	100	62	8:30	0.2	58.55
CB-4	100	0.0063	80	23	7:15	0.176	54.4

Table A - DA : Models with two vertical slots.

run no.	b mm	Q	y	d _{so}	t _e	Fr	% p
		m ³ /sec	mm	mm	hr:min		
DA-1	100	0.0099	100	68	10:00	0.2	42
DA-2	52	0.0099	100	44	11:20	0.2	40.38
DA-3	100	0.0063	80	39	10:30	0.176	42
DA-4	52	0.0063	80	24	9:00	0.176	40.38
DA-5	50	0.0063	80	25	10:10	0.176	50.98
DA-6	100	0.0063	80	34	10:00	0.176	49.5
DA-7	50	0.0099	100	36	9:35	0.2	50.98
DA-8	100	0.0099	100	60	9:45	0.2	49.5
DA-9	102	0.0099	100	83	8:00	0.2	31.37
DA-10	50	0.0099	100	52	10:00	0.2	32.65
DA-11	50	0.0063	80	28	9:30	0.176	32.65
DA-12	102	0.0063	80	33	10:30	0.176	31.37

Table A - DB : Models with three vertical slots.

run no.	b mm	Q	y	d _{so}	t _e	Fr	% p
		m ³ /sec	mm	mm	hr:min		
DB-1	50	0.0063	80	17	8:40	0.176	54
DB-2	100	0.0063	80	30	10:40	0.176	51
DB-3	50	0.0099	100	49	9:30	0.2	54
DB-4	100	0.0099	100	48	10:30	0.2	51
DB-5	50	0.0063	80	25	10:00	0.176	42
DB-6	100	0.0063	80	30	10:00	0.176	42
DB-7	50	0.0099	100	58	9:45	0.2	42
DB-8	100	0.0099	100	80.5	9:20	0.2	42
DB-9	50	0.0099	100	62	8:40	0.2	36
DB-10	100	0.0099	100	71	5:45	0.2	33
DB-11	50	0.0063	80	23	9:30	0.176	36
DB-12	100	0.0063	80	39	11:00	0.176	33

Table A - EA : Models with horizontal slots.

run no.	b mm	Q	y	d _{so}	t _e	Fr	% p
		m ³ /sec	mm	mm	hr:min		
EA-1	51	0.0099	100	43	5:30	0.2	50.23
EA-2	100	0.0099	100	80	10:08	0.2	49.35
EA-3	50	0.0063	80	13	6:30	0.176	43.05
EA-4	100	0.0063	80	32	8:00	0.176	41.47

Table A - EB : Models with horizontal slots.

run no.	b mm	Q m ³ /sec	y mm	d ₅₀ mm	t _e hr:min	Fr	% p
EB-1	50	0.0063	80	15	6:05	0.176	40
EB-2	100	0.0063	80	17	10:40	0.176	45
EB-3	50	0.0099	100	45	5:00	0.2	47.86
EB-4	100	0.0099	100	72	10:00	0.2	54

Table A - FA : Bamboo or wooden Pile Spur in form of pencils.

run no.	b mm	Q m ³ /sec	y mm	d ₅₀ mm	t _e hr:min	Fr	% p
FA-1	107	0.0099	100	32	8:00	0.2	84.12
FA-2	107	0.0063	80	12	8:15	0.176	84.12
FA-3	169	0.0099	100	32	7:05	0.2	78.48
FA-4	158	0.0063	80	17	7:00	0.176	78.48

Table A - FB : Bamboo or wooden Pile Spurs.

run no.	b mm	Q m ³ /sec	y mm	d ₅₀ mm	t _e hr:min	Fr	% p
FB-1	195	0.0099	100	32	6:00	0.2	79.5
FB-2	170	0.0063	80	17	5:00	0.176	76.18
FB-3	100	0.0099	100	64	7:15	0.2	51
FB-4	100	0.0063	80	25	3:00	0.176	51

Table A -P : Details of classification of pile spur model experimental runs of 2nd phase in clear water conditions in flume of width = 500mm, $d_{50} = 2.8\text{mm}$ fine gravel, with two model lengths (min. and max. permissible), $S = 1\text{ in } 2000$, all models in all experiments are placed at 90° to vertical rigid bank

Series	Type of experiments with:
P1A	Pile spur models 5cm in length with 15% permeability.
P2A	Pile spur models 10cm in length with 15% permeability.
P1B	Pile spur models 5cm in length with 25% permeability
P2B	Pile spur models 10cm in length with 25% permeability
P1C	Pile spur models 5cm in length with 40% permeability
P2C	Pile spur models 10cm in length with 40% permeability
P1D	Pile spur models 5cm in length with 60% permeability
P2D	Pile spur models 10cm in length with 60% permeability
P1E	Pile spur models 5cm in length with 80% permeability
P2E	Pile spur models 10cm in length with 80% permeability

Table A - PS : Details of classification of pile spur model experimental runs of 2nd phase in clear water conditions in flume of width = 500mm, $d_{50} = 0.424\text{mm}$, coarse sand, with two model lengths (min. and max. permissible), $S = 1\text{ in } 5000$, all models in all experiments are placed at 90° to vertical rigid bank

Series	Type of experiments with:
PS1A	Pile spur models 5cm in length with 15% permeability.
PS2A	Pile spur models 10cm in length with 15% permeability.
PS1B	Pile spur models 5cm in length with 25% permeability
PS1B	Pile spur models 10cm in length with 25% permeability
PS1C	Pile spur models 5cm in length with 40% permeability
PS2C	Pile spur models 10cm in length with 40% permeability
PS1D	Pile spur models 5cm in length with 60% permeability
PS2D	Pile spur models 10cm in length with 60% permeability
PS1E	Pile spur models 5cm in length with 80% permeability
PS2E	Pile spur models 10cm in length with 80% permeability

Tables A - PA : Data of P1A,P2A. Pile spur model runs with 15 % of permeabilities

run no.	b	Q	y	d _{so}	t _c	Fr	% p	t _{run}
	mm	m ³ /sec	mm	mm	hr:min			hr:min
P1A-1	50	0.0067	110	7	1:30	0.12	15	8:00
P2A-1	100	0.0067	110	10	0:30	0.12	15	8:00
P1A-2	50	0.0112	110	13	0:30	0.2	15	4:00
P2A-2	100	0.0112	110	18	0:30	0.2	15	4:00
P1A-3	50	0.0172	110	20	1:30	0.3079	15	4:00
P2A-3	100	0.0172	110	34	0:30	0.3079	15	4:00
P1A-4	50	0.0229	110	29	1:00	0.4095	15	5:00
P2A-4	100	0.0229	110	48	1:30	0.4095	15	5:00
P1A-5	50	0.027	110	38	0:30	0.483	15	4:00
P2A-5	100	0.027	110	60	0:30	0.483	15	4:00

Table A - PB : Data of P1B, P2B. Pile spur model runs with 25 % of permeabilities

run no.	b mm	Q	y	d _{so}	t _c	Fr	% p	t _{run}
		m ³ /sec	mm	mm	hr:min			hr:min
P1B-1	50	0.0067	110	6	3:00	0.12	25	8:00
P2B-1	100	0.0067	110	9	3:00	0.12	25	8:00
P1B-2	50	0.0112	110	12	1:30	0.2	25	4:00
P2B-2	100	0.0112	110	17	1:30	0.2	25	4:00
P1B-3	50	0.0172	110	18	1:30	0.3079	25	4:00
P2B-3	100	0.0172	110	26	1:00	0.3079	25	4:00
P1B-4	50	0.0229	110	28	5:00	0.4095	25	8:10
P2B-4	100	0.0229	110	42	3:00	0.4095	25	8:10
P1B-5	50	0.027	110	37	3:00	0.483	25	4:00
P2B-5	100	0.027	110	54	3:00	0.483	25	4:00

Table A - PC : Data of P1C, P2C. Pile spur model runs with 40 % of permeabilities

run no.	b mm	Q	y	d _{so}	t _e	Fr	% p	t _{run}
		m ³ /sec	mm	mm	hr:min			hr:min
P1C-1	50	0.0067	110	5.5	2:00	0.12	40	8:00
P2C-1	100	0.0067	110	7	0:30	0.12	40	4:00
P1C-2	50	0.0112	110	10	0:30	0.2	40	4:00
P2C-2	100	0.0112	110	13	1:30	0.2	40	4:00
P1C-3	50	0.0172	110	15	1:30	0.3079	40	4:30
P2C-3	100	0.0172	110	18	1:30	0.3079	40	4:00
P1C-4	50	0.0229	110	24	1:30	0.4095	40	4:00
P2C-4	100	0.0229	110	28	3:00	0.4095	40	4:00
P1C-5	50	0.027	110	32	2:00	0.483	40	7:00
P2C-5	100	0.027	110	44	3:00	0.483	40	7:00

Table A - PD : Data of P1D,P2D. Pile spur model runs with 60 % of permeabilities

run no.	b mm	Q	y	d _{so}	t _e	Fr	% p	t _{run}
		m ³ /sec	mm	mm	hr:min			hr:min
P1D-1	50	0.0067	110	4	1:30	0.12	60	4:00
P2D-1	100	0.0067	110	5	1:00	0.12	60	4:00
P1D-2	50	0.0112	110	8	0:30	0.2	60	4:00
P2D-2	100	0.0112	110	10	0:30	0.2	60	4:00
P1D-3	50	0.0172	110	11	0:30	0.3079	60	4:30
P2D-3	100	0.0172	110	13	1:30	0.3079	60	4:00
P1D-4	50	0.0229	110	18	1:30	0.4095	60	4:00
P2D-4	100	0.0229	110	22	5:00	0.4095	60	5:00
P1D-5	50	0.027	110	28	4:00	0.483	60	5:10
P2D-5	100	0.027	110	36	1:00	0.483	60	5:10

Table A - PE : Data of P1E, P2E. Pile spur model runs with 80 % of permeabilities

run no.	b mm	Q	y	d _{so}	t _e	Fr	% p	t _{run}
		m ³ /sec	mm	mm	hr:min			hr:min
P1E-1	50	0.0067	110	4	3:00	0.12	80	8:00
P2E-1	100	0.0067	110	5	1:00	0.12	80	4:00
P1E-2	50	0.0112	110	7	0:30	0.2	80	4:00
P2E-2	100	0.0112	110	9	0:30	0.2	80	4:00
P1E-3	50	0.0172	110	10	3:00	0.3079	80	4:30
P2E-3	100	0.0172	110	12	0:30	0.3079	80	4:00
P1E-4	50	0.0229	110	16	1:00	0.4095	80	4:30
P2E-4	100	0.0229	110	20	3:00	0.4095	80	4:00
P1E-5	50	0.027	110	24	1:00	0.483	80	4:00
P2E-5	100	0.027	110	29	2:00	0.483	80	4:00

Table A - PSA : PS1A, PS2A. Pile spurs with 15 % of permeabilities.

run no.	b mm	Q	y	d ₅₀	t _e	Fr	% p	t _{run}
		m ³ /sec	mm	mm	hr:min			hr:min
PS1A-1	50	0.00595	100	18	1:30	0.12	15	4:00
PS2A-1	100	0.00595	100	23	1:30	0.12	15	4:00
PS1A-2	50	0.009918	100	32	2:00	0.2	15	4:00
PS2A-2	100	0.009918	100	42	3:00	0.2	15	5:00
PS1A-3	50	0.014901	100	60	4:00	0.301	15	6:00
PS2A-3	100	0.014901	100	95	expl. below	0.301	15	1:00

Table A - PSB : PS1B, PS2B. Pile spurs with 25 % of permeabilities.

run no.	b mm	Q	y	d ₅₀	t _e	Fr	% p	t _{run}
		m ³ /sec	mm	mm	hr:min			hr:min
PS1B-1	50	0.00595	100	16	1:30	0.12	25	4:00
PS2B-1	100	0.00595	100	20	1:30	0.12	25	5:30
PS1B-2	50	0.009918	100	27	1:30	0.2	25	4:00
PS2B-2	100	0.009918	100	36	3:00	0.2	25	5:00
PS1B-3	50	0.014901	100	50	3:00	0.301	25	5:00
PS2B-3	100	0.014901	100	74	3:00	0.301	25	4:00

Table A - PSC : PS1C, PS2C. Pile spurs with 40 % of permeabilities.

run no.	b mm	Q	y	d ₅₀	t _e	Fr	% p	t _{run}
		m ³ /sec	mm	mm	hr:min			hr:min
PS1C-1	50	0.00595	100	14	1:30	0.12	40	5:00
PS2C-1	100	0.00595	100	17	1:30	0.12	40	6:30
PS1C-2	50	0.009918	100	24	2:00	0.2	40	5:00
PS2C-2	100	0.009918	100	30	3:00	0.2	40	6:00
PS1C-3	50	0.014901	100	45	3:00	0.301	40	4:00
PS2C-3	100	0.014901	100	60	4:00	0.301	40	7:00

Table A -PSD : PS1D, PS2D. Pile spurs with 60 % of permeabilities.

run no.	b mm	Q	y	d _{so}	t _e	Fr	% p	t _{run}
		m ³ /sec	mm	mm	hr:min			hr:min
PS1D-1	50	0.00595	100	11	0:30	0.12	60	5:00
PS2D-1	100	0.00595	100	13	0:30	0.12	60	5:00
PS1D-2	50	0.009918	100	20	0:30	0.2	60	6:00
PS2D-2	100	0.009918	100	25	4:00	0.2	60	6:00
PS1D-3	50	0.014901	100	40	3:00	0.301	60	5:00
PS2D-3	100	0.014901	100	52	3:00	0.301	60	5:00

Table A - PSE : PS1E, PS2E. Pile spurs with 80 % of permeabilities.

run no.	b mm	Q	y	d _{so}	t _e	Fr	% p	t _{run}
		m ³ /sec	mm	mm	hr:min			hr:min
PS1E-1	50	0.00595	100	9	0:30	0.12	80	5:00
PS2E-1	100	0.00595	100	11	0:30	0.12	80	5:00
PS1E-2	50	0.009918	100	16	0:30	0.2	80	5:00
PS2E-2	100	0.009918	100	19	3:00	0.2	80	5:00
PS1E-3	50	0.014901	100	29	3:00	0.301	80	5:00
PS2E-3	100	0.014901	100	40	3:00	0.301	80	5:00

**Table: A - R : Classification of field experimental runs with actual pile spurs in 3rd phase, $d_{50} = 0.21\text{mm}$, $S = 1$ in 1000, in live bed conditions
Channel width = 30 meters, dia of each bamboo = 6cm
all bamboo spurs in all experiments are placed at 90° to the river bank**

Series	Type of experiments with:
RA	bamboo spurs 3m in length with 20% permeability.
RB	bamboo spurs 3m in length with 40% permeability.
RC	bamboo spurs 3m in length with 60% permeability.
RD	bamboo spurs 3m in length with 80% permeability.

Table A - RS : Data of field experiments in river Solani, Roorkee.

run no.	Q	y	V	d_{50}	σ	τ_c	γ_s	t_{run}	F_r	% p
	m^3/sec	mm	m/s	mm	d.devia	N/m^2	gm/cc	hr		
RA-1	3.64	383	0.32	350	1	0.16	2.65	24	0.16	20
RA-2	3.76	390	0.32	600	1	0.16	2.65	48	0.16	20
RA-3	5.28	435	0.4	630	1	0.16	2.65	72	0.2	20
RA-4	6.28	439	0.48	700	1	0.16	2.65	96	0.23	20
RB-1	3.64	383	0.32	350	1	0.16	2.65	24	0.16	40
RB-2	3.76	390	0.32	370	1	0.16	2.65	48	0.16	40
RB-3	5.28	435	0.4	400	1	0.16	2.65	72	0.2	40
RB-4	6.28	439	0.48	450	1	0.16	2.65	96	0.23	40
RC-1	3.64	383	0.32	200	1	0.16	2.65	24	0.16	60
RC-2	3.76	390	0.32	200	1	0.16	2.65	48	0.16	60
RC-3	5.28	435	0.4	250	1	0.16	2.65	72	0.2	60
RC-4	6.28	439	0.48	300	1	0.16	2.65	96	0.23	60
RD-1	3.64	383	0.32	80	1	0.16	2.65	24	0.16	80
RD-2	3.76	390	0.32	100	1	0.16	2.65	48	0.16	80
RD-3	5.28	435	0.4	180	1	0.16	2.65	72	0.2	80
RD-4	6.28	439	0.48	200	1	0.16	2.65	96	0.23	80